

EUROPEAN ORGANISATION FOR NUCLEAR RESEARCH (CERN)



JHEP 09 (2016) 173
 DOI: [doi:10.1007/JHEP09\(2016\)173](https://doi.org/10.1007/JHEP09(2016)173)



CERN-EP-2016-106
 15th November 2021

Searches for heavy diboson resonances in pp collisions at $\sqrt{s} = 13$ TeV with the ATLAS detector

The ATLAS Collaboration

Abstract

Searches for new heavy resonances decaying to WW , WZ , and ZZ bosons are presented, using a data sample corresponding to 3.2 fb^{-1} of pp collisions at $\sqrt{s} = 13$ TeV collected with the ATLAS detector at the CERN Large Hadron Collider. Analyses selecting $vvqq$, ℓvqq , $\ell\ell qq$ and $qqqq$ final states are combined, searching for a narrow-width resonance with mass between 500 and 3000 GeV. The discriminating variable is either an invariant mass or a transverse mass. No significant deviations from the Standard Model predictions are observed. Three benchmark models are tested: a model predicting the existence of a new heavy scalar singlet, a simplified model predicting a heavy vector-boson triplet, and a bulk Randall-Sundrum model with a heavy spin-2 graviton. Cross-section limits are set at the 95% confidence level and are compared to theoretical cross-section predictions for a variety of models. The data exclude a scalar singlet with mass below 2650 GeV, a heavy vector-boson triplet with mass below 2600 GeV, and a graviton with mass below 1100 GeV. These results significantly extend the previous limits set using pp collisions at $\sqrt{s} = 8$ TeV.

Contents

1	Introduction	2
2	ATLAS detector and data sample	3
3	Signal and background simulation	3
4	Object reconstruction and selection	6
5	Event selection	8
6	Background estimation	10
7	Systematic uncertainties	12
8	Statistical analysis	14
9	Results	16
10	Conclusion	23

1 Introduction

Diboson resonances are predicted in several extensions to the Standard Model (SM), such as composite Higgs models [1, 2], technicolour [3–5], warped extra dimensions [6–8], Two-Higgs-doublet models (2HDM) [9], and Grand Unified Theories [10–13]. The search for high-mass resonances decaying into vector bosons benefits greatly from the increase in centre-of-mass energy of proton–proton collisions at the Large Hadron Collider (LHC) from $\sqrt{s} = 8$ TeV (Run 1) to 13 TeV (Run 2). This would result in more abundant production of new particles with masses significantly in excess of a TeV, in processes initiated by gg , gq or qq .¹

This paper reports a search for a charged or neutral resonant state, with a mass between 500 GeV and 3 TeV, decaying to WW , ZZ or WZ bosons, with subsequent decays of the W and Z bosons to quarks or leptons. Four different decay modes are considered: the fully hadronic mode ($qqqq$), and the semileptonic modes ($\ell\ell qq$, $\ell\nu qq$ and $\nu\nu qq$). Decays of the W or Z bosons to quarks are reconstructed as single jets with a large radius parameter. These jets are required to have features characteristic of a two-body decay, and are identified as W or Z bosons using the jet mass and jet substructure [14, 15].

Three specific signal models are used to assess the sensitivity of the search, to optimise the event selection, and to search for local excesses in the observed data. The first is an extension of the SM with an additional heavy, CP-even, scalar singlet decaying to longitudinally polarised bosons [16]. The second is the Heavy Vector Triplet (HVT) parameterisation [17], predicting $W' \rightarrow WZ$ and $Z' \rightarrow WW$ processes. The third model, known as a bulk Randall–Sundrum (RS) graviton model, features a spin-2 graviton (G^*) decaying to WW or ZZ . The G^* is the first Kaluza–Klein mode in a RS model [6, 18] with a warped extra dimension with curvature κ , where the SM fields are allowed to propagate in the bulk of the extra dimension [19–21].

¹ To simplify notation, antiparticles are denoted by the same symbol as the corresponding particles.

Both ATLAS and CMS have searched for heavy diboson resonances in various final states in the $\sqrt{s} = 7$ TeV and 8 TeV datasets [22–31]. As an example, CMS set a lower limit of 1.7 TeV at the 95% confidence level (CL) on the mass of a W' boson predicted by an Extended Gauge Model (EGM) [32] using the fully hadronic channel [26]. The $qqqq$, $\ell\ell qq$, $\ell\nu qq$ channels were combined by ATLAS using the bulk RS G^* model and the EGM W' boson as benchmarks [31]. Observed lower limits at 95% CL of 1.81 TeV on the EGM W' mass and of 810 GeV on the bulk G^* mass were obtained, assuming $\kappa/\bar{M}_{\text{Pl}} = 1$ (where \bar{M}_{Pl} is the reduced Planck mass) for the bulk G^* signal hypothesis. The largest deviation from the predicted background in that analysis was a 2.5σ local excess close to a mass of 2 TeV.

2 ATLAS detector and data sample

The ATLAS detector [33] is a general-purpose particle detector used to investigate a broad range of physics processes. It includes inner tracking devices surrounded by a superconducting solenoid, electromagnetic (EM) and hadronic calorimeters, and a muon spectrometer inside a system of toroid magnets. The inner detector (ID) consists of a silicon pixel detector including the newly installed Insertable B-Layer [34], a silicon microstrip detector and a straw tube tracker. It is situated inside a 2 T axial magnetic field from the solenoid and provides precision tracking of charged particles with pseudorapidity² $|\eta| < 2.5$. The straw tube tracker also provides transition radiation measurements for electron identification. The calorimeter system covers the pseudorapidity range $|\eta| < 4.9$. It is composed of sampling calorimeters with either liquid argon or scintillator tiles as the active medium. The muon spectrometer (MS) provides muon identification and measurement for $|\eta| < 2.7$ and detectors for triggering in the region $|\eta| < 2.4$. The ATLAS detector has a two-level trigger system to select events for offline analysis [35].

The data used in this analysis were recorded with the ATLAS detector during the 2015 run and correspond to an integrated luminosity of $3.2 \pm 0.2 \text{ fb}^{-1}$ of proton–proton collisions at $\sqrt{s} = 13$ TeV. The measurement of the integrated luminosity is derived, following a methodology similar to that detailed in Ref. [36], from a preliminary calibration of the luminosity scale using x – y beam-separation scans performed in August 2015. The data are required to satisfy a number of conditions ensuring that the detector was operating well while the data were recorded.

3 Signal and background simulation

The Monte Carlo (MC) simulation of three benchmark signal models is used to optimise the sensitivity of the search and to interpret the results.

The first model extends the SM by adding a new, heavy, neutral Higgs boson, using the narrow-width approximation (NWA) benchmark [37, 38]. Results are then interpreted within a model of a CP-even scalar singlet S [16]. The model is parameterised by: an energy scale $\Lambda = 1$ TeV; a coefficient c_H scaling the coupling of S to the Higgs boson; and a coefficient c_3 scaling the coupling of S to gluons. Two benchmark scenarios are considered, one in which c_3 is set via *naive dimensional analysis* (NDA) to be

² ATLAS uses a right-handed coordinate system with its origin at the nominal interaction point (IP) in the centre of the detector and the z -axis along the beam pipe. The x -axis points from the IP to the centre of the LHC ring, and the y -axis points upwards. Cylindrical coordinates (r, ϕ) are used in the transverse plane, ϕ being the azimuthal angle around the beam pipe. The pseudorapidity is defined in terms of the polar angle θ as $\eta = -\ln \tan(\theta/2)$. Rapidity is also defined relative to the beam axis as $y = 0.5 \ln[(E + p_z)/(E - p_z)]$. Angular distance is measured in units of $\Delta R \equiv \sqrt{(\Delta\eta)^2 + (\Delta\phi)^2}$.

$c_3 = (1/4\pi)^2$, with $c_H = 0.9$; and another in which the coupling to gluons is *Unsuppressed* and $c_3 = 1/8\pi$, with $c_H = 0.5$. The value of c_3 determines the production cross-section and the decay width to gluons, while decays to W or Z bosons account for the remaining decay width. In the Unsuppressed scenario considered in this paper, the total branching ratio to WW , ZZ or HH increases from 59% at 500 GeV, to 70% at 2 TeV and to 73% at 5 TeV. For the NDA scenario, this branching ratio is always above 99%. The ratio of $WW:ZZ:HH$ partial widths is approximately 2:1:1 in both scenarios, and couplings to fermions and transversely polarised bosons are set to zero.

The second model is based on the HVT phenomenological Lagrangian which introduces a new triplet of heavy vector bosons that contains three states with identical masses: the two electrically charged W' bosons and the electrically neutral Z' boson. The Lagrangian parameterises the couplings of the new HVT with the SM fields in a generic manner. This parameterisation allows a large class of models to be described, in which the new triplet field mixes with the SM vector bosons. The coupling between the new triplet and the SM fermions is given by the combination of parameters $g^2 c_F/g_V$, where g is the SM $SU(2)_L$ gauge coupling, c_F is a multiplicative factor that modifies the coupling to fermions, and g_V represents the coupling strength of the known W and Z bosons to the new vector bosons. Similarly, the coupling between the Higgs boson and the new triplet is given by the combination $g_V c_H$, where c_H is a multiplicative factor that modifies the coupling to the Higgs boson. Other coupling parameters involving more than one heavy vector boson give negligible contributions to the overall cross-sections for the processes of interest here. Two benchmarks are used [17]. In the first one, referred to as *model-A* with $g_V = 1$, the branching ratios of the new HVT to fermions and gauge bosons are similar to those predicted by some extensions of the SM gauge group [39]. This model, although severely constrained by searches for new resonances decaying to leptons [40–43], is included because of its similarity to the EGM W' model used as a benchmark in previous searches [31]. In the second model, referred to as *model-B* with $g_V = 3$, the fermionic couplings of the new HVT are suppressed, and branching ratios are similar to the ones predicted by composite Higgs boson models [44–46]. In both benchmarks the width of the HVT is narrower than the detector resolution, and the kinematic distributions relevant to this search are very similar. Off-shell and interference effects are not considered.

The third model considered is the so-called bulk RS model [19]. This model extends the original RS model with one warped extra dimension [6, 7] by allowing the SM fields to propagate in the bulk of the extra dimension. This avoids constraints on the original RS model from limits on flavour-changing neutral currents and electroweak precision measurements [47]. This model is characterised by the dimensionless coupling constant $\kappa/\bar{M}_{\text{Pl}} \sim O(1)$. In this model the branching ratio of the Kaluza–Klein graviton (G^*) to pairs of vector bosons, WW or ZZ , is larger than 30%.

For the NWA Higgs boson model, samples are generated for gluon fusion production with QCD corrections up to next-to-leading order (NLO), assuming a Higgs boson decay width of 4 MeV. Events are generated using POWHEG BOX [48] v1 r2856 with the CT10 parton distribution function (PDF) set [49] interfaced to PYTHIA 8.186 [50] using the AZNLO [51] tune of the underlying event.

Benchmark samples of the HVT and bulk RS graviton are generated using `MADGRAPH5_AMC@NLO` 2.2.2 [52] interfaced to PYTHIA 8.186 with the NNPDF23LO PDF set [53] for resonance masses ranging from 0.5 TeV to 5 TeV. For the HVT interpretation, samples are generated according to model A, for resonance masses ranging from 0.5 TeV to 3 TeV for the semileptonic channels and from 1.2 TeV to 3 TeV for the fully hadronic search. Interpretation in the HVT model-B, $g_V = 3$ scenario uses the model A signal samples rescaled to the predicted cross-sections from model-B. For the bulk RS graviton model, the curvature scale parameter $\kappa/\bar{M}_{\text{Pl}}$ is assumed to be 1. Table 1 shows the resonance width and the product of cross-sections and branching ratios for the various models.

Table 1: The resonance width (Γ) and the product of cross-section times branching ratio ($\sigma \times \text{BR}$) for diboson final states, for different values of the pole mass m of the resonances for a representative benchmark for the spin-0, spin-1 and spin-2 cases. The table shows the predictions by the CP-even scalar model ($\Lambda = 1$ TeV, $c_H = 0.9$, $c_3 = 1/16\pi^2$), by model-B of the HVT parameterisation ($g_V = 3$), and by the graviton model ($\kappa/\bar{M}_{\text{Pl}} = 1$). In the case of the scalar and HVT models, the alternate benchmarks (Unsuppressed scenario, model-A) correspond to a different cross-section but similar resonance width and ratios between the branching ratios into $WW/WZ/ZZ$.

m [TeV]	Scalar			HVT W' and Z'			G^*		
	WW		ZZ	WW		WZ	WW		ZZ
	Γ [GeV]	$\sigma \times \text{BR}$ [fb]	$\sigma \times \text{BR}$ [fb]	Γ [GeV]	$\sigma \times \text{BR}$ [fb]	$\sigma \times \text{BR}$ [fb]	Γ [GeV]	$\sigma \times \text{BR}$ [fb]	$\sigma \times \text{BR}$ [fb]
0.8	3.9	37	18	32	354	682	46	301	155
1.6	33	2.5	1.3	51	38.5	79.3	96	4.4	2.2
2.4	111	0.32	0.16	74	4.87	10.6	148	0.28	0.14

MC samples are used to model the shape and normalisation of the relevant kinematic distributions for most SM background processes in the $vvqq$, ℓvqq and $\ell\ell qq$ searches. Events containing W or Z bosons with associated jets are simulated using the **SHERPA** 2.1.1 [54] generator. Matrix elements (ME) are calculated for up to two partons at NLO and four partons at leading order (LO) using the Comix [55] and OpenLoops [56] ME generators. They are merged with the **SHERPA** parton shower (PS) [57] using the ME+PS@NLO prescription [58]. The CT10 PDF set is used in conjunction with a dedicated set of tuned parton-shower parameters developed by the **SHERPA** authors. For the generation of top–antitop pairs ($t\bar{t}$) and single top-quarks in the Wt - and s -channels the POWHEG BOX v2 [48, 59, 60] generator with the CT10 PDF set is used. Electroweak (t -channel) single-top-quark events are generated using the POWHEG BOX v1 generator. This generator uses the four-flavour scheme for the NLO ME calculations together with the four-flavour PDF set CT10f4 [49]. For all top-quark processes, top-quark spin correlations are preserved; for t -channel production, top-quarks are decayed using **MADSPIN** [61]. The parton shower, fragmentation, and the underlying event are simulated using **PYTHIA** 6.428 [62] with the CTEQ6L1[63] PDF sets and the set of tuned parameters known as the “Perugia 2012 tune” [64]. The top-quark mass is assumed to be 172.5 GeV. The **EvtGen** v1.2.0 program [65] is used for the bottom- and charm-hadron decays.

The cross-sections calculated at next-to-next-to-leading order (NNLO) accuracy for $W/Z+\text{jets}$ [66] and at NNLO+NNLL (next-to-next-to-leading-logarithm) accuracy for $t\bar{t}$ production [67] are used to normalise the samples for the optimisation studies, but the final normalisations of these dominant backgrounds are determined by fitting kinematic distributions to the data. For single-top-quark production, cross-sections are taken from Ref. [68].

Diboson processes with one boson decaying hadronically and the other decaying leptonically are simulated using the **SHERPA** 2.1.1 generator. They are calculated for up to one (ZZ) or no (WW , WZ) additional partons at NLO, and up to three additional partons at LO using the Comix and OpenLoops ME generators. They are merged with the **SHERPA** PS using the ME+PS@NLO prescription. The CT10 PDF set is used in conjunction with a dedicated parton-shower tuning developed by the **SHERPA** authors. Cross-section values from the generator, which are at NLO accuracy, are used.

The dominant background in the fully hadronic final state is from multi-jet events. While the background

in this search is estimated directly from data, samples of simulated dijet events are produced, using PYTHIA 8.186 with the NNPDF23LO PDFs and the parton-shower parameter set known as the “A14 tune” [69], to characterise the invariant mass distribution of the dijet final state and optimise the sensitivity of the search. The EvtGEN v1.2.0 program is used for the bottom- and charm-hadron decays.

All simulated MC samples include the effect of multiple proton–proton interactions in the same and neighbouring bunch crossings (pile-up) by overlaying simulated minimum-bias events, generated with PYTHIA 8.186, on each generated signal or background event. The generated samples are processed through the GEANT4-based ATLAS detector simulation [70, 71]. Simulated events are reconstructed with the standard ATLAS reconstruction software used for collision data. Table 2 summarises the background MC samples used.

Table 2: Generators and PDFs used in the simulation of the various background processes.

Process	PDF	Generator
$W/Z + \text{jets}$	CT10	SHERPA 2.1.1
$t\bar{t}$	CT10	POWHEG BOX v2+PYTHIA 6.428
Single top-quark (Wt , s -channel)	CT10	POWHEG BOX v2+PYTHIA 6.428
Single top-quark (t -channel)	CT104f	POWHEG BOX v1+PYTHIA 6.428 + MADSPIN 2.1.2
Diboson (WW , WZ , ZZ)	CT10	SHERPA 2.1.1
Dijet	NNPDF23LO	PYTHIA 8.186

4 Object reconstruction and selection

Electrons are reconstructed from clusters of energy deposits in the EM calorimeter that match a track reconstructed in the ID. The electrons used are required to have transverse momentum $p_T > 7 \text{ GeV}$ and $|\eta| < 2.47$. They are identified using a likelihood identification criterion described in Ref. [72]. The levels of identification are categorised as “loose”, “medium” and “tight”, which correspond to approximately 96%, 94% and 88% identification efficiency for an electron with transverse energy (E_T) of 100 GeV, where E_T is defined in terms of the energy E and of the polar angle θ as $E_T = E \sin \theta$.

Muons are reconstructed by combining ID and MS tracks. They are classified as “medium” if they satisfy identification requirements based on the number of hits in the different ID and MS subsystems and on the compatibility of track curvature measurements in the two subsystems [73]. An additional sample of “loose” muons is constructed including all medium muons, muons identified by combining an ID track with at least one track segment reconstructed in the MS, and muons reconstructed in the $|\eta| < 0.1$ region, where the MS is lacking coverage, by associating an ID track to an energy deposit in the calorimeters compatible with a minimum-ionising particle. Muons are required to have $p_T > 7 \text{ GeV}$ and $|\eta| < 2.7$. The loose and medium muons have average efficiencies of about 98% and 96% for $|\eta| < 2.5$, respectively.

In order to ensure that leptons originate from the interaction point, requirements of $|d_0^{\text{BL}}|/\sigma_{d_0^{\text{BL}}} < 5(3)$ and $|z_0^{\text{BL}} \sin \theta| < 0.5 \text{ mm}$ are imposed on the tracks associated with the electrons (muons), where d_0^{BL} is the transverse impact parameter of the track with respect to the measured beam line (BL) position determined at the point of closest approach of the track to the beam line, $\sigma_{d_0^{\text{BL}}}$ is the uncertainty in the measured d_0^{BL} , z_0^{BL} is the difference between the longitudinal position of the track along the beam line

at the point where d_0^{BL} is measured and the longitudinal position of the primary interaction vertex,³ and θ is the polar angle of the track. Lepton isolation criteria are defined based on low values for the scalar sum of transverse momenta of tracks with $p_T > 1 \text{ GeV}$ within a ΔR cone around the lepton, whose size depends upon its p_T , and excluding the track associated with the lepton (*track isolation*). These criteria are optimised for a uniform efficiency of 99% in the (p_T, η) plane for leptons from $Z \rightarrow \ell\ell$ decays in $Z + \text{jets}$ events. Calorimeter isolation is also used for the $\ell\nu qq$ channel, using an isolation variable constructed from calorimeter activity within a cone of radius $\Delta R = 0.2$ around the lepton candidate. The isolation criteria depend on both p_T and η , and accept 95% of $Z \rightarrow \ell\ell$ events while maximising the rejection of leptons originating in jets.

Jets are reconstructed from three-dimensional topological clusters of energy deposits in the calorimeter calibrated at the EM scale [74], using the anti- k_t algorithm [75] with two different radius parameters of $R = 1.0$ and $R = 0.4$, hereafter referred to as large- R jets (denoted by “ J ”) and small- R jets (denoted by “ j ”), respectively. The four-momenta of the jets are calculated as the sum of the four-momenta of the clusters, which are assumed to be massless.

The p_T of small- R jets are corrected for losses in passive material, the non-compensating response of the calorimeter, and contributions from pile-up [76]. They are required to have $p_T > 20 \text{ GeV}$ and $|\eta| < 2.4$. For small- R jets with $p_T < 50 \text{ GeV}$, a jet vertex tagger (JVT) [77] discriminant, based on tracking and vertexing information, is required to be larger than 0.64, where the JVT is a multivariate tagger used to identify and remove jets with a large contribution from pile-up. In addition, small- R jets are discarded if they are within a cone of size $\Delta R < 0.2$ around an electron candidate, or if they have less than three associated tracks and are within a cone of size $\Delta R < 0.2$ around a muon candidate. However, if a small- R jet with three or more associated tracks is within a cone of size $\Delta R < 0.4$ around a muon candidate, or any small- R jet is within a region $0.2 < \Delta R < 0.4$ around an electron candidate, the corresponding electron or muon candidate is discarded. Small- R track-jets are defined by applying the same jet reconstruction algorithms to inner-detector tracks treated as having the pion mass, and used to avoid overlap between $qqqq$ sideband regions and searches for Higgs boson pair production, as discussed in Section 6.

For the large- R jets, the original constituents are calibrated using the local cluster weighting algorithm [78] and reclustered using the k_\perp algorithm [79] with a radius parameter of $R_{\text{sub-jet}} = 0.2$, to form a collection of sub-jets. A sub-jet is discarded if it carries less than 5% of the p_T of the original jet. The constituents in the remaining sub-jets are then used to recalculate the large- R jet four-momentum, and the jet energy and mass are further calibrated to particle level using correction factors derived from simulation [80]. The resulting “trimmed”[81] large- R jets are required to have $p_T > 200 \text{ GeV}$ and $|\eta| < 2.0$. Large- R jets are required to have an angular separation of $\Delta R > 1.0$ from electron candidates.

The large- R jets are used to reconstruct the hadronically decaying W/Z (“ V ”) boson. A boson tagger [14, 15, 82, 83] is subsequently used to distinguish the boosted hadronically decaying V boson from jets originating from quarks (other than the top-quark) or gluons. The tagger is based on the mass of the jet m_J and a variable $D_2^{(\beta=1)}$, defined in Ref. [82], that is sensitive to the compatibility of the large- R jet with a two-prong decay topology. The large- R jet is identified by the boson tagger as a W (Z) candidate with its mass within 15 GeV of the expected W (Z) mass peak, which is estimated from simulated events to be 83.2 GeV (93.4 GeV). Large- R jets with mass within 15 GeV from both the W and Z peaks are assigned both hypotheses. For context, the resolution ranges from 8 GeV to 15 GeV in the jet p_T range used in the analysis. Additionally, a p_T -dependent selection on the $D_2^{(\beta=1)}$ variable is configured so that

³ If more than one vertex is reconstructed, the one with the highest sum of p_T^2 of the associated tracks is regarded as the primary vertex.

the average identification efficiency for longitudinally polarised, hadronically decaying W or Z bosons is 50%. This selection rejects more than 90% of the background. Large- R track-jets are defined by applying the same jet reconstruction and filtering algorithms to inner-detector tracks treated as having the pion mass. These jets are ghost-associated to large- R jets and used for the evaluation of systematic uncertainties, as discussed in Section 7.

Small- R jets and small- R track-jets containing b -hadrons are identified using the MV2 b -tagging algorithm [84], which has an efficiency of 85% in simulated $t\bar{t}$ events. The jets thus selected are referred to as b -jets in the following. The corresponding misidentification rate for selecting b -jet candidates originating from a light quark or gluon is less than 1%. The misidentification rate for selecting c -jets as b -jet candidates is approximately 17%.

The missing transverse momentum, $\mathbf{E}_T^{\text{miss}}$, with magnitude E_T^{miss} , is calculated as the negative vectorial sum of the transverse momenta of calibrated objects, such as electrons, muons, and small- R jets. Charged-particle tracks compatible with the primary vertex and not matched to any of those objects are also included in the $\mathbf{E}_T^{\text{miss}}$ reconstruction [85, 86]. For multi-jet background rejection, a similar quantity, $\mathbf{p}_T^{\text{miss}}$, is computed using only charged-particle tracks originating from the reconstructed primary vertex to substitute for the calorimeter-based measurements of jet four-momenta. Its magnitude is denoted by p_T^{miss} . Both tiers of the ATLAS trigger system also reconstruct E_T^{miss} . The triggers used in this paper reconstruct E_T^{miss} based on calorimeter information, and do not include corrections for muons.

The identification efficiency, energy scale, and resolution of jets, leptons and b -jets are measured in data and correction factors are derived, which are applied to the simulation to improve the modelling of the data.

5 Event selection

This analysis focuses on identifying diboson events in which at least one vector boson V decays hadronically, and is performed in four different channels identified by the decay of the other vector boson: $qqqq$, $vvqq$, ℓvqq and $\ell\ell qq$. Event selection criteria are chosen to guarantee the statistical independence of the channels. The criteria are summarised in Table 3, and described in more detail below.

Events are selected at trigger level by requiring at least one large- R jet with $p_T > 360$ GeV in the $qqqq$ channel, large E_T^{miss} in the $vvqq$ channel, large E_T^{miss} or at least one electron in the ℓvqq channel, and at least one electron or muon in the $\ell\ell qq$ channel. All trigger requirements guarantee full efficiency in the kinematic region considered in the analysis. A primary vertex is required to be reconstructed from at least three charged-particle tracks with $p_T > 400$ MeV.

At least one large- R jet is required, with $p_T > 200$ GeV, $|\eta| < 2.0$ and $m_J > 50$ GeV. Events are then divided by different pre-selection criteria into different channels according to the number of “baseline” and “good” leptons that are reconstructed. A baseline lepton is a loose muon or electron candidate with $p_T > 7$ GeV and $|\eta| < 2.7$ or $|\eta| < 2.47$, respectively, which passes a relaxed set of track-isolation and impact parameter requirements. A good lepton has $p_T > 25$ GeV and is either a muon with $|\eta| < 2.5$, or an electron with $|\eta| < 2.47$ excluding the transition region between barrel and endcap calorimeters ($1.37 < |\eta| < 1.52$), which passes identification and isolation requirements as discussed in Sec. 4.

Events with no reconstructed baseline lepton and with $E_T^{\text{miss}} > 250$ GeV are assigned to the $vvqq$ channel. Events are assigned to the $qqqq$ channel if they have no good leptons, $E_T^{\text{miss}} < 250$ GeV, an additional

large- R jet meeting the same selection criteria as the other large- R jet, and if the large- R jet with leading p_T satisfies a requirement of $p_T > 450$ GeV to ensure full trigger efficiency. Events with exactly one good lepton which satisfies tight track and calorimeter isolation requirements, and which is either a medium muon or tight electron, or a medium electron with $p_T > 300$ GeV, are assigned to the $\ell\nu qq$ channel. Events with exactly two same-flavour good leptons where one meets medium selection criteria, the invariant mass of the dilepton system passes a Z boson mass window selection of $83 < m_{ee}/\text{GeV} < 99$ or $66 < m_{\mu\mu}/\text{GeV} < 116$, and, in the case of muons, the two leptons are oppositely charged, are assigned to the $\ell\ell qq$ channel.

Additional event topology requirements are applied to pre-selected events in order to suppress backgrounds. In the $\nu\nu qq$ channel, contributions from non-collision backgrounds and multi-jet production are suppressed by requiring $p_T^{\text{miss}} > 30$ GeV, $|\Delta\phi(\mathbf{E}_T^{\text{miss}}, \mathbf{p}_T^{\text{miss}})| < \pi/2$ and by requiring that the minimum azimuthal separation between $\mathbf{E}_T^{\text{miss}}$ and any small- R jet is greater than 0.6.

In the $qqqq$ channel, the separation in rapidity between the two large- R jets, $|y_{J_1} - y_{J_2}|$, is required to be below 1.2, and their transverse momentum asymmetry, $(p_{T,J_1} - p_{T,J_2})/(p_{T,J_1} + p_{T,J_2})$, is required to be below 0.15. To further reduce the multi-jet background, large- R jets are required to have $N_{\text{trk}} < 30$ charged-particle tracks with $p_T > 500$ MeV, where the tracks must be consistent with the primary vertex and be matched to the calorimeter jet [87]. The matching is made prior to trimming, and is determined by representing each track by a collinear “ghost” constituent with negligible energy during jet reconstruction (“ghost association”).

In the $\ell\nu qq$ channel, events are required to have no small- R jet identified as a b -jet outside a cone of radius $\Delta R = 1.0$ around the selected large- R jet to reject backgrounds from $t\bar{t}$ production, and to have $E_T^{\text{miss}} > 100$ GeV in order to reject multi-jet background. The leptonically decaying W candidate is required to have $p_{T,\ell\nu} > 200$ GeV, where the neutrino is assigned transverse momentum $\mathbf{E}_T^{\text{miss}}$ and its momentum along the z -axis, p_z , is obtained by imposing a W boson mass constraint to the $\ell-\mathbf{E}_T^{\text{miss}}$ system.⁴ A new resonance with mass $m_{\ell\nu J}$ decaying into two bosons, both at fairly central rapidity, would often impart significant transverse momentum to the bosons relative to the resonance mass. The p_T of the two vector-boson candidates is therefore required to have $p_{T,J}/m_{\ell\nu J} > 0.4$ and $p_{T,\ell\nu}/m_{\ell\nu J} > 0.4$. In the $\ell\ell qq$ channel, similar requirements on the p_T of the two vector-boson candidates are applied, namely $p_{T,J}/m_{\ell\ell J} > 0.4$ and $p_{T,\ell\ell}/m_{\ell\ell J} > 0.4$.

Events are classified as WW , WZ , or ZZ by applying the corresponding selection criteria to the two boson candidates. If the number of boson-tagged jets exceeds the number of hadronically decaying bosons required by the decay channel, the leading- p_T jets are used. The final discrimination between resonant signal and backgrounds is done in a one-dimensional distribution either of mass or of transverse mass. In the $qqqq$ channel, the invariant mass of the jet pair, m_{JJ} , is used in the fiducial region $1 \text{ TeV} < m_{JJ} < 3.5 \text{ TeV}$ whose lower bound is chosen to guarantee full trigger efficiency. In the $\nu\nu qq$ channel, the transverse mass of the $J - \mathbf{E}_T^{\text{miss}}$ system, $m_T = \sqrt{(E_{T,J} + E_T^{\text{miss}})^2 - (\mathbf{p}_{T,J} + \mathbf{E}_T^{\text{miss}})^2}$ is used. In the $\ell\nu qq$ channel, $m_{\ell\nu J}$ is used. In the $\ell\ell qq$ channel, the p_T of the dilepton system is scaled event-by-event by a single multiplicative factor to set the dilepton invariant mass $m_{\ell\ell}$ to the mass of the Z boson (m_Z) in order to improve the diboson mass resolution. The invariant mass $m_{\ell\ell J}$ is used as the discriminant.

Table 3 shows a summary of the event selection criteria in the four channels. The combined acceptance times efficiency for a heavy resonance decaying to dibosons is as large as 18% for $W' \rightarrow WZ$ and also for

⁴ The longitudinal momentum p_z is taken to be the smaller in absolute value of the two solutions of the resulting quadratic equation. If a complex value is obtained, the real component is chosen.

Table 3: Event selection criteria in the four analysis channels. Baseline and good leptons are defined in the text.

Selection level	Channel			
	$qqqq$	$vvqq$	$\ell\nu qq$	$\ell\ell qq$
Trigger	Large-R jet, $p_T > 360$ GeV	E_T^{miss}	$E_T^{\text{miss}}(\mu\nu qq)$ or single electron ($e\nu qq$)	single electron or muon
Large-R jet	$\geq 2, N_{\text{trk}} < 30,$ $p_{T,J_1} > 450$ GeV, $p_{T,J_2} > 200$ GeV		$\geq 1,$ $p_{T,J} > 200$ GeV	
<i>Baseline leptons</i>	0	0	≥ 1	≥ 2
<i>Good leptons</i>	0	0	1 medium μ or tight [†] e	2 e or 2 μ , loose + medium
Topology	$E_T^{\text{miss}} < 250$ GeV, $ y_{J_1} - y_{J_2} < 1.2,$ $\frac{p_{T,J_1} - p_{T,J_2}}{p_{T,J_1} + p_{T,J_2}} < 0.15$	$E_T^{\text{miss}} > 250$ GeV, $p_T^{\text{miss}} > 30$ GeV, $ \Delta\phi(\mathbf{E}_T^{\text{miss}}, p_T^{\text{miss}}) < \frac{\pi}{2},$ $ \Delta\phi(\mathbf{E}_T^{\text{miss}}, j) > 0.6$	no b -jet with $\Delta R(j, J) < 1.0,$ $E_T^{\text{miss}} > 100$ GeV, $p_{T,\ell\nu} > 200$ GeV, $p_{T,J}/m_{\ell\nu J} > 0.4,$ $p_{T,\ell\nu}/m_{\ell\nu J} > 0.4$	$p_{T,J}/m_{\ell\ell J} > 0.4,$ $p_{T,\ell\ell}/m_{\ell\ell J} > 0.4,$ $83 < m_{ee}/\text{GeV} < 99,$ $66 < m_{\mu\mu}/\text{GeV} < 116$
Discriminant	m_{JJ}	m_T	$m_{\ell\nu J}$	$m_{\ell\ell J}$

[†] The electron, if over 300 GeV in p_T , need only be medium.

$Z' \rightarrow WW$ in the HVT model-A benchmark assuming $g_V = 1$. In the bulk RS benchmark with $\kappa/\bar{M}_{\text{Pl}} = 1$, it reaches up to 17% for $G^* \rightarrow WW$, and 14% for $G^* \rightarrow ZZ$. The acceptance times efficiency is estimated with respect to the branching ratio of the signal benchmarks to the specific diboson final state and takes into account the W and Z boson branching ratios. Figure 1 summarises the acceptance times efficiency for the different channels as a function of the scalar, HVT, and G^* masses, considering only decays of the resonance into VV . The mass ranges used in the different channels are reflected in the figure. After all selection criteria are applied, reconstructed diboson mass resolutions for a W' with a mass of 2 TeV, decaying to WZ , are 3% for $\ell\ell qq$, 5.5% for $\ell\nu qq$, and 6% for $qqqq$.

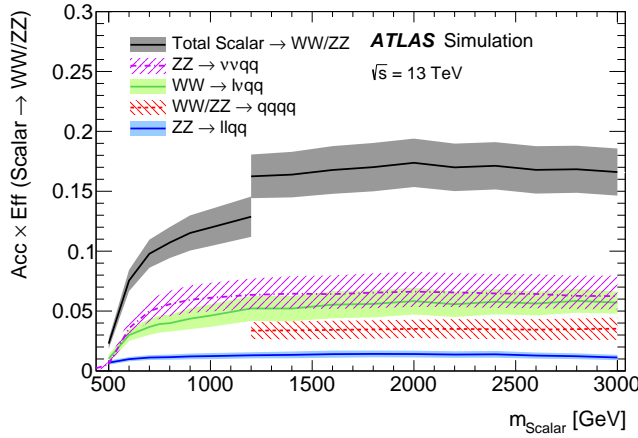
6 Background estimation

The background contamination in the signal regions is different for each of the channels studied. Different background estimation strategies are used for the fully hadronic and semileptonic channels.

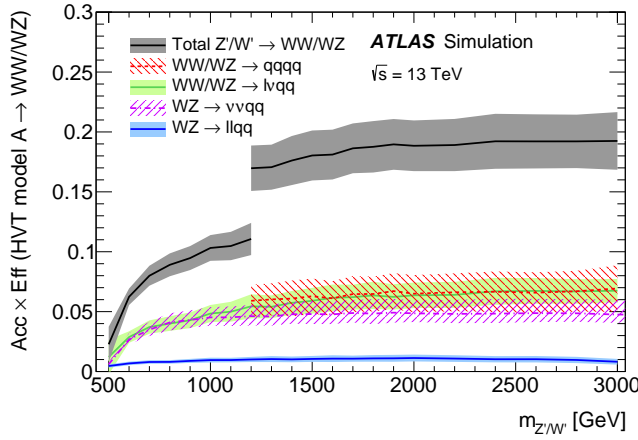
In the $qqqq$ channel, the dominant background originates from multi-jet events, with significantly smaller contributions due to SM $W/Z + \text{jet}$, diboson, $t\bar{t}$ and single-top-quark production. As all of these processes are expected to produce a smoothly falling m_{JJ} spectrum, the overall background is modelled in terms of a probability density function

$$f(x) = N(1 - x)^{p_2 + \xi p_3} x^{p_3}, \quad (1)$$

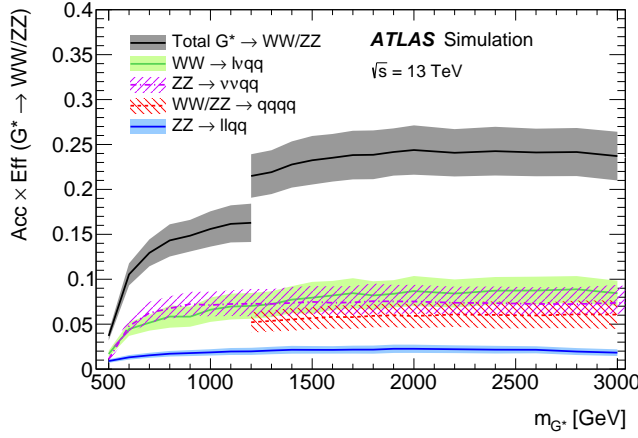
where $x = m_{JJ}/\sqrt{s}$, p_2 and p_3 are dimensionless shape parameters, ξ is a constant whose value is chosen to minimise the correlation between p_2 and p_3 , and N is an overall normalisation factor. The functional form in Eq. (1) is validated using background simulation and validation regions in data, defined to be similar to the signal region but with a few differences. Instead of selecting events where the mass of the large- R jet is consistent with the mass of the W or Z boson, events are selected to have a large- R jet with a mass in the sideband regions, 110–140 GeV or 50–65 GeV, and without applying the requirement on the track multiplicity. Specifically, it is required that either both jets have a mass in the range 110–140 GeV and there are less than two b -tagged track-jets matched by ghost-association to either jet, or that one jet has a mass in the range 110–140 GeV and the other in the range 50–65 GeV. These regions are defined



(a)



(b)



(c)

Figure 1: Signal acceptance times efficiency as a function of the resonance mass, for the different channels contributing to the searches for (a) a scalar resonance decaying to WW and ZZ , (b) HVT decaying to WW and WZ and (c) bulk RS gravitons decaying to WW and ZZ . The branching ratio of the new resonance decaying to dibosons is included in the denominator of the efficiency calculation. The coloured bands represent the total statistical and systematic uncertainties. In the case of the $qqqq$ channel, only signals with resonance masses beyond 1.2 TeV, for which the mass peak is fully reconstructed in the fiducial m_{JJ} region, are considered.

such that the kinematic properties of the selected events are similar to the signal region, and overlap with searches for Higgs boson pair production is avoided.

In the $vvqq$ channel, the dominant background is $Z + \text{jets}$ production with significant contributions from $W + \text{jets}$, tt , and SM diboson production. In the ℓvqq channel, the dominant backgrounds are $W + \text{jets}$ and tt production. In the $\ell\ell qq$ channel, where two same-flavour leptons with an invariant mass close to the Z mass are selected, $Z + \text{jets}$ production is by far the dominant background. All three channels also have contributions at the level of a few percent from single-top-quark and diboson production. The single-top-quark process contributes 15% of the total top-quark background in the ℓvqq channel, 10% in the $vvqq$, and a negligible amount for the $\ell\ell qq$ channel. The multi-jet background enters the signal regions of the semileptonic channels through semileptonic hadron decays and through jets misidentified as leptons, and this background is found to be negligibly small in all three channels.

In the $vvqq$, ℓvqq , and $\ell\ell qq$ channels, the modelling of $W/Z+\text{jets}$ backgrounds is constrained using dedicated control regions. A region enriched in $W + \text{jets}$ events is used to control the $W + \text{jets}$ background normalisation in the $vvqq$ and ℓvqq channels; events in this region are required to fall in the sidebands of the m_J distribution and to have one reconstructed good muon. A region enriched in $Z + \text{jets}$ events is used to control the $Z + \text{jets}$ backgrounds in the $vvqq$ and $\ell\ell qq$ channels; events in this region are also required to fall in the sidebands of the m_J distribution, but to have two reconstructed good leptons.

The tt background is estimated in the $vvqq$ and ℓvqq channels using a control region enriched in top-quark pairs. This control region is defined as the $W + \text{jets}$ control region, without the m_J sideband criterion and with the added requirement of at least one additional b -jet with a separation $\Delta R > 1$ from the large- R jet. The tt background for the $\ell\ell qq$ channel is estimated from MC simulation.

The W , Z and tt control regions are included in the combined profile likelihood fit described in Section 8 to help constrain the $W+\text{jets}$, $Z+\text{jets}$ and tt normalisation in the signal regions.

The diboson contributions to the $vvqq$, ℓvqq and $\ell\ell qq$ channels are estimated using MC simulation. Single-top-quark production is constrained by the tt control region using the same normalisation factor as for tt .

7 Systematic uncertainties

The most important sources of systematic uncertainty are those related to the energy scale and resolution of the large- R jet p_T , mass, and $D_2^{(\beta=1)}$. The systematic uncertainties related to the scales of the large- R jet p_T , mass and $D_2^{(\beta=1)}$ are extracted following the technique described in Ref. [80]. Track-jets are geometrically matched to calorimeter jets, and for each observable of interest, e.g. p_T , mass, or $D_2^{(\beta=1)}$, a systematic uncertainty is estimated from the comparison of the ratio of the matched track-jet observable to the calorimeter-jet observable between simulation and data. For the jet p_T and mass, $\sqrt{s} = 13$ TeV data and simulation are used. For $D_2^{(\beta=1)}$, $\sqrt{s} = 8$ TeV simulation and data are used, and an additional uncertainty is added to account for the differences between 8 TeV and 13 TeV [14]. The uncertainties in the large- R jet p_T , mass, and $D_2^{(\beta=1)}$ scale are 5%, 6% and 10%, respectively.

The resolution of each of these large- R jet observables is determined as the standard deviation of a Gaussian fit to the distribution of the observable response defined as the ratio of the calorimeter-jet observable to a simulated-particle-level jet observable. The relative uncertainties in these resolutions are estimated based on previous studies with $\sqrt{s} = 7$ TeV data and $\sqrt{s} = 13$ TeV simulation. For the large- R jet p_T [80]

and mass resolution a 20% uncertainty is assigned, while for the $D_2^{(\beta=1)}$ resolution a 10% uncertainty is assigned. The large- R jet mass resolution uncertainty is estimated from variations in data and simulation in the widths of the W -jet mass peaks in $t\bar{t}$ events [80]. The $D_2^{(\beta=1)}$ resolution uncertainty is estimated by comparing 13 TeV simulation samples from different generators and shower simulations [14].

Other subdominant experimental systematic uncertainties include those in the lepton energy and momentum scales, in lepton identification efficiency, in the efficiency of the trigger requirements, and in the small- R jet energy scale and resolution. All experimental systematic uncertainties are treated as fully correlated among all channels.

Uncertainties are also taken into account for possible differences between data and the simulation model that is used for each process.

In the $vvqq$ channel, an uncertainty on the shape of the m_T spectrum for the $W + \text{jets}$ and $Z + \text{jets}$ backgrounds is extracted by comparing the nominal shape obtained with **SHERPA** to the one obtained with an alternative sample generated with **MADGRAPH5_AMC@NLO**.

In the ℓvqq channel, an uncertainty on the shape of the $m_{\ell\nu J}$ distribution of the dominant $W + \text{jets}$ background is obtained by comparing the $m_{\ell\nu J}$ shape in simulation and in data in the $W + \text{jets}$ control region after the expected $t\bar{t}$ and diboson contributions are subtracted. The ratio of the data distribution to that predicted by MC is fitted with a first-order polynomial and its deviation from unity is used as a modelling uncertainty.

In the $\ell\ell qq$ channel, an uncertainty on the shape of the $m_{\ell\ell J}$ spectrum for the $Z + \text{jets}$ background is assessed by comparing the shape difference between the **SHERPA** predictions and the data-driven estimate using events in the Z control region.

The data and simulation agree very well for events in the top-quark control region. The uncertainty in the shape of the mass distributions for the $vvqq$, ℓvqq and $\ell\ell qq$ channels from the $t\bar{t}$ background is estimated by comparing a sample generated using **aMC@NLO** [52] interfaced with **Pythia** 8.186 to the nominal $t\bar{t}$ sample. Additional systematic uncertainties in parton showering and hadronisation are evaluated by comparing the nominal sample showered with **Pythia** to one showered with **Herwig** [88]. Samples of $t\bar{t}$ events generated with the factorisation and renormalisation scales doubled or halved are compared to the nominal sample, and the largest difference observed in the mass discriminants is taken as an additional uncertainty arising from the QCD scale uncertainty.

Theoretical uncertainties in the SM diboson production cross-section, including the effect of PDF and scale uncertainties, are taken into account and amount to about 10% [89]. An uncertainty in the shape of the predicted diboson $m_{\ell\ell J}$ spectrum in the $\ell\ell qq$ channel is derived by comparing MC samples generated by **SHERPA** and **POWHEG BOX**. Shape uncertainties are found to have negligible impact in the $vvqq$ and ℓvqq channels.

The uncertainties in the modelling of the $Z + \text{jets}$ and $W + \text{jets}$ backgrounds are treated as uncorrelated since they are evaluated differently in each channel. For the $t\bar{t}$ background, the modelling uncertainty is treated as correlated between the ℓvqq and $\ell\ell qq$ channels, and uncorrelated with the modelling uncertainty in the $vvqq$ channel. The diboson normalisation uncertainty is taken as correlated among the $vvqq$, ℓvqq and $\ell\ell qq$ channels.

Uncertainties in the signal acceptance arise from the choice of PDF and from the amount of initial- and final-state radiation present in simulated signal events. The PDF-induced uncertainties in the signal acceptance for semileptonic decay channels are derived using the **PDF4LHC** recommendations [90]; in

all channels the resulting uncertainty is at most 4%. PDF-induced uncertainties are not evaluated for the $qqqq$ channel, where they are subdominant to other acceptance effects. The uncertainty in the integrated luminosity has an impact of 5% on the signal normalisation. All signal acceptance uncertainties are treated as fully correlated across all search channels.

The uncertainty in modelling background distribution shapes in the $qqqq$ channel is found to be negligible compared to statistical uncertainties in the background fit parameters. An additional uncertainty in the signal normalisation is introduced in the $qqqq$ channel to take into account potentially different efficiencies of the $N_{\text{trk}} < 30$ requirement in data and simulation. This uncertainty is estimated in a data control sample enriched in $W/Z+\text{jets}$ events, where the W/Z bosons decay to quarks. This control sample is obtained by applying the $D_2^{(\beta=1)}$ selection only to the highest- p_T large- R jet in dijet events. The m_J distribution is fitted in subsamples with different track multiplicity selections to obtain the rates of W/Z decays in each sample. From these the uncertainty from the track multiplicity cut is estimated to be 6%.

For all the considered signal hypotheses, the impact of each source of uncertainty on the search is evaluated in terms of the corresponding contribution to the total uncertainty in the fitted number of signal events, as obtained after the statistical procedure described in the next section. The dominant contribution is due to large- R jet scale uncertainties and amounts to about 35% of the total uncertainty. Additional contributions are due to uncertainties in the modelling and normalisation of backgrounds in the $vvqq$, ℓvqq and $\ell \ell qq$ channels (about 20%), and small- R jet energy scale uncertainties (about 10%). Sub-leading contributions have an overall impact of less than about 15%.

8 Statistical analysis

In the combined analysis to search for a scalar resonance decaying to WW or ZZ , HVT decaying to WW or WZ , and bulk G^* decaying to WW or ZZ , all four individual channels are used. Table 4 summarises the signal region and mass range in which the individual channels contribute to the search.

Table 4: Channels, signal regions and mass ranges where the channels contribute to the search.

Channel	Signal region (selection)	Scalar mass range [TeV]	HVT W' and Z' mass range [TeV]	G^* mass range [TeV]
$qqqq$	$WW + ZZ$	1.2–3.0	–	1.2–3.0
	$WW + WZ$	–	1.2–3.0	–
$vvqq$	WZ	–	0.5–3.0	–
	ZZ	0.5–3.0	–	0.5–3.0
ℓvqq	$WW + WZ$	–	0.5–3.0	–
	WW	0.5–3.0	–	0.5–3.0
$\ell \ell qq$	WZ	–	0.5–3.0	–
	ZZ	0.5–3.0	–	0.5–3.0

The statistical interpretation of these results uses the data modelling and handling toolkits RooFit [91], RooStats [92] and HistFactory [93]. It proceeds by defining the likelihood function $L(\mu, \vec{\theta})$ for a particular model, with an implicit signal description, in terms of the signal strength μ , and the additional set of

nuisance parameters $\vec{\theta}$ which can be related to both background and signal. The likelihood function is computed considering in each channel bins of the discriminating variable; the binning is chosen based on the expected mass resolution and statistical uncertainty, as estimated from simulation. The nuisance parameters are either free to float, as in the case of the p_2 and p_3 parameters used in the $qqqq$ channel to estimate the background, or constrained from external studies represented by Gaussian terms. The likelihood for the combination of the four search channels is the product of the Poisson likelihoods for the individual channels, except in the case of common nuisance parameters,

$$L(\mu, \vec{\theta}) = \prod_c \prod_i \text{Pois}\left(n_{c_i}^{\text{obs}} | n_{c_i}^{\text{sig}}(\mu, \vec{\theta}) + n_{c_i}^{\text{bkg}}(\vec{\theta})\right) \prod_k f_k(\theta'_k | \theta_k). \quad (2)$$

The terms $n_{c_i}^{\text{obs}}$ represent the number of events observed, and the terms $n_{c_i}^{\text{sig}}$, $n_{c_i}^{\text{bkg}}$, the number of events expected from signal or background in bin i of the discriminant from channel c . The term $f_k(\theta'_k | \theta_k)$ represents the set of constraints on $\vec{\theta}$ from auxiliary measurements θ'_k : these constraints include normalisation and shape uncertainties in the signal and background models, and, except for the $qqqq$ channel, include the statistical uncertainties of the simulated bin content. The $W + \text{jets}$ normalisation is a free parameter in the combined likelihood fit in all the channels. The normalisation of the $Z + \text{jets}$ background in the $\ell\ell qq$ and $vvqq$ channels is a free parameter in the combined likelihood fit. In the ℓvqq channel, where the contribution from $Z + \text{jets}$ is small, the normalisation obtained from MC simulation is used instead, with an 11% systematic uncertainty assigned. The $t\bar{t}$ normalisation in the ℓvqq and $vvqq$ channels is a free parameter in the combined likelihood fit. In the $\ell\ell qq$ channel, where the $t\bar{t}$ background contribution is small, its normalisation is based on the theoretical cross-section with a 10% systematic uncertainty assigned.

The likelihood function $L(\mu, \vec{\theta})$ is used to construct the profile-likelihood-ratio test statistic [94], defined as:

$$t = -2 \ln \lambda(\mu) = -2 \ln \left(\frac{L(\mu, \hat{\vec{\theta}}(\mu))}{L(\hat{\mu}, \hat{\vec{\theta}})} \right), \quad (3)$$

where $\hat{\mu}$ and $\hat{\vec{\theta}}$ are the values of the parameters that maximise the likelihood function $L(\mu, \vec{\theta})$ globally, and $\hat{\vec{\theta}}(\mu)$ are the values of $\vec{\theta}$ which maximise the likelihood function given a certain value of μ . The parameter $\hat{\mu}$ is required to be non-negative. This test statistic is used to derive the statistical results of the analysis.

For calculating p -values, which test the compatibility of the data with the background-only model, the numerator of Eq. (3) is evaluated for the background-only hypothesis, i.e. signal strength $\mu = 0$. In extracting upper limits, the calculation is modified such that if $\hat{\mu} > \mu$, $\lambda(\mu)$ is taken to be 1; this ensures that a signal larger than expected is not taken as evidence against a model. The asymptotic distributions of the above test statistic are known and described in Ref. [95], and this methodology is used to obtain the results in this paper.

Upper limits on the production cross-section times branching ratio to diboson final states for the benchmark signals are set using the modified-frequentist CL_s prescription [96], where the probability of observing λ to be larger than a particular value, is calculated using a one-sided profile likelihood. The calculations are done using the lowest-order asymptotic approximation, which was validated to better than 10% accuracy using pseudo-experiments. All limits are set at the 95% confidence level (CL).

Table 5: Expected and observed yields in signal and control regions for the $W' \rightarrow WZ$ signal hypothesis. Yields and uncertainties are evaluated after a background-only fit to the data. The background for the $qqqq$ channel is evaluated *in situ* and only the total background yield is indicated. The $W+jets$ background for the $Z+jets$ control region and the $\ell\ell qq$ signal region is negligible. The uncertainty in the total background estimate can be smaller than the sum in quadrature of the individual background contributions due to anti-correlations between the estimates of different background sources.

	Control Regions			Signal Regions			
	$W+jets$	$Z+jets$	tt	$vvqq$	$\ell\ell qq$	ℓvqq	$qqqq$
SM Diboson	53 ± 8	15 ± 4	12 ± 3	70 ± 8	12 ± 2	64 ± 9	
tt , single- t	325 ± 49	1.4 ± 0.8	780 ± 34	170 ± 15	1.2 ± 0.9	230 ± 31	
$Z+jets$	17 ± 3	387 ± 19	2.5 ± 0.7	385 ± 24	102 ± 7	11 ± 2	
$W+jets$	797 ± 66		54 ± 13	208 ± 23		397 ± 31	
Total Background	1193 ± 31	403 ± 19	849 ± 29	832 ± 26	115 ± 7	702 ± 20	128 ± 11
Observed	1200	406	848	838	109	691	128

9 Results

The background estimation techniques described in Section 6 are applied to the selected data, and the results in the four different analysis channels are shown in Figure 2 for the channels relevant to the HVT (WZ , WW) search and in Figure 3 for those relevant to the scalar resonance and bulk RS $G^* \rightarrow WW, ZZ$ searches, respectively. Both figures represent background-only fits to the data. The total yields in the different signal and control regions for the HVT WZ channel are also shown in Table 5. Good agreement is found between the data and the background-only hypothesis. The most significant excess over the expected background is observed in the scalar selection for a mass of 1.6 TeV, with a p -value equivalent to a local significance of 2.5 standard deviations. Upper limits at the 95% CL are set on the production cross-section times the branching ratio of new resonances decaying to diboson final states.

Figure 4 shows the observed and expected 95% CL model-independent limits on the production cross-section times branching ratio of a narrow-width scalar resonance, as a function of its mass, in the WW and ZZ channels combined. The constraints are compared with the CP-even scalar singlet model described in Section 3, for the NDA and Unsuppressed scenarios. Masses below 2650 GeV are excluded for the Unsuppressed scenario. Figure 5 shows the exclusion contours in the $(c_H/\Lambda, c_3/\Lambda)$ parameter space, derived from the cross-section limits for three sample masses.

Figure 6 shows the observed and expected limits obtained in the search for an HVT decaying to WW or WZ states as a function of the mass of the HVT, compared to the theoretical predictions for the HVT model A assuming $g_V = 1$ and the HVT model-B assuming $g_V = 3$. For HVT model-B, new gauge bosons with masses below 2600 GeV are excluded at the 95% CL. Results are also shown in Figure 7 in terms of exclusion contours in the HVT parameter space $(g^2 c_F/g_V, g_V c_H)$ for different resonance masses [97].

Similarly, in Figure 8 the observed and expected limits obtained in the search for a bulk G^* decaying to WW or ZZ final states are shown and compared to the theoretical prediction for the bulk RS G^* model assuming $\kappa/\bar{M}_{\text{Pl}} = 1$. Bulk RS G^* decaying to WW or ZZ in this model are excluded if their mass is below 1100 GeV.

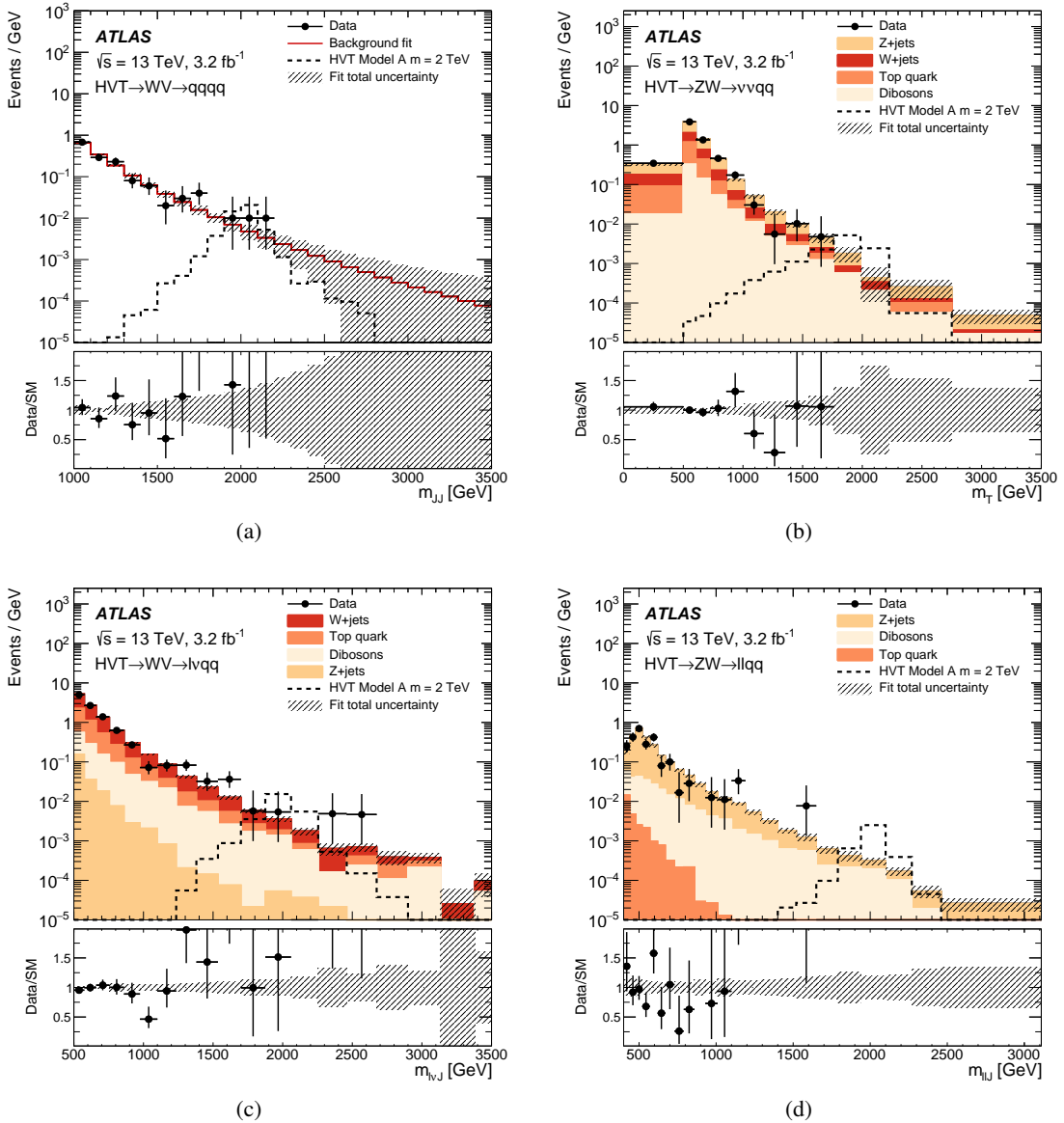


Figure 2: Distribution of the data compared to the background estimate for the analysis discriminant in the signal regions for the HVT search; (a) the m_{JJ} distribution in the $qqqq$ channel, (b) the m_T distribution in the $vvqq$ channel, (c) m_{lvJ} in the $lvqq$ channel, and (d) m_{llJ} in the $llqq$ channel. The “Top quark” distribution includes both the $t\bar{t}$ and single-top-quark backgrounds. The upper panels show the distribution of the observed data and estimated backgrounds as a function of the analysis discriminants. The observed data are shown as points, solid colours represent the different background contributions and the shaded bands reflect the systematic uncertainties in the estimated background. The lower panels show the ratio of the observed data to the estimated background as a function of the analysis discriminant. The decay modes “ WV ” or “ ZW ” indicate the mass requirements placed on the hadronically decaying boson, where a “ W ” or “ Z ” indicates a narrow mass window around the corresponding boson mass, and a “ V ” indicates the wider mass window including both the W and Z boson masses. More details are given in the text.

No combination of these results with those at 8 TeV [31] has been performed. However, the results of the 8 TeV data analysis in the EGM W' model have been used to estimate its sensitivity to the HVT model A,

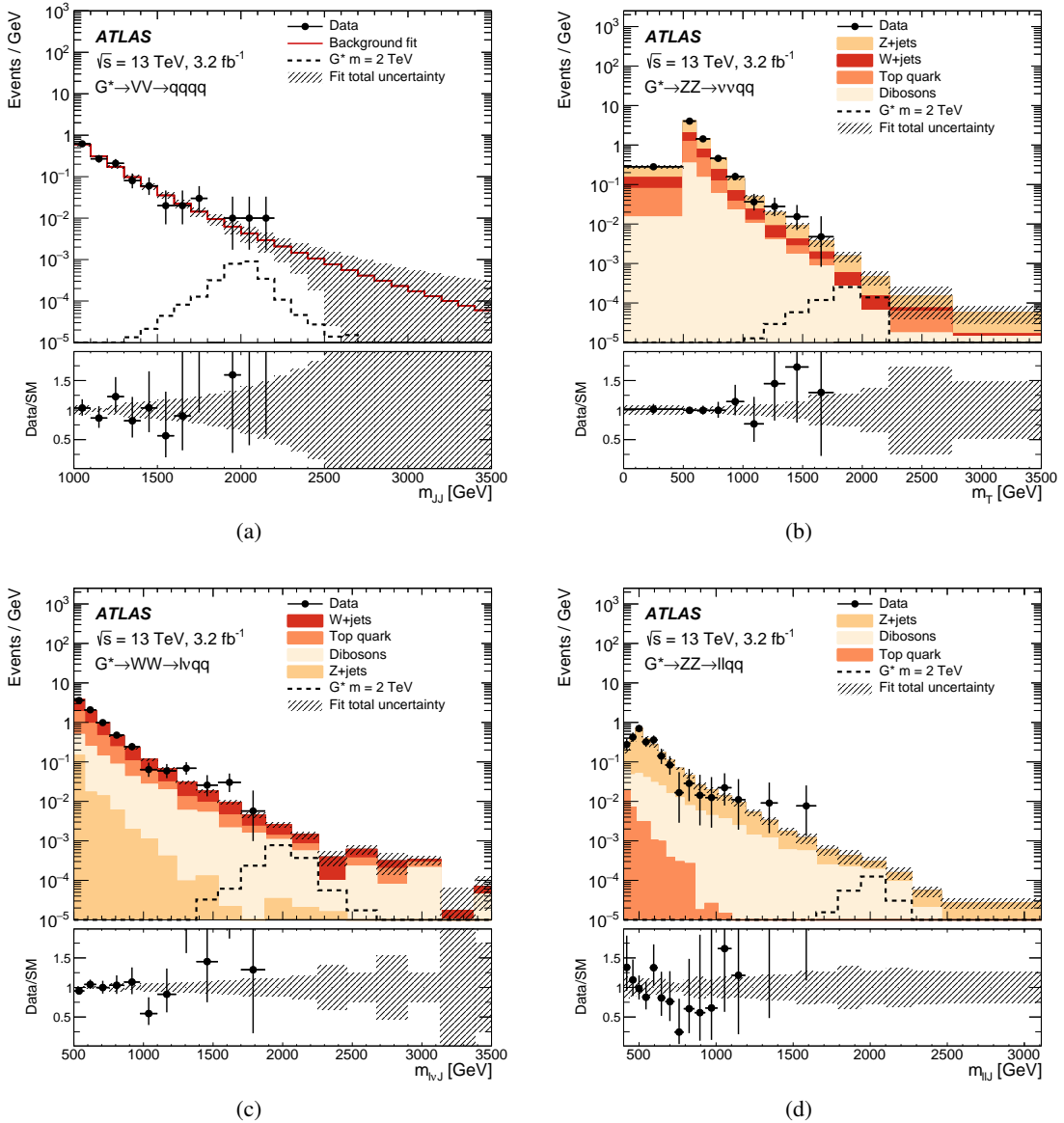


Figure 3: Distribution of the data compared to the background estimate for the analysis discriminant in the signal regions for the scalar and bulk RS G^* searches; (a) the m_{JJ} distribution in the $qqqq$ channel, (b) the m_T distribution in the $vvqq$ channel, (c) $m_{\ell\nu J}$ in the $\ell\nu qq$ channel, and (d) $m_{\ell\ell J}$ in the $\ell\ell qq$ channel. The “Top quark” distribution includes both the $t\bar{t}$ and single-top-quark backgrounds. The upper panels show the distribution of the observed data and estimated backgrounds as a function of the analysis discriminants. The observed data are shown as points, solid colours represent the different background contributions and the shaded bands reflect the systematic uncertainties in the estimated background. The lower panels show the ratio of the observed data to the estimated background as a function of the analysis discriminant. The decay modes “ WW ”, “ ZZ ”, or “ VV ” indicate the mass requirements placed on the hadronically decaying boson, where a “ W ” or “ Z ” indicates a narrow mass window around the corresponding boson mass, and a “ V ” indicates the wider mass window including both the W and Z boson masses. More details are given in the text.

including corrections for the difference in beam energy and the line-shape of the resonance. This study shows that the current analysis is more sensitive to the HVT model A for triplet masses above 1.6 TeV,

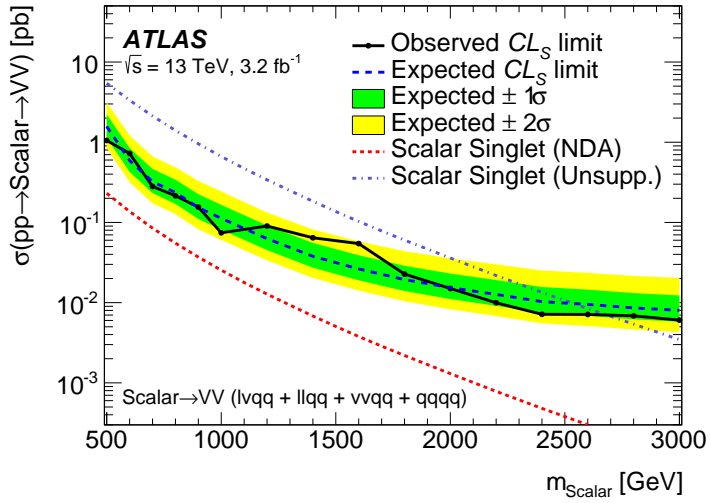


Figure 4: Observed and expected 95% CL limits on the cross-section times branching ratio to diboson final states for a narrow-width scalar resonance, as a function of its mass, combining the WW and ZZ decay modes.

and that the ratio of the expected cross-section limit to the theoretical cross-section improves by a factor two for triplet masses of 2 TeV.

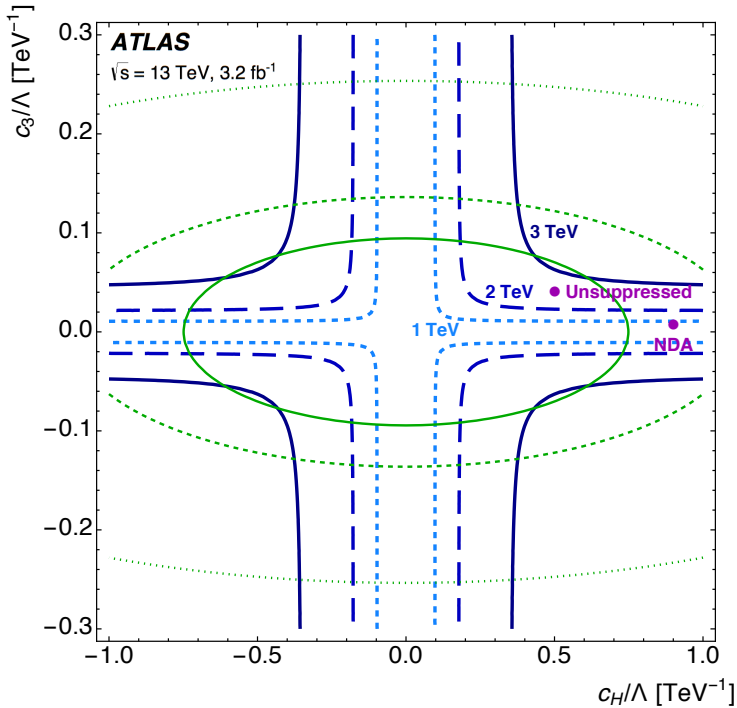


Figure 5: Observed 95% CL exclusion contours in the parameter space $(c_H/\Lambda, c_3/\Lambda)$ for scalar resonances of mass 1 TeV, 2 TeV and 3 TeV. The region inside each green ellipse indicates, for the corresponding assumed mass, the part of the parameter space in which the ratio of the resonance's total width Γ to its mass m is below 5%, which is comparable to the experimental mass resolution. Points inside the ellipse, but where the absolute values of the c_H/Λ and c_3/Λ parameters are larger than at the exclusion contour, are considered to be excluded at a CL greater than 95%. The solid lines correspond to results for a resonance mass of 3 TeV; the long-dashed lines correspond to a resonance mass of 2 TeV; the short-dashed lines correspond to a resonance mass of 1 TeV. Parameters for the Unsuppressed and NDA benchmark models are also shown.

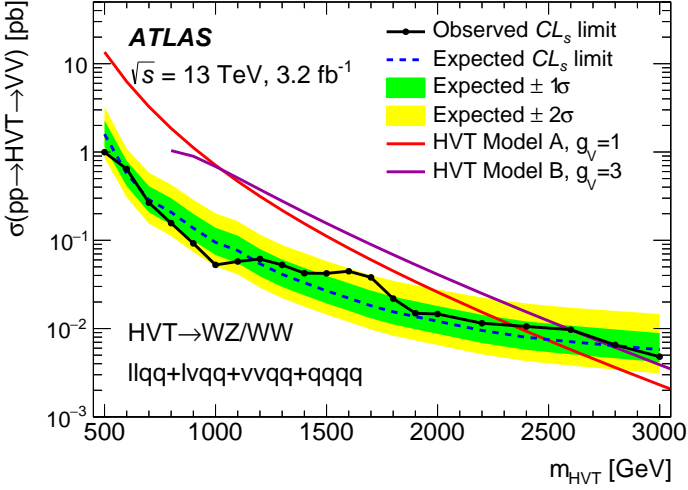


Figure 6: The observed and expected 95% CL limits on the cross-section times branching ratio to diboson final states for the HVT scenario, compared to the theoretical predictions for the HVT model-A with $g_V = 1$ (red line) and model-B with $g_V = 3$ (purple line).

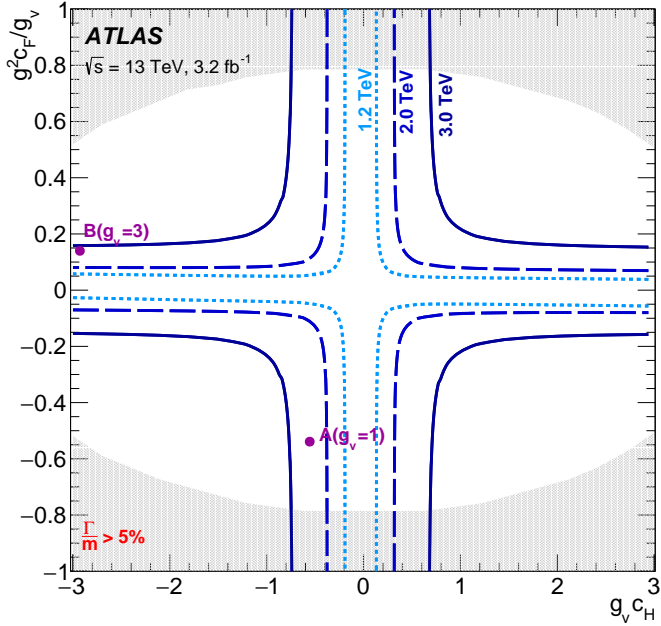


Figure 7: Observed 95% CL exclusion contours in the HVT parameter space ($g^2 c_F / g_V, g_V c_H$) for resonances of mass 1 TeV, 2 TeV and 3 TeV. Parameters for the benchmark models-A and -B are also shown. The grey area indicates the part of the parameter space in which the ratio of the resonance's total width Γ to its mass m is higher than 5%, which is comparable to the experimental mass resolution.

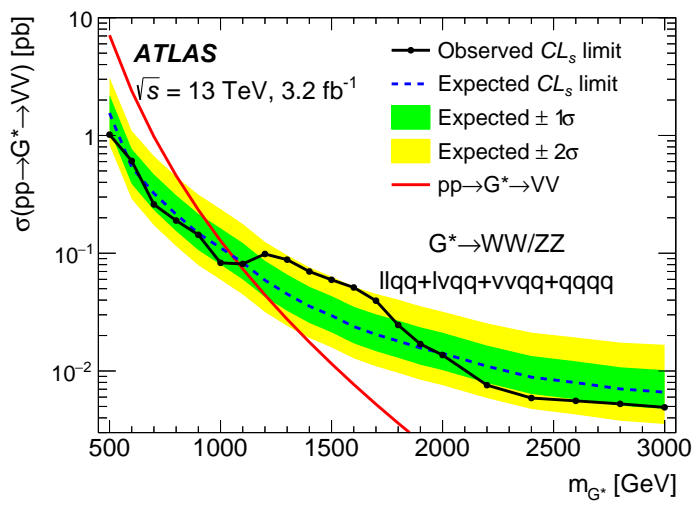


Figure 8: The observed and expected 95% CL limits on the cross-section times branching ratio to diboson final states for bulk RS G^* , compared to the theoretical prediction for $\kappa/\bar{M}_{\text{Pl}} = 1$ (red line).

10 Conclusion

A search is performed for resonant WW , WZ or ZZ production in final states with at least one hadronically decaying vector boson, using 3.2 fb^{-1} of proton–proton collisions at $\sqrt{s} = 13\text{ TeV}$ recorded in 2015 by the ATLAS detector at the LHC. No significant excesses are found in data compared to the SM predictions. Limits on the production cross-section times branching ratio into vector-boson pairs are obtained as a function of the resonance mass for resonances arising from a model predicting the existence of a new heavy scalar singlet, from a simplified model predicting a heavy vector-boson triplet, or from a bulk Randall–Sundrum model with a heavy spin-2 graviton. A scalar resonance with mass below 2650 GeV predicted by the Unsuppressed model, a heavy vector-boson triplet predicted by model-B with $g_v = 3$ of the HVT parameterisation with mass below 2600 GeV , and a graviton in the bulk Randall–Sundrum model ($\kappa/\tilde{M}_{\text{Pl}} = 1$) with mass below 1100 GeV are excluded at the 95% confidence level. Limits are also expressed in terms of the parameters characterising the simplified models considered.

Acknowledgements

We thank CERN for the very successful operation of the LHC, as well as the support staff from our institutions without whom ATLAS could not be operated efficiently.

We acknowledge the support of ANPCyT, Argentina; YerPhI, Armenia; ARC, Australia; BMWFW and FWF, Austria; ANAS, Azerbaijan; SSTC, Belarus; CNPq and FAPESP, Brazil; NSERC, NRC and CFI, Canada; CERN; CONICYT, Chile; CAS, MOST and NSFC, China; COLCIENCIAS, Colombia; MSMT CR, MPO CR and VSC CR, Czech Republic; DNRF and DNSRC, Denmark; IN2P3-CNRS, CEA-DSM/IRFU, France; GNSF, Georgia; BMBF, HGF, and MPG, Germany; GSRT, Greece; RGC, Hong Kong SAR, China; ISF, I-CORE and Benoziyo Center, Israel; INFN, Italy; MEXT and JSPS, Japan; CNRST, Morocco; FOM and NWO, Netherlands; RCN, Norway; MNiSW and NCN, Poland; FCT, Portugal; MNE/IFA, Romania; MES of Russia and NRC KI, Russian Federation; JINR; MESTD, Serbia; MSSR, Slovakia; ARRS and MIZŠ, Slovenia; DST/NRF, South Africa; MINECO, Spain; SRC and Wallenberg Foundation, Sweden; SERI, SNSF and Cantons of Bern and Geneva, Switzerland; MOST, Taiwan; TAEK, Turkey; STFC, United Kingdom; DOE and NSF, United States of America. In addition, individual groups and members have received support from BCKDF, the Canada Council, CANARIE, CRC, Compute Canada, FQRNT, and the Ontario Innovation Trust, Canada; EPLANET, ERC, FP7, Horizon 2020 and Marie Skłodowska-Curie Actions, European Union; Investissements d’Avenir Labex and Idex, ANR, Région Auvergne and Fondation Partager le Savoir, France; DFG and AvH Foundation, Germany; Herakleitos, Thales and Aristeia programmes co-financed by EU-ESF and the Greek NSRF; BSF, GIF and Minerva, Israel; BRF, Norway; Generalitat de Catalunya, Generalitat Valenciana, Spain; the Royal Society and Leverhulme Trust, United Kingdom.

The crucial computing support from all WLCG partners is acknowledged gratefully, in particular from CERN, the ATLAS Tier-1 facilities at TRIUMF (Canada), NDGF (Denmark, Norway, Sweden), CC-IN2P3 (France), KIT/GridKA (Germany), INFN-CNAF (Italy), NL-T1 (Netherlands), PIC (Spain), ASGC (Taiwan), RAL (UK) and BNL (USA), the Tier-2 facilities worldwide and large non-WLCG resource providers. Major contributors of computing resources are listed in Ref. [98].

References

- [1] M. J. Dugan, H. Georgi and D. B. Kaplan, *Anatomy of a Composite Higgs Model*, *Nucl. Phys. B* **254** (1985) 299.
- [2] K. Agashe, R. Contino and A. Pomarol, *The Minimal composite Higgs model*, *Nucl. Phys. B* **719** (2005) 165–187, arXiv:[hep-ph/0412089](#).
- [3] E. Eichten and K. Lane, *Low-scale technicolor at the Tevatron and LHC*, *Phys. Lett. B* **669** (2008) 235–238, arXiv:[0706.2339 \[hep-ph\]](#).
- [4] F. Sannino and K. Tuominen, *Orientifold theory dynamics and symmetry breaking*, *Phys. Rev. D* **71** (2005) 051901, arXiv:[hep-ph/0405209 \[hep-ph\]](#).
- [5] J. Andersen et al., *Discovering Technicolor*, *Eur. Phys. J. Plus* **126** (2011) 81, arXiv:[1104.1255 \[hep-ph\]](#).
- [6] L. Randall and R. Sundrum, *A Large mass hierarchy from a small extra dimension*, *Phys. Rev. Lett.* **83** (1999) 3370–3373, arXiv:[hep-ph/9905221](#).
- [7] L. Randall and R. Sundrum, *An Alternative to compactification*, *Phys. Rev. Lett.* **83** (1999) 4690–4693, arXiv:[hep-th/9906064](#).
- [8] H. Davoudiasl, J. Hewett and T. Rizzo, *Experimental probes of localized gravity: On and off the wall*, *Phys. Rev. D* **63** (2001) 075004, arXiv:[hep-ph/0006041](#).
- [9] G. C. Branco et al., *Theory and phenomenology of two-Higgs-doublet models*, *Phys. Rept.* **516** (2012) 1–102, arXiv:[1106.0034 \[hep-ph\]](#).
- [10] J. C. Pati and A. Salam, *Lepton Number as the Fourth Color*, *Phys. Rev. D* **10** (1974) 275–289.
- [11] H. Georgi and S. Glashow, *Unity of All Elementary Particle Forces*, *Phys. Rev. Lett.* **32** (1974) 438–441.
- [12] H. Georgi, *The State of the Art - Gauge Theories. (Talk)*, *AIP Conf. Proc.* **23** (1975) 575–582.
- [13] H. Fritzsch and P. Minkowski, *Unified Interactions of Leptons and Hadrons*, *Annals Phys.* **93** (1975) 193–266.
- [14] ATLAS Collaboration, *Identification of boosted, hadronically-decaying W and Z bosons in $\sqrt{s} = 13 \text{ TeV}$ Monte Carlo Simulations for ATLAS*, (2015), URL: <http://cds.cern.ch/record/2041461>.
- [15] ATLAS Collaboration, *Identification of boosted, hadronically decaying W bosons and comparisons with ATLAS data taken at $\sqrt{s} = 8 \text{ TeV}$* , *Eur. Phys. J. C* **76** (2016) 1, arXiv:[1510.05821 \[hep-ex\]](#).
- [16] R. Franceschini et al., *What is the $\gamma\gamma$ resonance at 750 GeV?*, *JHEP* **03** (2016) 144, arXiv:[1512.04933 \[hep-ph\]](#).
- [17] D. Pappadopulo et al., *Heavy Vector Triplets: Bridging Theory and Data*, *JHEP* **09** (2014) 060, arXiv:[1402.4431 \[hep-ph\]](#).
- [18] T. Han, J. D. Lykken and R.-J. Zhang, *On Kaluza-Klein states from large extra dimensions*, *Phys. Rev. D* **59** (1999) 105006, arXiv:[hep-ph/9811350](#).
- [19] K. Agashe et al., *Warped Gravitons at the LHC and Beyond*, *Phys. Rev. D* **76** (2007) 036006, arXiv:[hep-ph/0701186](#).

- [20] O. Antipin, D. Atwood and A. Soni, *Search for RS gravitons via $W_L W_L$ decays*, *Phys. Lett. B* **666** (2008) 155–161, arXiv:[0711.3175 \[hep-ph\]](#).
- [21] O. Antipin and A. Soni, *Towards establishing the spin of warped gravitons*, *JHEP* **10** (2008) 018, arXiv:[0806.3427 \[hep-ph\]](#).
- [22] ATLAS Collaboration, *Search for WZ resonances in the fully leptonic channel using pp collisions at $\sqrt{s} = 8$ TeV with the ATLAS detector*, *Phys. Lett. B* **737** (2014) 223–243, arXiv:[1406.4456 \[hep-ex\]](#).
- [23] ATLAS Collaboration, *Search for resonant diboson production in the $\ell\ell q\bar{q}$ final state in pp collisions at $\sqrt{s} = 8$ TeV with the ATLAS detector*, *Eur. Phys. J. C* **75** (2015) 69, arXiv:[1409.6190 \[hep-ex\]](#).
- [24] ATLAS Collaboration, *Search for production of WW/WZ resonances decaying to a lepton, neutrino and jets in pp collisions at $\sqrt{s} = 8$ TeV with the ATLAS detector*, *Eur. Phys. J. C* **75** (2015) 209, arXiv:[1503.04677 \[hep-ex\]](#).
- [25] ATLAS Collaboration, *Search for high-mass diboson resonances with boson-tagged jets in proton-proton collisions at $\sqrt{s} = 8$ TeV with the ATLAS detector*, *JHEP* **12** (2015) 055, arXiv:[1506.00962 \[hep-ex\]](#).
- [26] CMS Collaboration, *Search for massive resonances in dijet systems containing jets tagged as W or Z boson decays in pp collisions at $\sqrt{s} = 8$ TeV*, *JHEP* **08** (2014) 173, arXiv:[1405.1994 \[hep-ex\]](#).
- [27] CMS Collaboration, *Search for massive resonances decaying into pairs of boosted bosons in semi-leptonic final states at $\sqrt{s} = 8$ TeV*, *JHEP* **08** (2014) 174, arXiv:[1405.3447 \[hep-ex\]](#).
- [28] CMS Collaboration, *Search for new resonances decaying via WZ to leptons in proton-proton collisions at $\sqrt{s} = 8$ TeV*, *Phys. Lett. B* **740** (2015) 83–104, arXiv:[1407.3476 \[hep-ex\]](#).
- [29] ATLAS Collaboration, *Search for an additional, heavy Higgs boson in the $H \rightarrow ZZ$ decay channel at $\sqrt{s} = 8$ TeV in pp collision data with the ATLAS detector*, *Eur. Phys. J. C* **76** (2016) 45, arXiv:[1507.05930 \[hep-ex\]](#).
- [30] ATLAS Collaboration, *Search for a high-mass Higgs boson decaying to a W boson pair in pp collisions at $\sqrt{s} = 8$ TeV with the ATLAS detector*, *JHEP* **01** (2015) 032, arXiv:[1509.00389 \[hep-ex\]](#).
- [31] ATLAS Collaboration, *Combination of searches for WW , WZ , and ZZ resonances in pp collisions at $\sqrt{s} = 8$ TeV with the ATLAS detector*, *Phys. Lett. B* **755** (2016) 285, arXiv:[1512.05099 \[hep-ex\]](#).
- [32] G. Altarelli, B. Mele and M. Ruiz-Altaba, *Searching for New Heavy Vector Bosons in $p\bar{p}$ Colliders*, *Z.Phys. C* **45** (1989) 109.
- [33] ATLAS Collaboration, *The ATLAS Experiment at the CERN Large Hadron Collider*, *JINST* **3** (2008) S08003.
- [34] ATLAS Collaboration, *ATLAS Insertable B-Layer Technical Design Report*, (2010), URL: <http://cds.cern.ch/record/1291633>, ATLAS Insertable B-Layer Technical Design Report Addendum, ATLAS-TDR-19-ADD-1 (2012), URL: <http://cds.cern.ch/record/1451888>.

- [35] ATLAS Collaboration, *2015 start-up trigger menu and initial performance assessment of the ATLAS trigger using Run-2 data*, (2016), URL: <http://cds.cern.ch/record/2136007>.
- [36] ATLAS Collaboration, *Improved Luminosity Determination in pp Collisions at $\sqrt{s} = 7 \text{ TeV}$ using the ATLAS Detector at the LHC*, *Eur. Phys. J. C* **73** (2013) 2518, arXiv:1302.4393.
- [37] A. Hill and J. J. van der Bij, *Strongly interacting singlet-doublet Higgs model*, *Phys. Rev. D* **36** (1987) 3463–3473.
- [38] V. Barger et al., *LHC Phenomenology of an Extended Standard Model with a Real Scalar Singlet*, *Phys. Rev. D* **77** (2008) 035005, arXiv:0706.4311 [hep-ph].
- [39] V. D. Barger, W.-Y. Keung and E. Ma, *A Gauge Model With Light W and Z Bosons*, *Phys. Rev. D* **22** (1980) 727.
- [40] ATLAS Collaboration, *Search for high-mass dilepton resonances in pp collisions at $\sqrt{s} = 8 \text{ TeV}$ with the ATLAS detector*, *Phys. Rev. D* **90** (2014) 052005, arXiv:1405.4123 [hep-ex].
- [41] ATLAS Collaboration, *Search for new particles in events with one lepton and missing transverse momentum in pp collisions at $\sqrt{s} = 8 \text{ TeV}$ with the ATLAS detector*, *JHEP* **09** (2014) 037, arXiv:1407.7494 [hep-ex].
- [42] CMS Collaboration, *Search for physics beyond the standard model in dilepton mass spectra in proton-proton collisions at $\sqrt{s} = 8 \text{ TeV}$* , *JHEP* **04** (2015) 025, arXiv:1412.6302 [hep-ex].
- [43] CMS Collaboration, *Search for physics beyond the standard model in final states with a lepton and missing transverse energy in proton-proton collisions at $\sqrt{s} = 8 \text{ TeV}$* , *Phys. Rev. D* **91** (2015) 092005, arXiv:1408.2745 [hep-ex].
- [44] R. Contino et al., *On the effect of resonances in composite Higgs phenomenology*, *JHEP* **10** (2011) 081, arXiv:1109.1570 [hep-ph].
- [45] B. Bellazzini, C. Csáki and J. Serra, *Composite Higgses*, *Eur. Phys. J. C* **74** (2014) 2766, arXiv:1401.2457 [hep-ph].
- [46] G. Panico and A. Wulzer, *The Composite Nambu-Goldstone Higgs*, *Lect. Notes Phys.* **913** (2016), arXiv:1506.01961 [hep-ph].
- [47] K. Agashe et al., *Warped Gravitons at the LHC and Beyond*, *Phys. Rev. D* **76** (2007) 036006, arXiv:hep-ph/0701186.
- [48] S. Alioli et al., *A general framework for implementing NLO calculations in shower Monte Carlo programs: the POWHEG BOX*, *JHEP* **06** (2010) 043, arXiv:1002.2581 [hep-ph].
- [49] H.-L. Lai et al., *New parton distributions for collider physics*, *Phys. Rev. D* **82** (2010) 074024, arXiv:1007.2241 [hep-ph].
- [50] T. Sjöstrand, S. Mrenna and P. Z. Skands, *A Brief Introduction to PYTHIA 8.1*, *Comput. Phys. Commun.* **178** (2008) 852–867, arXiv:0710.3820 [hep-ph].
- [51] ATLAS Collaboration, *Measurement of the Z/γ^* boson transverse momentum distribution in pp collisions at $\sqrt{s} = 7 \text{ TeV}$ with the ATLAS detector*, *JHEP* **09** (2014) 145, arXiv:1406.3660 [hep-ex].
- [52] J. Alwall et al., *The automated computation of tree-level and next-to-leading order differential cross sections, and their matching to parton shower simulations*, *JHEP* **07** (2014) 079, arXiv:1405.0301 [hep-ph].

- [53] R. D. Ball et al., *Parton distributions with LHC data*, *Nucl. Phys.* **B867** (2013) 244–289, arXiv:[1207.1303 \[hep-ph\]](#).
- [54] T. Gleisberg et al., *Event generation with SHERPA 1.1*, *JHEP* **02** (2009) 007, arXiv:[0811.4622 \[hep-ph\]](#).
- [55] T. Gleisberg and S. Höche, *Comix, a new matrix element generator*, *JHEP* **12** (2008) 039, arXiv:[0808.3674 \[hep-ph\]](#).
- [56] F. Caccioli, P. Maierhofer and S. Pozzorini, *Scattering Amplitudes with Open Loops*, *Phys. Rev. Lett.* **108** (2012) 111601, arXiv:[1111.5206 \[hep-ph\]](#).
- [57] S. Schumann and F. Krauss,
A Parton shower algorithm based on Catani-Seymour dipole factorisation, *JHEP* **03** (2008) 038, arXiv:[0709.1027 \[hep-ph\]](#).
- [58] S. Höche et al., *QCD matrix elements + parton showers: The NLO case*, *JHEP* **04** (2013) 027, arXiv:[1207.5030 \[hep-ph\]](#).
- [59] P. Nason, *A new method for combining NLO QCD with shower Monte Carlo algorithms*, *JHEP* **11** (2004) 040, arXiv:[hep-ph/0409146](#).
- [60] S. Frixione, P. Nason and C. Oleari,
Matching NLO QCD computations with Parton Shower simulations: the POWHEG method, *JHEP* **11** (2007) 070, arXiv:[0709.2092 \[hep-ph\]](#).
- [61] P. Artoisenet et al.,
Automatic spin-entangled decays of heavy resonances in Monte Carlo simulations, *JHEP* **03** (2013) 015, arXiv:[1212.3460 \[hep-ph\]](#).
- [62] T. Sjöstrand, S. Mrenna and P. Z. Skands, *PYTHIA 6.4 Physics and Manual*, *JHEP* **05** (2006) 026, arXiv:[hep-ph/0603175](#).
- [63] J. Pumplin et al.,
New generation of parton distributions with uncertainties from global QCD analysis, *JHEP* **07** (2002) 012, arXiv:[hep-ph/0201195](#).
- [64] P. Z. Skands, *Tuning Monte Carlo Generators: The Perugia Tunes*, *Phys. Rev. D* **82** (2010) 074018, arXiv:[1005.3457 \[hep-ph\]](#).
- [65] D. J. Lange, *The EvtGen particle decay simulation package*, *Nucl. Instrum. Meth. A* **462** (2001) 152.
- [66] K. Melnikov and F. Petriello,
Electroweak gauge boson production at hadron colliders through $O(\alpha_s^2)$, *Phys. Rev. D* **74** (2006) 114017, arXiv:[hep-ph/0609070](#).
- [67] M. Czakon, P. Fiedler and A. Mitov,
Total Top-Quark Pair-Production Cross Section at Hadron Colliders Through $O(\alpha_s^4)$, *Phys. Rev. Lett.* **110** (2013) 252004, arXiv:[1303.6254 \[hep-ph\]](#).
- [68] N. Kidonakis, *Next-to-next-to-leading-order collinear and soft gluon corrections for t-channel single top quark production*, *Phys. Rev. D* **83** (2011) 091503, arXiv:[1103.2792 \[hep-ph\]](#).
- [69] ATLAS Collaboration, *ATLAS Run 1 Pythia8 tunes*, ATL-PHYS-PUB-2014-021 (2014), URL: <http://cds.cern.ch/record/1966419>.
- [70] S. Agostinelli et al., GEANT4 Collaboration, *GEANT4 - a simulation toolkit*, *Nucl. Instrum. Meth. A* **506** (2003) 250–303.

- [71] ATLAS Collaboration, *The ATLAS simulation infrastructure*, *Eur. Phys. J. C* **70** (2010) 823–874, arXiv:[1005.4568 \[physics.ins-det\]](#).
- [72] ATLAS Collaboration, *Electron efficiency measurements with the ATLAS detector using the 2012 LHC proton-proton collision data*, (2014), URL: <http://cds.cern.ch/record/1706245>.
- [73] G. Aad et al., *Muon reconstruction performance of the ATLAS detector in proton–proton collision data at $\sqrt{s} = 13$ TeV*, *Eur. Phys. J. C* **76** (2016) 292, arXiv:[1603.05598 \[hep-ex\]](#).
- [74] ATLAS Collaboration, *Topological cell clustering in the ATLAS calorimeters and its performance in LHC Run 1*, (2016), submitted to EPJC, arXiv:[1603.02934 \[hep-ex\]](#).
- [75] M. Cacciari, G. P. Salam and G. Soyez, *The anti- k_t jet clustering algorithm*, *JHEP* **04** (2008) 063, arXiv:[0802.1189 \[hep-ph\]](#).
- [76] ATLAS Collaboration, *Jet energy measurement with the ATLAS detector in proton-proton collisions at $\sqrt{s} = 7$ TeV*, *Eur. Phys. J. C* **73** (2013) 2304, arXiv:[1112.6426 \[hep-ex\]](#).
- [77] ATLAS Collaboration, *Performance of pile-up mitigation techniques for jets in pp collisions at $\sqrt{s} = 8$ TeV using the ATLAS detector*, (2015), submitted to EPJC, arXiv:[1510.03823 \[hep-ex\]](#).
- [78] T Barillari et al., *Local Hadronic Calibration*, ATL-LARG-PUB-2009-001-2 (2008), URL: <http://cds.cern.ch/record/1112035>.
- [79] S. Catani et al., *Longitudinally invariant k_\perp clustering algorithms for hadron hadron collisions*, *Nucl. Phys. B* **406** (1993) 187–224.
- [80] ATLAS Collaboration, *Performance of jet substructure techniques for large-R jets in proton-proton collisions at $\sqrt{s} = 7$ TeV using the ATLAS detector*, *JHEP* **09** (2013) 076, arXiv:[1306.4945 \[hep-ex\]](#).
- [81] D. Krohn, J. Thaler and L.-T. Wang, *Jet Trimming*, *JHEP* **02** (2010) 084, arXiv:[0912.1342 \[hep-ph\]](#).
- [82] A. J. Larkoski, I. Moult and D. Neill, *Power Counting to Better Jet Observables*, *JHEP* **12** (2014) 009, arXiv:[1409.6298 \[hep-ph\]](#).
- [83] A. J. Larkoski, G. P. Salam and J. Thaler, *Energy Correlation Functions for Jet Substructure*, *JHEP* **06** (2013) 108, arXiv:[1305.0007 \[hep-ph\]](#).
- [84] ATLAS Collaboration, *Performance of b-Jet Identification in the ATLAS Experiment*, *JINST* **11** (2015) P04008, arXiv:[1512.01094 \[hep-ex\]](#).
- [85] ATLAS Collaboration, *Performance of missing transverse momentum reconstruction for the ATLAS detector in the first proton-proton collisions at $\sqrt{s} = 13$ TeV*, (2015), URL: <http://cds.cern.ch/record/2037904>.
- [86] ATLAS Collaboration, *Expected performance of missing transverse momentum reconstruction for the ATLAS detector at $\sqrt{s} = 13$ TeV*, (2015), URL: <http://cds.cern.ch/record/2037700>.
- [87] M. Cacciari, G. P. Salam and G. Soyez, *The Catchment Area of Jets*, *JHEP* **04** (2008) 005, arXiv:[0802.1188 \[hep-ph\]](#).
- [88] M. Bahr et al., *Herwig++ Physics and Manual*, *Eur. Phys. J. C* **58** (2008) 639–707, arXiv:[0803.0883 \[hep-ph\]](#).

- [89] J. M. Campbell and R. K. Ellis, *An Update on vector boson pair production at hadron colliders*, Phys. Rev. D **60** (1999) 113006, arXiv:[hep-ph/9905386](#).
- [90] M. Botje et al., *The PDF4LHC Working Group Interim Recommendations*, (2011), arXiv:[1101.0538 \[hep-ph\]](#).
- [91] W. Verkerke and D. P. Kirkby, *The RooFit toolkit for data modeling*, eConf **C0303241** (2003) MOLT007, arXiv:[physics/0306116 \[physics\]](#).
- [92] L. Moneta et al., *The RooStats Project*, PoS **ACAT2010** (2010) 057, arXiv:[1009.1003 \[physics.data-an\]](#).
- [93] K. Cranmer et al.,
HistFactory: A tool for creating statistical models for use with RooFit and RooStats, CERN-OPEN-2012-016 (2012), URL: <http://cds.cern.ch/record/1456844/>.
- [94] ATLAS and CMS Collaborations,
Procedure for the LHC Higgs boson search combination in summer 2011, (2011), URL: <http://cds.cern.ch/record/1375842>.
- [95] G. Cowan et al., *Asymptotic formulae for likelihood-based test of new physics*, (2010), arXiv:[1007.1727v2 \[physics.data-an\]](#).
- [96] A. L. Read, *Presentation of search results: The CL_s technique*, J. Phys. G **28** (2002) 2693–2704.
- [97] D. Pappadopulo et al.,
URL: http://rtorre.web.cern.ch/rtorre/Riccardotorre/vector_triplet_t.html.
- [98] ATLAS Collaboration, *ATLAS Computing Acknowledgements 2016-2017*, ATL-GEN-PUB-2016-002, 2016, URL: <http://cds.cern.ch/record/2202407>.

The ATLAS Collaboration

M. Aaboud^{135d}, G. Aad⁸⁶, B. Abbott¹¹³, J. Abdallah⁶⁴, O. Abdinov¹², B. Abelsoos¹¹⁷, R. Aben¹⁰⁷, O.S. AbouZeid¹³⁷, N.L. Abraham¹⁴⁹, H. Abramowicz¹⁵³, H. Abreu¹⁵², R. Abreu¹¹⁶, Y. Abulaiti^{146a,146b}, B.S. Acharya^{163a,163b,a}, L. Adamczyk^{40a}, D.L. Adams²⁷, J. Adelman¹⁰⁸, S. Adomeit¹⁰⁰, T. Adye¹³¹, A.A. Affolder⁷⁵, T. Agatonovic-Jovin¹⁴, J. Agricola⁵⁶, J.A. Aguilar-Saavedra^{126a,126f}, S.P. Ahlen²⁴, F. Ahmadov^{66,b}, G. Aielli^{133a,133b}, H. Akerstedt^{146a,146b}, T.P.A. Åkesson⁸², A.V. Akimov⁹⁶, G.L. Alberghi^{22a,22b}, J. Albert¹⁶⁸, S. Albrand⁵⁷, M.J. Alconada Verzini⁷², M. Alekса³², I.N. Aleksandrov⁶⁶, C. Alexa^{28b}, G. Alexander¹⁵³, T. Alexopoulos¹⁰, M. Alhroob¹¹³, B. Ali¹²⁸, M. Aliev^{74a,74b}, G. Alimonti^{92a}, J. Alison³³, S.P. Alkire³⁷, B.M.M. Allbrooke¹⁴⁹, B.W. Allen¹¹⁶, P.P. Allport¹⁹, A. Aloisio^{104a,104b}, A. Alonso³⁸, F. Alonso⁷², C. Alpigiani¹³⁸, M. Alstaty⁸⁶, B. Alvarez Gonzalez³², D. Álvarez Piqueras¹⁶⁶, M.G. Alviggi^{104a,104b}, B.T. Amadio¹⁶, K. Amako⁶⁷, Y. Amaral Coutinho^{26a}, C. Amelung²⁵, D. Amidei⁹⁰, S.P. Amor Dos Santos^{126a,126c}, A. Amorim^{126a,126b}, S. Amoroso³², G. Amundsen²⁵, C. Anastopoulos¹³⁹, L.S. Ancu⁵¹, N. Andari¹⁹, T. Andeen¹¹, C.F. Anders^{59b}, G. Anders³², J.K. Anders⁷⁵, K.J. Anderson³³, A. Andreazza^{92a,92b}, V. Andrei^{59a}, S. Angelidakis⁹, I. Angelozzi¹⁰⁷, P. Anger⁴⁶, A. Angerami³⁷, F. Anghinolfi³², A.V. Anisenkov^{109,c}, N. Anjos¹³, A. Annovi^{124a,124b}, C. Antel^{59a}, M. Antonelli⁴⁹, A. Antonov^{98,*}, F. Anulli^{132a}, M. Aoki⁶⁷, L. Aperio Bella¹⁹, G. Arabidze⁹¹, Y. Arai⁶⁷, J.P. Araque^{126a}, A.T.H. Arce⁴⁷, F.A. Arduh⁷², J.-F. Arguin⁹⁵, S. Argyropoulos⁶⁴, M. Arik^{20a}, A.J. Armbruster¹⁴³, L.J. Armitage⁷⁷, O. Arnaez³², H. Arnold⁵⁰, M. Arratia³⁰, O. Arslan²³, A. Artamonov⁹⁷, G. Artoni¹²⁰, S. Artz⁸⁴, S. Asai¹⁵⁵, N. Asbah⁴⁴, A. Ashkenazi¹⁵³, B. Åsman^{146a,146b}, L. Asquith¹⁴⁹, K. Assamagan²⁷, R. Astalos^{144a}, M. Atkinson¹⁶⁵, N.B. Atlay¹⁴¹, K. Augsten¹²⁸, G. Avolio³², B. Axen¹⁶, M.K. Ayoub¹¹⁷, G. Azuelos^{95,d}, M.A. Baak³², A.E. Baas^{59a}, M.J. Baca¹⁹, H. Bachacou¹³⁶, K. Bachas^{74a,74b}, M. Backes¹⁴⁸, M. Backhaus³², P. Bagiacchi^{132a,132b}, P. Bagnaia^{132a,132b}, Y. Bai^{35a}, J.T. Barnes¹³¹, O.K. Baker¹⁷⁵, E.M. Baldin^{109,c}, P. Balek¹⁷¹, T. Balestri¹⁴⁸, F. Balli¹³⁶, W.K. Balunas¹²², E. Banas⁴¹, Sw. Banerjee^{172,e}, A.A.E. Bannoura¹⁷⁴, L. Barak³², E.L. Barberio⁸⁹, D. Barberis^{52a,52b}, M. Barbero⁸⁶, T. Barillari¹⁰¹, M-S Barisits³², T. Barklow¹⁴³, N. Barlow³⁰, S.L. Barnes⁸⁵, B.M. Barnett¹³¹, R.M. Barnett¹⁶, Z. Barnovska-Blenessy⁵, A. Baroncelli^{134a}, G. Barone²⁵, A.J. Barr¹²⁰, L. Barranco Navarro¹⁶⁶, F. Barreiro⁸³, J. Barreiro Guimarães da Costa^{35a}, R. Bartoldus¹⁴³, A.E. Barton⁷³, P. Bartos^{144a}, A. Basalaev¹²³, A. Bassalat¹¹⁷, R.L. Bates⁵⁵, S.J. Batista¹⁵⁸, J.R. Batley³⁰, M. Battaglia¹³⁷, M. Bauce^{132a,132b}, F. Bauer¹³⁶, H.S. Bawa^{143,f}, J.B. Beacham¹¹¹, M.D. Beattie⁷³, T. Beau⁸¹, P.H. Beauchemin¹⁶¹, P. Bechtle²³, H.P. Beck^{18,g}, K. Becker¹²⁰, M. Becker⁸⁴, M. Beckingham¹⁶⁹, C. Becot¹¹⁰, A.J. Beddall^{20e}, A. Beddall^{20b}, V.A. Bednyakov⁶⁶, M. Bedognetti¹⁰⁷, C.P. Bee¹⁴⁸, L.J. Beemster¹⁰⁷, T.A. Beermann³², M. Begel²⁷, J.K. Behr⁴⁴, C. Belanger-Champagne⁸⁸, A.S. Bell⁷⁹, G. Bella¹⁵³, L. Bellagamba^{22a}, A. Bellerive³¹, M. Bellomo⁸⁷, K. Belotskiy⁹⁸, O. Beltramello³², N.L. Belyaev⁹⁸, O. Benary¹⁵³, D. Benchekroun^{135a}, M. Bender¹⁰⁰, K. Bendtz^{146a,146b}, N. Benekos¹⁰, Y. Benhammou¹⁵³, E. Benhar Noccioli¹⁷⁵, J. Benitez⁶⁴, D.P. Benjamin⁴⁷, J.R. Bensinger²⁵, S. Bentvelsen¹⁰⁷, L. Beresford¹²⁰, M. Beretta⁴⁹, D. Berge¹⁰⁷, E. Bergeaas Kuutmann¹⁶⁴, N. Berger⁵, J. Beringer¹⁶, S. Berlendis⁵⁷, N.R. Bernard⁸⁷, C. Bernius¹¹⁰, F.U. Bernlochner²³, T. Berry⁷⁸, P. Berta¹²⁹, C. Bertella⁸⁴, G. Bertoli^{146a,146b}, F. Bertolucci^{124a,124b}, I.A. Bertram⁷³, C. Bertsche⁴⁴, D. Bertsche¹¹³, G.J. Besjes³⁸, O. Bessidskaia Bylund^{146a,146b}, M. Bessner⁴⁴, N. Besson¹³⁶, C. Betancourt⁵⁰, A. Bethani⁵⁷, S. Bethke¹⁰¹, A.J. Bevan⁷⁷, R.M. Bianchi¹²⁵, L. Bianchini²⁵, M. Bianco³², O. Biebel¹⁰⁰, D. Biedermann¹⁷, R. Bielski⁸⁵, N.V. Biesuz^{124a,124b}, M. Biglietti^{134a}, J. Bilbao De Mendizabal⁵¹, T.R.V. Billoud⁹⁵, H. Bilokon⁴⁹, M. Bindi⁵⁶, S. Binet¹¹⁷, A. Bingul^{20b}, C. Bini^{132a,132b}, S. Biondi^{22a,22b}, T. Bisanz⁵⁶, D.M. Bjergaard⁴⁷, C.W. Black¹⁵⁰, J.E. Black¹⁴³, K.M. Black²⁴, D. Blackburn¹³⁸, R.E. Blair⁶, J.-B. Blanchard¹³⁶, T. Blazek^{144a}, I. Bloch⁴⁴, C. Blocker²⁵, W. Blum^{84,*},

U. Blumenschein⁵⁶, S. Blunier^{34a}, G.J. Bobbink¹⁰⁷, V.S. Bobrovnikov^{109,c}, S.S. Bocchetta⁸², A. Bocci⁴⁷, C. Bock¹⁰⁰, M. Boehler⁵⁰, D. Boerner¹⁷⁴, J.A. Bogaerts³², D. Bogavac¹⁴, A.G. Bogdanchikov¹⁰⁹, C. Bohm^{146a}, V. Boisvert⁷⁸, P. Bokan¹⁴, T. Bold^{40a}, A.S. Boldyrev^{163a,163c}, M. Bomben⁸¹, M. Bona⁷⁷, M. Boonekamp¹³⁶, A. Borisov¹³⁰, G. Borissov⁷³, J. Bortfeldt³², D. Bortoletto¹²⁰, V. Bortolotto^{61a,61b,61c}, K. Bos¹⁰⁷, D. Boscherini^{22a}, M. Bosman¹³, J.D. Bossio Sola²⁹, J. Boudreau¹²⁵, J. Bouffard², E.V. Bouhova-Thacker⁷³, D. Boumediene³⁶, C. Bourdarios¹¹⁷, S.K. Boutle⁵⁵, A. Boveia³², J. Boyd³², I.R. Boyko⁶⁶, J. Bracinik¹⁹, A. Brandt⁸, G. Brandt⁵⁶, O. Brandt^{59a}, U. Bratzler¹⁵⁶, B. Brau⁸⁷, J.E. Brau¹¹⁶, H.M. Braun^{174,*}, W.D. Breaden Madden⁵⁵, K. Brendlinger¹²², A.J. Brennan⁸⁹, L. Brenner¹⁰⁷, R. Brenner¹⁶⁴, S. Bressler¹⁷¹, T.M. Bristow⁴⁸, D. Britton⁵⁵, D. Britzger⁴⁴, F.M. Brochu³⁰, I. Brock²³, R. Brock⁹¹, G. Brooijmans³⁷, T. Brooks⁷⁸, W.K. Brooks^{34b}, J. Brosamer¹⁶, E. Brost¹⁰⁸, J.H. Broughton¹⁹, P.A. Bruckman de Renstrom⁴¹, D. Bruncko^{144b}, R. Bruneliere⁵⁰, A. Bruni^{22a}, G. Bruni^{22a}, L.S. Bruni¹⁰⁷, BH Brunt³⁰, M. Bruschi^{22a}, N. Bruscino²³, P. Bryant³³, L. Bryngemark⁸², T. Buanes¹⁵, Q. Buat¹⁴², P. Buchholz¹⁴¹, A.G. Buckley⁵⁵, I.A. Budagov⁶⁶, F. Buehrer⁵⁰, M.K. Bugge¹¹⁹, O. Bulekov⁹⁸, D. Bullock⁸, H. Burckhart³², S. Burdin⁷⁵, C.D. Burgard⁵⁰, B. Burghgrave¹⁰⁸, K. Burka⁴¹, S. Burke¹³¹, I. Burmeister⁴⁵, J.T.P. Burr¹²⁰, E. Busato³⁶, D. Büscher⁵⁰, V. Büscher⁸⁴, P. Bussey⁵⁵, J.M. Butler²⁴, C.M. Buttar⁵⁵, J.M. Butterworth⁷⁹, P. Butti¹⁰⁷, W. Buttinger²⁷, A. Buzatu⁵⁵, A.R. Buzykaev^{109,c}, S. Cabrera Urbán¹⁶⁶, D. Caforio¹²⁸, V.M. Cairo^{39a,39b}, O. Cakir^{4a}, N. Calace⁵¹, P. Calafiura¹⁶, A. Calandri⁸⁶, G. Calderini⁸¹, P. Calfayan¹⁰⁰, G. Callea^{39a,39b}, L.P. Caloba^{26a}, S. Calvente Lopez⁸³, D. Calvet³⁶, S. Calvet³⁶, T.P. Calvet⁸⁶, R. Camacho Toro³³, S. Camarda³², P. Camarri^{133a,133b}, D. Cameron¹¹⁹, R. Caminal Armadans¹⁶⁵, C. Camincher⁵⁷, S. Campana³², M. Campanelli⁷⁹, A. Camplani^{92a,92b}, A. Campoverde¹⁴¹, V. Canale^{104a,104b}, A. Canepa^{159a}, M. Cano Bret^{35e}, J. Cantero¹¹⁴, R. Cantrill^{126a}, T. Cao⁴², M.D.M. Capeans Garrido³², I. Caprini^{28b}, M. Caprini^{28b}, M. Capua^{39a,39b}, R. Caputo⁸⁴, R.M. Carbone³⁷, R. Cardarelli^{133a}, F. Cardillo⁵⁰, I. Carli¹²⁹, T. Carli³², G. Carlino^{104a}, L. Carminati^{92a,92b}, S. Caron¹⁰⁶, E. Carquin^{34b}, G.D. Carrillo-Montoya³², J.R. Carter³⁰, J. Carvalho^{126a,126c}, D. Casadei¹⁹, M.P. Casado^{13,h}, M. Casolino¹³, D.W. Casper¹⁶², E. Castaneda-Miranda^{145a}, R. Castelijn¹⁰⁷, A. Castelli¹⁰⁷, V. Castillo Gimenez¹⁶⁶, N.F. Castro^{126a,i}, A. Catinaccio³², J.R. Catmore¹¹⁹, A. Cattai³², J. Caudron²³, V. Cavalieri¹⁶⁵, E. Cavallaro¹³, D. Cavalli^{92a}, M. Cavalli-Sforza¹³, V. Cavasinni^{124a,124b}, F. Ceradini^{134a,134b}, L. Cerdá Alberich¹⁶⁶, B.C. Cerio⁴⁷, A.S. Cerqueira^{26b}, A. Cerri¹⁴⁹, L. Cerrito^{133a,133b}, F. Cerutti¹⁶, M. Cerv³², A. Cervelli¹⁸, S.A. Cetin^{20d}, A. Chafaq^{135a}, D. Chakraborty¹⁰⁸, S.K. Chan⁵⁸, Y.L. Chan^{61a}, P. Chang¹⁶⁵, J.D. Chapman³⁰, D.G. Charlton¹⁹, A. Chatterjee⁵¹, C.C. Chau¹⁵⁸, C.A. Chavez Barajas¹⁴⁹, S. Che¹¹¹, S. Cheatham⁷³, A. Chegwidden⁹¹, S. Chekanov⁶, S.V. Chekulaev^{159a}, G.A. Chelkov^{66,j}, M.A. Chelstowska⁹⁰, C. Chen⁶⁵, H. Chen²⁷, K. Chen¹⁴⁸, S. Chen^{35c}, S. Chen¹⁵⁵, X. Chen^{35f}, Y. Chen⁶⁸, H.C. Cheng⁹⁰, H.J. Cheng^{35a}, Y. Cheng³³, A. Cheplakov⁶⁶, E. Cheremushkina¹³⁰, R. Cherkaoui El Moursli^{135e}, V. Chernyatin^{27,*}, E. Cheu⁷, L. Chevalier¹³⁶, V. Chiarella⁴⁹, G. Chiarelli^{124a,124b}, G. Chiodini^{74a}, A.S. Chisholm¹⁹, A. Chitan^{28b}, M.V. Chizhov⁶⁶, K. Choi⁶², A.R. Chomont³⁶, S. Chouridou⁹, B.K.B. Chow¹⁰⁰, V. Christodoulou⁷⁹, D. Chromek-Burckhart³², J. Chudoba¹²⁷, A.J. Chuinard⁸⁸, J.J. Chwastowski⁴¹, L. Chytka¹¹⁵, G. Ciapetti^{132a,132b}, A.K. Ciftci^{4a}, D. Cinca⁴⁵, V. Cindro⁷⁶, I.A. Cioara²³, C. Ciocca^{22a,22b}, A. Ciocio¹⁶, F. Cirotto^{104a,104b}, Z.H. Citron¹⁷¹, M. Citterio^{92a}, M. Ciubancan^{28b}, A. Clark⁵¹, B.L. Clark⁵⁸, M.R. Clark³⁷, P.J. Clark⁴⁸, R.N. Clarke¹⁶, C. Clement^{146a,146b}, Y. Coadou⁸⁶, M. Cobal^{163a,163c}, A. Coccaro⁵¹, J. Cochran⁶⁵, L. Colasurdo¹⁰⁶, B. Cole³⁷, A.P. Colijn¹⁰⁷, J. Collot⁵⁷, T. Colombo³², G. Compostella¹⁰¹, P. Conde Muiño^{126a,126b}, E. Coniavitis⁵⁰, S.H. Connell^{145b}, I.A. Connelly⁷⁸, V. Consorti⁵⁰, S. Constantinescu^{28b}, G. Conti³², F. Conventi^{104a,k}, M. Cooke¹⁶, B.D. Cooper⁷⁹, A.M. Cooper-Sarkar¹²⁰, K.J.R. Cormier¹⁵⁸, T. Cornelissen¹⁷⁴, M. Corradi^{132a,132b}, F. Corriveau^{88,l}, A. Corso-Radu¹⁶², A. Cortes-Gonzalez³², G. Cortiana¹⁰¹, G. Costa^{92a}, M.J. Costa¹⁶⁶, D. Costanzo¹³⁹, G. Cottin³⁰, G. Cowan⁷⁸, B.E. Cox⁸⁵, K. Cranmer¹¹⁰, S.J. Crawley⁵⁵, G. Cree³¹, S. Crépé-Renaudin⁵⁷, F. Crescioli⁸¹, W.A. Cribbs^{146a,146b},

M. Crispin Ortuzar¹²⁰, M. Cristinziani²³, V. Croft¹⁰⁶, G. Crosetti^{39a,39b}, A. Cueto⁸³,
 T. Cuhadar Donszelmann¹³⁹, J. Cummings¹⁷⁵, M. Curatolo⁴⁹, J. Cúth⁸⁴, H. Czirr¹⁴¹, P. Czodrowski³,
 G. D'amen^{22a,22b}, S. D'Auria⁵⁵, M. D'Onofrio⁷⁵, M.J. Da Cunha Sargedas De Sousa^{126a,126b},
 C. Da Via⁸⁵, W. Dabrowski^{40a}, T. Dado^{144a}, T. Dai⁹⁰, O. Dale¹⁵, F. Dallaire⁹⁵, C. Dallapiccola⁸⁷,
 M. Dam³⁸, J.R. Dandoy³³, N.P. Dang⁵⁰, A.C. Daniells¹⁹, N.S. Dann⁸⁵, M. Danninger¹⁶⁷,
 M. Dano Hoffmann¹³⁶, V. Dao⁵⁰, G. Darbo^{52a}, S. Darmora⁸, J. Dassoulas³, A. Dattagupta¹¹⁶,
 W. Davey²³, C. David¹⁶⁸, T. Davidek¹²⁹, M. Davies¹⁵³, P. Davison⁷⁹, E. Dawe⁸⁹, I. Dawson¹³⁹,
 R.K. Daya-Ishmukhametova⁸⁷, K. De⁸, R. de Asmundis^{104a}, A. De Benedetti¹¹³, S. De Castro^{22a,22b},
 S. De Cecco⁸¹, N. De Groot¹⁰⁶, P. de Jong¹⁰⁷, H. De la Torre⁸³, F. De Lorenzi⁶⁵, A. De Maria⁵⁶,
 D. De Pedis^{132a}, A. De Salvo^{132a}, U. De Sanctis¹⁴⁹, A. De Santo¹⁴⁹, J.B. De Vivie De Regie¹¹⁷,
 W.J. Dearnaley⁷³, R. Debbe²⁷, C. Debenedetti¹³⁷, D.V. Dedovich⁶⁶, N. Dehghanian³, I. Deigaard¹⁰⁷,
 M. Del Gaudio^{39a,39b}, J. Del Peso⁸³, T. Del Prete^{124a,124b}, D. Delgove¹¹⁷, F. Deliot¹³⁶, C.M. Delitzsch⁵¹,
 M. Deliyergiyev⁷⁶, A. Dell'Acqua³², L. Dell'Asta²⁴, M. Dell'Orso^{124a,124b}, M. Della Pietra^{104a,k},
 D. della Volpe⁵¹, M. Delmastro⁵, P.A. Delsart⁵⁷, D.A. DeMarco¹⁵⁸, S. Demers¹⁷⁵, M. Demichev⁶⁶,
 A. Demilly⁸¹, S.P. Denisov¹³⁰, D. Denysiuk¹³⁶, D. Derendarz⁴¹, J.E. Derkaoui^{135d}, F. Derue⁸¹,
 P. Dervan⁷⁵, K. Desch²³, C. Deterre⁴⁴, K. Dette⁴⁵, P.O. Deviveiros³², A. Dewhurst¹³¹, S. Dhaliwal²⁵,
 A. Di Ciaccio^{133a,133b}, L. Di Ciaccio⁵, W.K. Di Clemente¹²², C. Di Donato^{132a,132b}, A. Di Girolamo³²,
 B. Di Girolamo³², B. Di Micco^{134a,134b}, R. Di Nardo³², A. Di Simone⁵⁰, R. Di Sipio¹⁵⁸,
 D. Di Valentino³¹, C. Diaconu⁸⁶, M. Diamond¹⁵⁸, F.A. Dias⁴⁸, M.A. Diaz^{34a}, E.B. Diehl⁹⁰, J. Dietrich¹⁷,
 S. Diglio⁸⁶, A. Dimitrieva¹⁴, J. Dingfelder²³, P. Dita^{28b}, S. Dita^{28b}, F. Dittus³², F. Djama⁸⁶,
 T. Djobava^{53b}, J.I. Djuvsland^{59a}, M.A.B. do Vale^{26c}, D. Dobos³², M. Dobre^{28b}, C. Doglioni⁸²,
 J. Dolejsi¹²⁹, Z. Dolezal¹²⁹, M. Donadelli^{26d}, S. Donati^{124a,124b}, P. Dondero^{121a,121b}, J. Donini³⁶,
 J. Dopke¹³¹, A. Doria^{104a}, M.T. Dova⁷², A.T. Doyle⁵⁵, E. Drechsler⁵⁶, M. Dris¹⁰, Y. Du^{35d},
 J. Duarte-Campderros¹⁵³, E. Duchovni¹⁷¹, G. Duckeck¹⁰⁰, O.A. Ducu^{95,m}, D. Duda¹⁰⁷, A. Dudarev³²,
 A.Chr. Dudder⁸⁴, E.M. Duffield¹⁶, L. Duflot¹¹⁷, M. Dührssen³², M. Dumancic¹⁷¹, M. Dunford^{59a},
 H. Duran Yildiz^{4a}, M. Düren⁵⁴, A. Durglishvili^{53b}, D. Duschinger⁴⁶, B. Dutta⁴⁴, M. Dyndal⁴⁴,
 C. Eckardt⁴⁴, K.M. Ecker¹⁰¹, R.C. Edgar⁹⁰, N.C. Edwards⁴⁸, T. Eifert³², G. Eigen¹⁵, K. Einsweiler¹⁶,
 T. Ekelof¹⁶⁴, M. El Kacimi^{135c}, V. Ellajosyula⁸⁶, M. Ellert¹⁶⁴, S. Elles⁵, F. Ellinghaus¹⁷⁴, A.A. Elliot¹⁶⁸,
 N. Ellis³², J. Elmsheuser²⁷, M. Elsing³², D. Emeliyanov¹³¹, Y. Enari¹⁵⁵, O.C. Endner⁸⁴, J.S. Ennis¹⁶⁹,
 J. Erdmann⁴⁵, A. Ereditato¹⁸, G. Ernis¹⁷⁴, J. Ernst², M. Ernst²⁷, S. Errede¹⁶⁵, E. Ertel⁸⁴, M. Escalier¹¹⁷,
 H. Esch⁴⁵, C. Escobar¹²⁵, B. Esposito⁴⁹, A.I. Etienne¹³⁶, E. Etzion¹⁵³, H. Evans⁶², A. Ezhilov¹²³,
 F. Fabbri^{22a,22b}, L. Fabbri^{22a,22b}, G. Facini³³, R.M. Fakhrutdinov¹³⁰, S. Falciano^{132a}, R.J. Falla⁷⁹,
 J. Faltova³², Y. Fang^{35a}, M. Fanti^{92a,92b}, A. Farbin⁸, A. Farilla^{134a}, C. Farina¹²⁵, E.M. Farina^{121a,121b},
 T. Farooque¹³, S. Farrell¹⁶, S.M. Farrington¹⁶⁹, P. Farthouat³², F. Fassi^{135e}, P. Fassnacht³²,
 D. Fassouliotis⁹, M. Faucci Giannelli⁷⁸, A. Favaretto^{52a,52b}, W.J. Fawcett¹²⁰, L. Fayard¹¹⁷,
 O.L. Fedin^{123,n}, W. Fedorko¹⁶⁷, S. Feigl¹¹⁹, L. Feligioni⁸⁶, C. Feng^{35d}, E.J. Feng³², H. Feng⁹⁰,
 A.B. Fenyuk¹³⁰, L. Feremenga⁸, P. Fernandez Martinez¹⁶⁶, S. Fernandez Perez¹³, J. Ferrando⁵⁵,
 A. Ferrari¹⁶⁴, P. Ferrari¹⁰⁷, R. Ferrari^{121a}, D.E. Ferreira de Lima^{59b}, A. Ferrer¹⁶⁶, D. Ferrere⁵¹,
 C. Ferretti⁹⁰, A. Ferretto Parodi^{52a,52b}, F. Fiedler⁸⁴, A. Filipčič⁷⁶, M. Filipuzzi⁴⁴, F. Filthaut¹⁰⁶,
 M. Fincke-Keeler¹⁶⁸, K.D. Finelli¹⁵⁰, M.C.N. Fiolhais^{126a,126c}, L. Fiorini¹⁶⁶, A. Firan⁴², A. Fischer²,
 C. Fischer¹³, J. Fischer¹⁷⁴, W.C. Fisher⁹¹, N. Flaschel⁴⁴, I. Fleck¹⁴¹, P. Fleischmann⁹⁰, G.T. Fletcher¹³⁹,
 R.R.M. Fletcher¹²², T. Flick¹⁷⁴, A. Floderus⁸², L.R. Flores Castillo^{61a}, M.J. Flowerdew¹⁰¹,
 G.T. Forcolin⁸⁵, A. Formica¹³⁶, A. Forti⁸⁵, A.G. Foster¹⁹, D. Fournier¹¹⁷, H. Fox⁷³, S. Fracchia¹³,
 P. Francavilla⁸¹, M. Franchini^{22a,22b}, D. Francis³², L. Franconi¹¹⁹, M. Franklin⁵⁸, M. Frate¹⁶²,
 M. Fraternali^{121a,121b}, D. Freeborn⁷⁹, S.M. Fressard-Batraneanu³², F. Friedrich⁴⁶, D. Froidevaux³²,
 J.A. Frost¹²⁰, C. Fukunaga¹⁵⁶, E. Fullana Torregrosa⁸⁴, T. Fusayasu¹⁰², J. Fuster¹⁶⁶, C. Gabaldon⁵⁷,
 O. Gabizon¹⁷⁴, A. Gabrielli^{22a,22b}, A. Gabrielli¹⁶, G.P. Gach^{40a}, S. Gadatsch³², S. Gadomski⁵¹,

G. Gagliardi^{52a,52b}, L.G. Gagnon⁹⁵, P. Gagnon⁶², C. Galea¹⁰⁶, B. Galhardo^{126a,126c}, E.J. Gallas¹²⁰,
 B.J. Gallop¹³¹, P. Gallus¹²⁸, G. Galster³⁸, K.K. Gan¹¹¹, J. Gao^{35b}, Y. Gao⁴⁸, Y.S. Gao^{143,f},
 F.M. Garay Walls⁴⁸, C. García Navarro¹⁶⁶, M. Garcia-Sciveres¹⁶, R.W. Gardner³³,
 N. Garelli¹⁴³, V. Garonne¹¹⁹, A. Gascon Bravo⁴⁴, K. Gasnikova⁴⁴, C. Gatti⁴⁹, A. Gaudiello^{52a,52b},
 G. Gaudio^{121a}, L. Gauthier⁹⁵, I.L. Gavrilenko⁹⁶, C. Gay¹⁶⁷, G. Gaycken²³, E.N. Gazis¹⁰, Z. Gecse¹⁶⁷,
 C.N.P. Gee¹³¹, Ch. Geich-Gimbel²³, M. Geisen⁸⁴, M.P. Geisler^{59a}, C. Gemme^{52a}, M.H. Genest⁵⁷,
 C. Geng^{35b,o}, S. Gentile^{132a,132b}, C. Gentsos¹⁵⁴, S. George⁷⁸, D. Gerbaudo¹³, A. Gershon¹⁵³,
 S. Ghasemi¹⁴¹, H. Ghazlane^{135b}, M. Ghneimat²³, B. Giacobbe^{22a}, S. Giagu^{132a,132b}, P. Giannetti^{124a,124b},
 B. Gibbard²⁷, S.M. Gibson⁷⁸, M. Gignac¹⁶⁷, M. Gilchriese¹⁶, T.P.S. Gillam³⁰, D. Gillberg³¹,
 G. Gilles¹⁷⁴, D.M. Gingrich^{3,d}, N. Giokaris⁹, M.P. Giordani^{163a,163c}, F.M. Giorgi^{22a}, F.M. Giorgi¹⁷,
 P.F. Giraud¹³⁶, P. Giromini⁵⁸, D. Giugni^{92a}, F. Giuli¹²⁰, C. Giuliani¹⁰¹, M. Giulini^{59b}, B.K. Gjelsten¹¹⁹,
 S. Gkaitatzis¹⁵⁴, I. Gkialas¹⁵⁴, E.L. Gkougkousis¹¹⁷, L.K. Gladilin⁹⁹, C. Glasman⁸³, J. Glatzer⁵⁰,
 P.C.F. Glaysher⁴⁸, A. Glazov⁴⁴, M. Goblirsch-Kolb²⁵, J. Godlewski⁴¹, S. Goldfarb⁸⁹, T. Golling⁵¹,
 D. Golubkov¹³⁰, A. Gomes^{126a,126b,126d}, R. Gonçalo^{126a}, J. Goncalves Pinto Firmino Da Costa¹³⁶,
 G. Gonella⁵⁰, L. Gonella¹⁹, A. Gongadze⁶⁶, S. González de la Hoz¹⁶⁶, G. Gonzalez Parra¹³,
 S. Gonzalez-Sevilla⁵¹, L. Goossens³², P.A. Gorbounov⁹⁷, H.A. Gordon²⁷, I. Gorelov¹⁰⁵, B. Gorini³²,
 E. Gorini^{74a,74b}, A. Gorišek⁷⁶, E. Gornicki⁴¹, A.T. Goshaw⁴⁷, C. Gössling⁴⁵, M.I. Gostkin⁶⁶,
 C.R. Goudet¹¹⁷, D. Goujdami^{135c}, A.G. Goussiou¹³⁸, N. Govender^{145b,p}, E. Gozani¹⁵², L. Graber⁵⁶,
 I. Grabowska-Bold^{40a}, P.O.J. Gradin⁵⁷, P. Grafström^{22a,22b}, J. Gramling⁵¹, E. Gramstad¹¹⁹,
 S. Grancagnolo¹⁷, V. Gratchev¹²³, P.M. Gravila^{28e}, H.M. Gray³², E. Graziani^{134a}, Z.D. Greenwood^{80,q},
 C. Grefe²³, K. Gregersen⁷⁹, I.M. Gregor⁴⁴, P. Grenier¹⁴³, K. Grevtsov⁵, J. Griffiths⁸, A.A. Grillo¹³⁷,
 K. Grimm⁷³, S. Grinstein^{13,r}, Ph. Gris³⁶, J.-F. Grivaz¹¹⁷, S. Groh⁸⁴, J.P. Grohs⁴⁶, E. Gross¹⁷¹,
 J. Grosse-Knetter⁵⁶, G.C. Grossi⁸⁰, Z.J. Grout⁷⁹, L. Guan⁹⁰, W. Guan¹⁷², J. Guenther⁶³, F. Guescini⁵¹,
 D. Guest¹⁶², O. Gueta¹⁵³, E. Guido^{52a,52b}, T. Guillemin⁵, S. Guindon², U. Gul⁵⁵, C. Gumpert³²,
 J. Guo^{35e}, Y. Guo^{35b,o}, R. Gupta⁴², S. Gupta¹²⁰, G. Gustavino^{132a,132b}, P. Gutierrez¹¹³,
 N.G. Gutierrez Ortiz⁷⁹, C. Gutschow⁴⁶, C. Guyot¹³⁶, C. Gwenlan¹²⁰, C.B. Gwilliam⁷⁵, A. Haas¹¹⁰,
 C. Haber¹⁶, H.K. Hadavand⁸, N. Haddad^{135e}, A. Hadef⁸⁶, S. Hageböck²³, Z. Hajduk⁴¹,
 H. Hakobyan^{176,*}, M. Haleem⁴⁴, J. Haley¹¹⁴, G. Halladjian⁹¹, G.D. Hallewell⁸⁶, K. Hamacher¹⁷⁴,
 P. Hamal¹¹⁵, K. Hamano¹⁶⁸, A. Hamilton^{145a}, G.N. Hamity¹³⁹, P.G. Hamnett⁴⁴, L. Han^{35b},
 K. Hanagaki^{67,s}, K. Hanawa¹⁵⁵, M. Hance¹³⁷, B. Haney¹²², P. Hanke^{59a}, R. Hanna¹³⁶, J.B. Hansen³⁸,
 J.D. Hansen³⁸, M.C. Hansen²³, P.H. Hansen³⁸, K. Hara¹⁶⁰, A.S. Hard¹⁷², T. Harenberg¹⁷⁴, F. Hariri¹¹⁷,
 S. Harkusha⁹³, R.D. Harrington⁴⁸, P.F. Harrison¹⁶⁹, F. Hartjes¹⁰⁷, N.M. Hartmann¹⁰⁰, M. Hasegawa⁶⁸,
 Y. Hasegawa¹⁴⁰, A. Hasib¹¹³, S. Hassani¹³⁶, S. Haug¹⁸, R. Hauser⁹¹, L. Hauswald⁴⁶, M. Havranek¹²⁷,
 C.M. Hawkes¹⁹, R.J. Hawkings³², D. Hayakawa¹⁵⁷, D. Hayden⁹¹, C.P. Hays¹²⁰, J.M. Hays⁷⁷,
 H.S. Hayward⁷⁵, S.J. Haywood¹³¹, S.J. Head¹⁹, T. Heck⁸⁴, V. Hedberg⁸², L. Heelan⁸, S. Heim¹²²,
 T. Heim¹⁶, B. Heinemann¹⁶, J.J. Heinrich¹⁰⁰, L. Heinrich¹¹⁰, C. Heinz⁵⁴, J. Hejbal¹²⁷, L. Helary³²,
 S. Hellman^{146a,146b}, C. Helsens³², J. Henderson¹²⁰, R.C.W. Henderson⁷³, Y. Heng¹⁷², S. Henkelmann¹⁶⁷,
 A.M. Henriques Correia³², S. Henrot-Versille¹¹⁷, G.H. Herbert¹⁷, V. Herget¹⁷³,
 Y. Hernández Jiménez¹⁶⁶, G. Herten⁵⁰, R. Hertenberger¹⁰⁰, L. Hervas³², G.G. Hesketh⁷⁹, N.P. Hessey¹⁰⁷,
 J.W. Hetherly⁴², R. Hickling⁷⁷, E. Higón-Rodriguez¹⁶⁶, E. Hill¹⁶⁸, J.C. Hill³⁰, K.H. Hiller⁴⁴,
 S.J. Hillier¹⁹, I. Hinchliffe¹⁶, E. Hines¹²², R.R. Hinman¹⁶, M. Hirose⁵⁰, D. Hirschbuehl¹⁷⁴, J. Hobbs¹⁴⁸,
 N. Hod^{159a}, M.C. Hodgkinson¹³⁹, P. Hodgson¹³⁹, A. Hoecker³², M.R. Hoeferkamp¹⁰⁵, F. Hoenig¹⁰⁰,
 D. Hohn²³, T.R. Holmes¹⁶, M. Homann⁴⁵, T.M. Hong¹²⁵, B.H. Hooberman¹⁶⁵, W.H. Hopkins¹¹⁶,
 Y. Horii¹⁰³, A.J. Horton¹⁴², J-Y. Hostachy⁵⁷, S. Hou¹⁵¹, A. Hoummada^{135a}, J. Howarth⁴⁴,
 M. Hrabovsky¹¹⁵, I. Hristova¹⁷, J. Hrvnac¹¹⁷, T. Hrynevich⁹⁴, C. Hsu^{145c}, P.J. Hsu^{151,t},
 S.-C. Hsu¹³⁸, D. Hu³⁷, Q. Hu^{35b}, S. Hu^{35e}, Y. Huang⁴⁴, Z. Hubacek¹²⁸, F. Hubaut⁸⁶, F. Huegging²³,
 T.B. Huffman¹²⁰, E.W. Hughes³⁷, G. Hughes⁷³, M. Huhtinen³², P. Huo¹⁴⁸, N. Huseynov^{66,b}, J. Huston⁹¹,

J. Huth⁵⁸, G. Iacobucci⁵¹, G. Iakovidis²⁷, I. Ibragimov¹⁴¹, L. Iconomidou-Fayard¹¹⁷, E. Ideal¹⁷⁵,
 Z. Idrissi^{135e}, P. Iengo³², O. Igolkina^{107,u}, T. Iizawa¹⁷⁰, Y. Ikegami⁶⁷, M. Ikeno⁶⁷, Y. Ilchenko^{11,v},
 D. Iliadis¹⁵⁴, N. Ilic¹⁴³, T. Ince¹⁰¹, G. Introzzi^{121a,121b}, P. Ioannou^{9,*}, M. Iodice^{134a}, K. Iordanidou³⁷,
 V. Ippolito⁵⁸, N. Ishijima¹¹⁸, M. Ishino¹⁵⁵, M. Ishitsuka¹⁵⁷, R. Ishmukhametov¹¹¹, C. Issever¹²⁰,
 S. Isti^{20a}, F. Ito¹⁶⁰, J.M. Iturbe Ponce⁸⁵, R. Iuppa^{133a,133b}, W. Iwanski⁶³, H. Iwasaki⁶⁷, J.M. Izen⁴³,
 V. Izzo^{104a}, S. Jabbar³, B. Jackson¹²², P. Jackson¹, V. Jain², K.B. Jakobi⁸⁴, K. Jakobs⁵⁰, S. Jakobsen³²,
 T. Jakoubek¹²⁷, D.O. Jamin¹¹⁴, D.K. Jana⁸⁰, E. Jansen⁷⁹, R. Jansky⁶³, J. Janssen²³, M. Janus⁵⁶,
 G. Jarlskog⁸², N. Javadov^{66,b}, T. Javurek⁵⁰, F. Jeanneau¹³⁶, L. Jeanty¹⁶, G.-Y. Jeng¹⁵⁰, D. Jennens⁸⁹,
 P. Jenni^{50,w}, C. Jeske¹⁶⁹, S. Jézéquel⁵, H. Ji¹⁷², J. Jia¹⁴⁸, H. Jiang⁶⁵, Y. Jiang^{35b}, S. Jiggins⁷⁹,
 J. Jimenez Pena¹⁶⁶, S. Jin^{35a}, A. Jinaru^{28b}, O. Jinnouchi¹⁵⁷, P. Johansson¹³⁹, K.A. Johns⁷,
 W.J. Johnson¹³⁸, K. Jon-And^{146a,146b}, G. Jones¹⁶⁹, R.W.L. Jones⁷³, S. Jones⁷, T.J. Jones⁷⁵,
 J. Jongmanns^{59a}, P.M. Jorge^{126a,126b}, J. Jovicevic^{159a}, X. Ju¹⁷², A. Juste Rozas^{13,r}, M.K. Köhler¹⁷¹,
 A. Kaczmarcka⁴¹, M. Kado¹¹⁷, H. Kagan¹¹¹, M. Kagan¹⁴³, S.J. Kahn⁸⁶, T. Kaji¹⁷⁰, E. Kajomovitz⁴⁷,
 C.W. Kalderon¹²⁰, A. Kaluza⁸⁴, S. Kama⁴², A. Kamenshchikov¹³⁰, N. Kanaya¹⁵⁵, S. Kaneti³⁰,
 L. Kanjur⁷⁶, V.A. Kantserov⁹⁸, J. Kanzaki⁶⁷, B. Kaplan¹¹⁰, L.S. Kaplan¹⁷², A. Kapliy³³, D. Kar^{145c},
 K. Karakostas¹⁰, A. Karamaoun³, N. Karastathis¹⁰, M.J. Kareem⁵⁶, E. Karentzos¹⁰, M. Karnevskiy⁸⁴,
 S.N. Karpov⁶⁶, Z.M. Karpova⁶⁶, K. Karthik¹¹⁰, V. Kartvelishvili⁷³, A.N. Karyukhin¹³⁰, K. Kasahara¹⁶⁰,
 L. Kashif¹⁷², R.D. Kass¹¹¹, A. Kastanas¹⁵, Y. Kataoka¹⁵⁵, C. Kato¹⁵⁵, A. Katre⁵¹, J. Katzy⁴⁴,
 K. Kawagoe⁷¹, T. Kawamoto¹⁵⁵, G. Kawamura⁵⁶, V.F. Kazanin^{109,c}, R. Keeler¹⁶⁸, R. Kehoe⁴²,
 J.S. Keller⁴⁴, J.J. Kempster⁷⁸, K. Kawade¹⁰³, H. Keoshkerian¹⁵⁸, O. Kepka¹²⁷, B.P. Kerševan⁷⁶,
 S. Kersten¹⁷⁴, R.A. Keyes⁸⁸, M. Khader¹⁶⁵, F. Khalil-zada¹², A. Khanov¹¹⁴, A.G. Kharlamov^{109,c},
 T.J. Khoo⁵¹, V. Khovanskiy⁹⁷, E. Khramov⁶⁶, J. Khubua^{53b,x}, S. Kido⁶⁸, C.R. Kilby⁷⁸, H.Y. Kim⁸,
 S.H. Kim¹⁶⁰, Y.K. Kim³³, N. Kimura¹⁵⁴, O.M. Kind¹⁷, B.T. King⁷⁵, M. King¹⁶⁶, S.B. King¹⁶⁷,
 J. Kirk¹³¹, A.E. Kiryunin¹⁰¹, T. Kishimoto¹⁵⁵, D. Kisielewska^{40a}, F. Kiss⁵⁰, K. Kiuchi¹⁶⁰,
 O. Kiverny¹³⁶, E. Kladiva^{144b}, M.H. Klein³⁷, M. Klein⁷⁵, U. Klein⁷⁵, K. Kleinknecht⁸⁴, P. Klimek¹⁰⁸,
 A. Klimentov²⁷, R. Klingenberg⁴⁵, J.A. Klinger¹³⁹, T. Klioutchnikova³², E.-E. Kluge^{59a}, P. Kluit¹⁰⁷,
 S. Kluth¹⁰¹, J. Knapik⁴¹, E. Kneringer⁶³, E.B.F.G. Knoops⁸⁶, A. Knue⁵⁵, A. Kobayashi¹⁵⁵,
 D. Kobayashi¹⁵⁷, T. Kobayashi¹⁵⁵, M. Kobel⁴⁶, M. Kocian¹⁴³, P. Kodys¹²⁹, N.M. Koehler¹⁰¹, T. Koffas³¹,
 E. Koffeman¹⁰⁷, T. Koi¹⁴³, H. Kolanoski¹⁷, M. Kolb^{59b}, I. Koletsou⁵, A.A. Komar^{96,*}, Y. Komori¹⁵⁵,
 T. Kondo⁶⁷, N. Kondrashova⁴⁴, K. Köneke⁵⁰, A.C. König¹⁰⁶, T. Kono^{67,y}, R. Konoplich^{110,z},
 N. Konstantinidis⁷⁹, R. Kopeliansky⁶², S. Koperny^{40a}, L. Köpke⁸⁴, A.K. Kopp⁵⁰, K. Korcyl⁴¹,
 K. Kordas¹⁵⁴, A. Korn⁷⁹, A.A. Korol^{109,c}, I. Korolkov¹³, E.V. Korolkova¹³⁹, O. Kortner¹⁰¹, S. Kortner¹⁰¹,
 T. Kosek¹²⁹, V.V. Kostyukhin²³, A. Kotwal⁴⁷, A. Kourkoumeli-Charalampidi^{121a,121b}, C. Kourkoumelis⁹,
 V. Kouskoura²⁷, A.B. Kowalewska⁴¹, R. Kowalewski¹⁶⁸, T.Z. Kowalski^{40a}, C. Kozakai¹⁵⁵,
 W. Kozanecki¹³⁶, A.S. Kozhin¹³⁰, V.A. Kramarenko⁹⁹, G. Kramberger⁷⁶, D. Krasnopalovtsev⁹⁸,
 M.W. Krasny⁸¹, A. Krasznahorkay³², A. Kravchenko²⁷, M. Kretz^{59c}, J. Kretzschmar⁷⁵, K. Kreutzfeldt⁵⁴,
 P. Krieger¹⁵⁸, K. Krizka³³, K. Kroeninger⁴⁵, H. Kroha¹⁰¹, J. Kroll¹²², J. Kroeseberg²³, J. Krstic¹⁴,
 U. Kruchonak⁶⁶, H. Krüger²³, N. Krumnack⁶⁵, A. Kruse¹⁷², M.C. Kruse⁴⁷, M. Kruskal²⁴, T. Kubota⁸⁹,
 H. Kucuk⁷⁹, S. Kuday^{4b}, J.T. Kuechler¹⁷⁴, S. Kuehn⁵⁰, A. Kugel^{59c}, F. Kuger¹⁷³, A. Kuhl¹³⁷, T. Kuhl⁴⁴,
 V. Kukhtin⁶⁶, R. Kukla¹³⁶, Y. Kulchitsky⁹³, S. Kuleshov^{34b}, M. Kuna^{132a,132b}, T. Kunigo⁶⁹, A. Kupco¹²⁷,
 H. Kurashige⁶⁸, Y.A. Kurochkin⁹³, V. Kus¹²⁷, E.S. Kuwertz¹⁶⁸, M. Kuze¹⁵⁷, J. Kvita¹¹⁵, T. Kwan¹⁶⁸,
 D. Kyriazopoulos¹³⁹, A. La Rosa¹⁰¹, J.L. La Rosa Navarro^{26d}, L. La Rotonda^{39a,39b}, C. Lacasta¹⁶⁶,
 F. Lacava^{132a,132b}, J. Lacey³¹, H. Lacker¹⁷, D. Lacour⁸¹, V.R. Lacuesta¹⁶⁶, E. Ladygin⁶⁶, R. Lafaye⁵,
 B. Laforge⁸¹, T. Lagouri¹⁷⁵, S. Lai⁵⁶, S. Lammers⁶², W. Lampl⁷, E. Lançon¹³⁶, U. Landgraf⁵⁰,
 M.P.J. Landon⁷⁷, M.C. Lanfermann⁵¹, V.S. Lang^{59a}, J.C. Lange¹³, A.J. Lankford¹⁶², F. Lanni²⁷,
 K. Lantzsch²³, A. Lanza^{121a}, S. Laplace⁸¹, C. Lapoire³², J.F. Laporte¹³⁶, T. Lari^{92a},
 F. Lasagni Manghi^{22a,22b}, M. Lassnig³², P. Laurelli⁴⁹, W. Lavrijesen¹⁶, A.T. Law¹³⁷, P. Laycock⁷⁵,

T. Lazovich⁵⁸, M. Lazzaroni^{92a,92b}, B. Le⁸⁹, O. Le Dortz⁸¹, E. Le Guirriec⁸⁶, E.P. Le Quilleuc¹³⁶,
 M. LeBlanc¹⁶⁸, T. LeCompte⁶, F. Ledroit-Guillon⁵⁷, C.A. Lee²⁷, S.C. Lee¹⁵¹, L. Lee¹, B. Lefebvre⁸⁸,
 G. Lefebvre⁸¹, M. Lefebvre¹⁶⁸, F. Legger¹⁰⁰, C. Leggett¹⁶, A. Lehan⁷⁵, G. Lehmann Miotto³², X. Lei⁷,
 W.A. Leight³¹, A. Leisos^{154,aa}, A.G. Leister¹⁷⁵, M.A.L. Leite^{26d}, R. Leitner¹²⁹, D. Lellouch¹⁷¹,
 B. Lemmer⁵⁶, K.J.C. Leney⁷⁹, T. Lenz²³, B. Lenzi³², R. Leone⁷, S. Leone^{124a,124b}, C. Leonidopoulos⁴⁸,
 S. Leontsinis¹⁰, G. Lerner¹⁴⁹, C. Leroy⁹⁵, A.A.J. Lesage¹³⁶, C.G. Lester³⁰, M. Levchenko¹²³,
 J. Levêque⁵, D. Levin⁹⁰, L.J. Levinson¹⁷¹, M. Levy¹⁹, D. Lewis⁷⁷, A.M. Leyko²³, M. Leyton⁴³,
 B. Li^{35b,o}, C. Li^{35b}, H. Li¹⁴⁸, H.L. Li³³, L. Li⁴⁷, L. Li^{35e}, Q. Li^{35a}, S. Li⁴⁷, X. Li⁸⁵, Y. Li¹⁴¹, Z. Liang^{35a},
 B. Liberti^{133a}, A. Liblong¹⁵⁸, P. Lichard³², K. Lie¹⁶⁵, J. Liebal²³, W. Liebig¹⁵, A. Limosani¹⁵⁰,
 S.C. Lin^{151,ab}, T.H. Lin⁸⁴, B.E. Lindquist¹⁴⁸, A.E. Lioni⁵¹, E. Lipeles¹²², A. Lipniacka¹⁵, M. Lisovyi^{59b},
 T.M. Liss¹⁶⁵, A. Lister¹⁶⁷, A.M. Litke¹³⁷, B. Liu^{151,ac}, D. Liu¹⁵¹, H. Liu⁹⁰, H. Liu²⁷, J. Liu⁸⁶,
 J.B. Liu^{35b}, K. Liu⁸⁶, L. Liu¹⁶⁵, M. Liu⁴⁷, M. Liu^{35b}, Y.L. Liu^{35b}, Y. Liu^{35b}, M. Livan^{121a,121b},
 A. Lleres⁵⁷, J. Llorente Merino^{35a}, S.L. Lloyd⁷⁷, F. Lo Sterzo¹⁵¹, E.M. Lobodzinska⁴⁴, P. Loch⁷,
 W.S. Lockman¹³⁷, F.K. Loebinger⁸⁵, A.E. Loevschall-Jensen³⁸, K.M. Loew²⁵, A. Loginov^{175,*},
 T. Lohse¹⁷, K. Lohwasser⁴⁴, M. Lokajicek¹²⁷, B.A. Long²⁴, J.D. Long¹⁶⁵, R.E. Long⁷³, L. Longo^{74a,74b},
 K.A.Looper¹¹¹, L. Lopes^{126a}, D. Lopez Mateos⁵⁸, B. Lopez Paredes¹³⁹, I. Lopez Paz¹³,
 A. Lopez Solis⁸¹, J. Lorenz¹⁰⁰, N. Lorenzo Martinez⁶², M. Losada²¹, P.J. Lösel¹⁰⁰, X. Lou^{35a},
 A. Lounis¹¹⁷, J. Love⁶, P.A. Love⁷³, H. Lu^{61a}, N. Lu⁹⁰, H.J. Lubatti¹³⁸, C. Luci^{132a,132b}, A. Lucotte⁵⁷,
 C. Luedtke⁵⁰, F. Luehring⁶², W. Lukas⁶³, L. Luminari^{132a}, O. Lundberg^{146a,146b}, B. Lund-Jensen¹⁴⁷,
 P.M. Luzi⁸¹, D. Lynn²⁷, R. Lysak¹²⁷, E. Lytken⁸², V. Lyubushkin⁶⁶, H. Ma²⁷, L.L. Ma^{35d}, Y. Ma^{35d},
 G. Maccarrone⁴⁹, A. Macchioli¹⁰¹, C.M. Macdonald¹³⁹, B. Maček⁷⁶, J. Machado Miguens^{122,126b},
 D. Madaffari⁸⁶, R. Madar³⁶, H.J. Maddocks¹⁶⁴, W.F. Mader⁴⁶, A. Madsen⁴⁴, J. Maeda⁶⁸, S. Maeland¹⁵,
 T. Maeno²⁷, A. Maevskiy⁹⁹, E. Magradze⁵⁶, J. Mahlstedt¹⁰⁷, C. Maiani¹¹⁷, C. Maidantchik^{26a},
 A.A. Maier¹⁰¹, T. Maier¹⁰⁰, A. Maio^{126a,126b,126d}, S. Majewski¹¹⁶, Y. Makida⁶⁷, N. Makovec¹¹⁷,
 B. Malaescu⁸¹, Pa. Malecki⁴¹, V.P. Maleev¹²³, F. Malek⁵⁷, U. Mallik⁶⁴, D. Malon⁶, C. Malone¹⁴³,
 S. Maltezos¹⁰, S. Malyukov³², J. Mamuzic¹⁶⁶, G. Mancini⁴⁹, B. Mandelli³², L. Mandelli^{92a}, I. Mandić⁷⁶,
 J. Maneira^{126a,126b}, L. Manhaes de Andrade Filho^{26b}, J. Manjarres Ramos^{159b}, A. Mann¹⁰⁰,
 A. Manousos³², B. Mansoulie¹³⁶, J.D. Mansour^{35a}, R. Mantifel⁸⁸, M. Mantoani⁵⁶, S. Manzoni^{92a,92b},
 L. Mapelli³², G. Marceca²⁹, L. March⁵¹, G. Marchiori⁸¹, M. Marcisovsky¹²⁷, M. Marjanovic¹⁴,
 D.E. Marley⁹⁰, F. Marroquim^{26a}, S.P. Marsden⁸⁵, Z. Marshall¹⁶, S. Marti-Garcia¹⁶⁶, B. Martin⁹¹,
 T.A. Martin¹⁶⁹, V.J. Martin⁴⁸, B. Martin dit Latour¹⁵, M. Martinez^{13,r}, V.I. Martinez Outschoorn¹⁶⁵,
 S. Martin-Haugh¹³¹, V.S. Martiou^{28b}, A.C. Martyniuk⁷⁹, M. Marx¹³⁸, A. Marzin³², L. Masetti⁸⁴,
 T. Mashimo¹⁵⁵, R. Mashinistov⁹⁶, J. Masik⁸⁵, A.L. Maslenikov^{109,c}, I. Massa^{22a,22b}, L. Massa^{22a,22b},
 P. Mastrandrea⁵, A. Mastroberardino^{39a,39b}, T. Masubuchi¹⁵⁵, P. Mättig¹⁷⁴, J. Mattmann⁸⁴, J. Maurer^{28b},
 S.J. Maxfield⁷⁵, D.A. Maximov^{109,c}, R. Mazini¹⁵¹, S.M. Mazza^{92a,92b}, N.C. Mc Fadden¹⁰⁵,
 G. Mc Goldrick¹⁵⁸, S.P. Mc Kee⁹⁰, A. McCarn⁹⁰, R.L. McCarthy¹⁴⁸, T.G. McCarthy¹⁰¹,
 L.I. McClymont⁷⁹, E.F. McDonald⁸⁹, J.A. McFayden⁷⁹, G. Mchedlidze⁵⁶, S.J. McMahon¹³¹,
 R.A. McPherson^{168,l}, M. Medinnis⁴⁴, S. Meehan¹³⁸, S. Mehlhase¹⁰⁰, A. Mehta⁷⁵, K. Meier^{59a},
 C. Meineck¹⁰⁰, B. Meirose⁴³, D. Melini¹⁶⁶, B.R. Mellado Garcia^{145c}, M. Melo^{144a}, F. Meloni¹⁸,
 A. Mengarelli^{22a,22b}, S. Menke¹⁰¹, E. Meoni¹⁶¹, S. Mergelmeyer¹⁷, P. Mermod⁵¹, L. Merola^{104a,104b},
 C. Meroni^{92a}, F.S. Merritt³³, A. Messina^{132a,132b}, J. Metcalfe⁶, A.S. Mete¹⁶², C. Meyer⁸⁴, C. Meyer¹²²,
 J.-P. Meyer¹³⁶, J. Meyer¹⁰⁷, H. Meyer Zu Theenhausen^{59a}, F. Miano¹⁴⁹, R.P. Middleton¹³¹,
 S. Miglioranzi^{52a,52b}, L. Mijović⁴⁸, G. Mikenberg¹⁷¹, M. Mikestikova¹²⁷, M. Mikuž⁷⁶, M. Milesi⁸⁹,
 A. Milic⁶³, D.W. Miller³³, C. Mills⁴⁸, A. Milov¹⁷¹, D.A. Milstead^{146a,146b}, A.A. Minaenko¹³⁰,
 Y. Minami¹⁵⁵, I.A. Minashvili⁶⁶, A.I. Mincer¹¹⁰, B. Mindur^{40a}, M. Mineev⁶⁶, Y. Ming¹⁷², L.M. Mir¹³,
 K.P. Mistry¹²², T. Mitani¹⁷⁰, J. Mitrevski¹⁰⁰, V.A. Mitsou¹⁶⁶, A. Miucci¹⁸, P.S. Miyagawa¹³⁹,
 J.U. Mjörnmark⁸², T. Moa^{146a,146b}, K. Mochizuki⁹⁵, S. Mohapatra³⁷, S. Molander^{146a,146b},

R. Moles-Valls²³, R. Monden⁶⁹, M.C. Mondragon⁹¹, K. Mönig⁴⁴, J. Monk³⁸, E. Monnier⁸⁶,
 A. Montalbano¹⁴⁸, J. Montejo Berlingen³², F. Monticelli⁷², S. Monzani^{92a,92b}, R.W. Moore³,
 N. Morange¹¹⁷, D. Moreno²¹, M. Moreno Llácer⁵⁶, P. Morettini^{52a}, S. Morgenstern³², D. Mori¹⁴²,
 T. Mori¹⁵⁵, M. Morii⁵⁸, M. Morinaga¹⁵⁵, V. Morisbak¹¹⁹, S. Moritz⁸⁴, A.K. Morley¹⁵⁰, G. Mornacchi³²,
 J.D. Morris⁷⁷, S.S. Mortensen³⁸, L. Morvaj¹⁴⁸, M. Mosidze^{53b}, J. Moss^{143,ad}, K. Motohashi¹⁵⁷,
 R. Mount¹⁴³, E. Mountricha²⁷, S.V. Mouraviev^{96,*}, E.J.W. Moyse⁸⁷, S. Muanza⁸⁶, R.D. Mudd¹⁹,
 F. Mueller¹⁰¹, J. Mueller¹²⁵, R.S.P. Mueller¹⁰⁰, T. Mueller³⁰, D. Muenstermann⁷³, P. Mullen⁵⁵,
 G.A. Mullier¹⁸, F.J. Munoz Sanchez⁸⁵, J.A. Murillo Quijada¹⁹, W.J. Murray^{169,131}, H. Musheghyan⁵⁶,
 M. Muškinja⁷⁶, A.G. Myagkov^{130,ae}, M. Myska¹²⁸, B.P. Nachman¹⁴³, O. Nackenhorst⁵¹, K. Nagai¹²⁰,
 R. Nagai^{67,y}, K. Nagano⁶⁷, Y. Nagasaka⁶⁰, K. Nagata¹⁶⁰, M. Nagel⁵⁰, E. Nagy⁸⁶, A.M. Nairz³²,
 Y. Nakahama¹⁰³, K. Nakamura⁶⁷, T. Nakamura¹⁵⁵, I. Nakano¹¹², H. Namasivayam⁴³,
 R.F. Naranjo Garcia⁴⁴, R. Narayan¹¹, D.I. Narrias Villar^{59a}, I. Naryshkin¹²³, T. Naumann⁴⁴,
 G. Navarro²¹, R. Nayyar⁷, H.A. Neal⁹⁰, P.Yu. Nechaeva⁹⁶, T.J. Neep⁸⁵, A. Negri^{121a,121b}, M. Negrini^{22a},
 S. Nektarijevic¹⁰⁶, C. Nellist¹¹⁷, A. Nelson¹⁶², S. Nemecek¹²⁷, P. Nemethy¹¹⁰, A.A. Nepomuceno^{26a},
 M. Nessi^{32,af}, M.S. Neubauer¹⁶⁵, M. Neumann¹⁷⁴, R.M. Neves¹¹⁰, P. Nevski²⁷, P.R. Newman¹⁹,
 D.H. Nguyen⁶, T. Nguyen Manh⁹⁵, R.B. Nickerson¹²⁰, R. Nicolaïdou¹³⁶, J. Nielsen¹³⁷, A. Nikiforov¹⁷,
 V. Nikolaenko^{130,ae}, I. Nikolic-Audit⁸¹, K. Nikolopoulos¹⁹, J.K. Nilsen¹¹⁹, P. Nilsson²⁷, Y. Ninomiya¹⁵⁵,
 A. Nisati^{132a}, R. Nisius¹⁰¹, T. Nobe¹⁵⁵, M. Nomachi¹¹⁸, I. Nomidis³¹, T. Nooney⁷⁷, S. Norberg¹¹³,
 M. Nordberg³², N. Norjoharuddeen¹²⁰, O. Novgorodova⁴⁶, S. Nowak¹⁰¹, M. Nozaki⁶⁷, L. Nozka¹¹⁵,
 K. Ntekas¹⁰, E. Nurse⁷⁹, F. Nuti⁸⁹, F. O'grady⁷, D.C. O'Neil¹⁴², A.A. O'Rourke⁴⁴, V. O'Shea⁵⁵,
 F.G. Oakham^{31,d}, H. Oberlack¹⁰¹, T. Obermann²³, J. Ocariz⁸¹, A. Ochi⁶⁸, I. Ochoa³⁷,
 J.P. Ochoa-Ricoux^{34a}, S. Oda⁷¹, S. Odaka⁶⁷, H. Ogren⁶², A. Oh⁸⁵, S.H. Oh⁴⁷, C.C. Ohm¹⁶,
 H. Ohman¹⁶⁴, H. Oide³², H. Okawa¹⁶⁰, Y. Okumura¹⁵⁵, T. Okuyama⁶⁷, A. Olariu^{28b},
 L.F. Oleiro Seabra^{126a}, S.A. Olivares Pino⁴⁸, D. Oliveira Damazio²⁷, A. Olszewski⁴¹, J. Olszowska⁴¹,
 A. Onofre^{126a,126e}, K. Onogi¹⁰³, P.U.E. Onyisi^{11,v}, M.J. Oreglia³³, Y. Oren¹⁵³, D. Orestano^{134a,134b},
 N. Orlando^{61b}, R.S. Orr¹⁵⁸, B. Osculati^{52a,52b,*}, R. Ospanov⁸⁵, G. Otero y Garzon²⁹, H. Otono⁷¹,
 M. Ouchrif^{135d}, F. Ould-Saada¹¹⁹, A. Ouraou¹³⁶, K.P. Oussoren¹⁰⁷, Q. Ouyang^{35a}, M. Owen⁵⁵,
 R.E. Owen¹⁹, V.E. Ozcan^{20a}, N. Ozturk⁸, K. Pachal¹⁴², A. Pacheco Pages¹³, L. Pacheco Rodriguez¹³⁶,
 C. Padilla Aranda¹³, M. Pagáčová⁵⁰, S. Pagan Griso¹⁶, F. Paige²⁷, P. Pais⁸⁷, K. Pajchel¹¹⁹,
 G. Palacino^{159b}, S. Palazzo^{39a,39b}, S. Palestini³², M. Palka^{40b}, D. Pallin³⁶, E.St. Panagiotopoulou¹⁰,
 C.E. Pandini⁸¹, J.G. Panduro Vazquez⁷⁸, P. Pani^{146a,146b}, S. Panitkin²⁷, D. Pantea^{28b}, L. Paolozzi⁵¹,
 Th.D. Papadopoulou¹⁰, K. Papageorgiou¹⁵⁴, A. Paramonov⁶, D. Paredes Hernandez¹⁷⁵, A.J. Parker⁷³,
 M.A. Parker³⁰, K.A. Parker¹³⁹, F. Parodi^{52a,52b}, J.A. Parsons³⁷, U. Parzefall⁵⁰, V.R. Pascuzzi¹⁵⁸,
 E. Pasqualucci^{132a}, S. Passaggio^{52a}, Fr. Pastore⁷⁸, G. Pásztor^{31,ag}, S. Pataraia¹⁷⁴, J.R. Pater⁸⁵, T. Pauly³²,
 J. Pearce¹⁶⁸, B. Pearson¹¹³, L.E. Pedersen³⁸, M. Pedersen¹¹⁹, S. Pedraza Lopez¹⁶⁶, R. Pedro^{126a,126b},
 S.V. Peleganchuk^{109,c}, O. Penc¹²⁷, C. Peng^{35a}, H. Peng^{35b}, J. Penwell⁶², B.S. Peralva^{26b},
 M.M. Perego¹³⁶, D.V. Perepelitsa²⁷, E. Perez Codina^{159a}, L. Perini^{92a,92b}, H. Pernegger³²,
 S. Perrella^{104a,104b}, R. Peschke⁴⁴, V.D. Peshekhanov⁶⁶, K. Peters⁴⁴, R.F.Y. Peters⁸⁵, B.A. Petersen³²,
 T.C. Petersen³⁸, E. Petit⁵⁷, A. Petridis¹, C. Petridou¹⁵⁴, P. Petroff¹¹⁷, E. Petrolo^{132a}, M. Petrov¹²⁰,
 F. Petrucci^{134a,134b}, N.E. Petterson⁸⁷, A. Peyaud¹³⁶, R. Pezoa^{34b}, P.W. Phillips¹³¹, G. Piacquadio^{143,ah},
 E. Pianori¹⁶⁹, A. Picazio⁸⁷, E. Piccaro⁷⁷, M. Piccinini^{22a,22b}, M.A. Pickering¹²⁰, R. Piegaia²⁹,
 J.E. Pilcher³³, A.D. Pilkington⁸⁵, A.W.J. Pin⁸⁵, M. Pinamonti^{163a,163c,ai}, J.L. Pinfold³, A. Pingel³⁸,
 S. Pires⁸¹, H. Pirumov⁴⁴, M. Pitt¹⁷¹, L. Plazak^{144a}, M.-A. Pleier²⁷, V. Pleskot⁸⁴, E. Plotnikova⁶⁶,
 P. Plucinski⁹¹, D. Pluth⁶⁵, R. Poettgen^{146a,146b}, L. Poggiali¹¹⁷, D. Pohl²³, G. Polesello^{121a}, A. Poley⁴⁴,
 A. Policicchio^{39a,39b}, R. Polifka¹⁵⁸, A. Polini^{22a}, C.S. Pollard⁵⁵, V. Polychronakos²⁷, K. Pommès³²,
 L. Pontecorvo^{132a}, B.G. Pope⁹¹, G.A. Popeneciu^{28c}, D.S. Popovic¹⁴, A. Poppleton³², S. Pospisil¹²⁸,
 K. Potamianos¹⁶, I.N. Potrap⁶⁶, C.J. Potter³⁰, C.T. Potter¹¹⁶, G. Poulard³², J. Poveda³²,

V. Pozdnyakov⁶⁶, M.E. Pozo Astigarraga³², P. Pralavorio⁸⁶, A. Pranko¹⁶, S. Prell⁶⁵, D. Price⁸⁵,
 L.E. Price⁶, M. Primavera^{74a}, S. Prince⁸⁸, K. Prokofiev^{61c}, F. Prokoshin^{34b}, S. Protopopescu²⁷,
 J. Proudfoot⁶, M. Przybycien^{40a}, D. Puddu^{134a,134b}, M. Purohit^{27,aj}, P. Puzo¹¹⁷, J. Qian⁹⁰, G. Qin⁵⁵,
 Y. Qin⁸⁵, A. Quadt⁵⁶, W.B. Quayle^{163a,163b}, M. Queitsch-Maitland⁸⁵, D. Quilty⁵⁵, S. Raddum¹¹⁹,
 V. Radeka²⁷, V. Radescu¹²⁰, S.K. Radhakrishnan¹⁴⁸, P. Radloff¹¹⁶, P. Rados⁸⁹, F. Ragusa^{92a,92b},
 G. Rahal¹⁷⁷, J.A. Raine⁸⁵, S. Rajagopalan²⁷, M. Rammensee³², C. Rangel-Smith¹⁶⁴, M.G. Ratti^{92a,92b},
 F. Rauscher¹⁰⁰, S. Rave⁸⁴, T. Ravenscroft⁵⁵, I. Ravinovich¹⁷¹, M. Raymond³², A.L. Read¹¹⁹,
 N.P. Readioff⁷⁵, M. Reale^{74a,74b}, D.M. Rebuzzi^{121a,121b}, A. Redelbach¹⁷³, G. Redlinger²⁷, R. Reece¹³⁷,
 K. Reeves⁴³, L. Rehnisch¹⁷, J. Reichert¹²², H. Reisin²⁹, C. Rembser³², H. Ren^{35a}, M. Rescigno^{132a},
 S. Resconi^{92a}, O.L. Rezanova^{109,c}, P. Reznicek¹²⁹, R. Rezvani⁹⁵, R. Richter¹⁰¹, S. Richter⁷⁹,
 E. Richter-Was^{40b}, O. Ricken²³, M. Ridel⁸¹, P. Rieck¹⁷, C.J. Riegel¹⁷⁴, J. Rieger⁵⁶, O. Rifki¹¹³,
 M. Rijssenbeek¹⁴⁸, A. Rimoldi^{121a,121b}, M. Rimoldi¹⁸, L. Rinaldi^{22a}, B. Ristic⁵¹, E. Ritsch³², I. Riu¹³,
 F. Rizatdinova¹¹⁴, E. Rizvi⁷⁷, C. Rizzi¹³, S.H. Robertson^{88,l}, A. Robichaud-Veronneau⁸⁸, D. Robinson³⁰,
 J.E.M. Robinson⁴⁴, A. Robson⁵⁵, C. Roda^{124a,124b}, Y. Rodina⁸⁶, A. Rodriguez Perez¹³,
 D. Rodriguez Rodriguez¹⁶⁶, S. Roe³², C.S. Rogan⁵⁸, O. Røhne¹¹⁹, A. Romaniouk⁹⁸, M. Romano^{22a,22b},
 S.M. Romano Saez³⁶, E. Romero Adam¹⁶⁶, N. Rompotis¹³⁸, M. Ronzani⁵⁰, L. Roos⁸¹, E. Ros¹⁶⁶,
 S. Rosati^{132a}, K. Rosbach⁵⁰, P. Rose¹³⁷, O. Rosenthal¹⁴¹, N.-A. Rosien⁵⁶, V. Rossetti^{146a,146b},
 E. Rossi^{104a,104b}, L.P. Rossi^{52a}, J.H.N. Rosten³⁰, R. Rosten¹³⁸, M. Rotaru^{28b}, I. Roth¹⁷¹, J. Rothberg¹³⁸,
 D. Rousseau¹¹⁷, C.R. Royon¹³⁶, A. Rozanov⁸⁶, Y. Rozen¹⁵², X. Ruan^{145c}, F. Rubbo¹⁴³,
 M.S. Rudolph¹⁵⁸, F. Rühr⁵⁰, A. Ruiz-Martinez³¹, Z. Rurikova⁵⁰, N.A. Rusakovich⁶⁶, A. Ruschke¹⁰⁰,
 H.L. Russell¹³⁸, J.P. Rutherford⁷, N. Ruthmann³², Y.F. Ryabov¹²³, M. Rybar¹⁶⁵, G. Rybkin¹¹⁷, S. Ryu⁶,
 A. Ryzhov¹³⁰, G.F. Rzehorz⁵⁶, A.F. Saavedra¹⁵⁰, G. Sabato¹⁰⁷, S. Sacerdoti²⁹, H.F-W. Sadrozinski¹³⁷,
 R. Sadykov⁶⁶, F. Safai Tehrani^{132a}, P. Saha¹⁰⁸, M. Sahinsoy^{59a}, M. Saimpert¹³⁶, T. Saito¹⁵⁵,
 H. Sakamoto¹⁵⁵, Y. Sakurai¹⁷⁰, G. Salamanna^{134a,134b}, A. Salamon^{133a,133b}, J.E. Salazar Loyola^{34b},
 D. Salek¹⁰⁷, P.H. Sales De Bruin¹³⁸, D. Salihagic¹⁰¹, A. Salnikov¹⁴³, J. Salt¹⁶⁶, D. Salvatore^{39a,39b},
 F. Salvatore¹⁴⁹, A. Salvucci^{61a}, A. Salzburger³², D. Sammel⁵⁰, D. Sampsonidis¹⁵⁴, A. Sanchez^{104a,104b},
 J. Sánchez¹⁶⁶, V. Sanchez Martinez¹⁶⁶, H. Sandaker¹¹⁹, R.L. Sandbach⁷⁷, H.G. Sander⁸⁴,
 M. Sandhoff¹⁷⁴, C. Sandoval²¹, R. Sandstroem¹⁰¹, D.P.C. Sankey¹³¹, M. Sannino^{52a,52b}, A. Sansoni⁴⁹,
 C. Santoni³⁶, R. Santonico^{133a,133b}, H. Santos^{126a}, I. Santoyo Castillo¹⁴⁹, K. Sapp¹²⁵, A. Sapronov⁶⁶,
 J.G. Saraiva^{126a,126d}, B. Sarrazin²³, O. Sasaki⁶⁷, Y. Sasaki¹⁵⁵, K. Sato¹⁶⁰, G. Sauvage^{5,*}, E. Sauvan⁵,
 G. Savage⁷⁸, P. Savard^{158,d}, N. Savic¹⁰¹, C. Sawyer¹³¹, L. Sawyer^{80,4}, J. Saxon³³, C. Sbarra^{22a},
 A. Sbrizzi^{22a,22b}, T. Scanlon⁷⁹, D.A. Scannicchio¹⁶², M. Scarcella¹⁵⁰, V. Scarfone^{39a,39b},
 J. Schaarschmidt¹⁷¹, P. Schacht¹⁰¹, B.M. Schachtner¹⁰⁰, D. Schaefer³², R. Schaefer⁴⁴, J. Schaeffer⁸⁴,
 S. Schaepe²³, S. Schaetzl^{59b}, U. Schäfer⁸⁴, A.C. Schaffer¹¹⁷, D. Schaile¹⁰⁰, R.D. Schamberger¹⁴⁸,
 V. Scharf^{59a}, V.A. Schegelsky¹²³, D. Scheirich¹²⁹, M. Schernau¹⁶², C. Schiavi^{52a,52b}, S. Schier¹³⁷,
 C. Schillo⁵⁰, M. Schioppa^{39a,39b}, S. Schlenker³², K.R. Schmidt-Sommerfeld¹⁰¹, K. Schmieden³²,
 C. Schmitt⁸⁴, S. Schmitt⁴⁴, S. Schmitz⁸⁴, B. Schneider^{159a}, U. Schnoor⁵⁰, L. Schoeffel¹³⁶,
 A. Schoening^{59b}, B.D. Schoenrock⁹¹, E. Schopf²³, M. Schott⁸⁴, J. Schovancova⁸, S. Schramm⁵¹,
 M. Schreyer¹⁷³, N. Schuh⁸⁴, A. Schulte⁸⁴, M.J. Schultens²³, H.-C. Schultz-Coulon^{59a}, H. Schulz¹⁷,
 M. Schumacher⁵⁰, B.A. Schumm¹³⁷, Ph. Schune¹³⁶, A. Schwartzman¹⁴³, T.A. Schwarz⁹⁰,
 H. Schweiger⁸⁵, Ph. Schwemling¹³⁶, R. Schwienhorst⁹¹, J. Schwindling¹³⁶, T. Schwindt²³, G. Sciolla²⁵,
 F. Scuri^{124a,124b}, F. Scutti⁸⁹, J. Searcy⁹⁰, P. Seema²³, S.C. Seidel¹⁰⁵, A. Seiden¹³⁷, F. Seifert¹²⁸,
 J.M. Seixas^{26a}, G. Sekhniaidze^{104a}, K. Sekhon⁹⁰, S.J. Sekula⁴², D.M. Seliverstov^{123,*},
 N. Semprini-Cesari^{22a,22b}, C. Serfon¹¹⁹, L. Serin¹¹⁷, L. Serkin^{163a,163b}, M. Sessa^{134a,134b}, R. Seuster¹⁶⁸,
 H. Severini¹¹³, T. Sfiligoj⁷⁶, F. Sforza³², A. Sfyrla⁵¹, E. Shabalina⁵⁶, N.W. Shaikh^{146a,146b}, L.Y. Shan^{35a},
 R. Shang¹⁶⁵, J.T. Shank²⁴, M. Shapiro¹⁶, P.B. Shatalov⁹⁷, K. Shaw^{163a,163b}, S.M. Shaw⁸⁵,
 A. Shcherbakova^{146a,146b}, C.Y. Shehu¹⁴⁹, P. Sherwood⁷⁹, L. Shi^{151,ak}, S. Shimizu⁶⁸, C.O. Shimmin¹⁶²,

M. Shimojima¹⁰², M. Shiyakova^{66,al}, A. Shmeleva⁹⁶, D. Shoaleh Saadi⁹⁵, M.J. Shochet³³,
 S. Shojaii^{92a,92b}, S. Shrestha¹¹¹, E. Shulga⁹⁸, M.A. Shupe⁷, P. Sicho¹²⁷, A.M. Sickles¹⁶⁵, P.E. Sidebo¹⁴⁷,
 O. Sidiropoulou¹⁷³, D. Sidorov¹¹⁴, A. Sidoti^{22a,22b}, F. Siegert⁴⁶, Dj. Sijacki¹⁴, J. Silva^{126a,126d},
 S.B. Silverstein^{146a}, V. Simak¹²⁸, Lj. Simic¹⁴, S. Simion¹¹⁷, E. Simioni⁸⁴, B. Simmons⁷⁹, D. Simon³⁶,
 M. Simon⁸⁴, P. Sinervo¹⁵⁸, N.B. Sinev¹¹⁶, M. Sioli^{22a,22b}, G. Siragusa¹⁷³, S.Yu. Sivoklokov⁹⁹,
 J. Sjölin^{146a,146b}, M.B. Skinner⁷³, H.P. Skottowe⁵⁸, P. Skubic¹¹³, M. Slater¹⁹, T. Slavicek¹²⁸,
 M. Slawinska¹⁰⁷, K. Sliwa¹⁶¹, R. Slovac¹²⁹, V. Smakhtin¹⁷¹, B.H. Smart⁵, L. Smestad¹⁵, J. Smiesko^{144a},
 S.Yu. Smirnov⁹⁸, Y. Smirnov⁹⁸, L.N. Smirnova^{99,an}, O. Smirnova⁸², M.N.K. Smith³⁷, R.W. Smith³⁷,
 M. Smizanska⁷³, K. Smolek¹²⁸, A.A. Snesarev⁹⁶, S. Snyder²⁷, R. Sobie^{168,l}, F. Socher⁴⁶, A. Soffer¹⁵³,
 D.A. Soh¹⁵¹, G. Sokhrannyi⁷⁶, C.A. Solans Sanchez³², M. Solar¹²⁸, E.Yu. Soldatov⁹⁸, U. Soldevila¹⁶⁶,
 A.A. Solodkov¹³⁰, A. Soloshenko⁶⁶, O.V. Solovyanov¹³⁰, V. Solovyev¹²³, P. Sommer⁵⁰, H. Son¹⁶¹,
 H.Y. Song^{35b,an}, A. Sood¹⁶, A. Sopczak¹²⁸, V. Sopko¹²⁸, V. Sorin¹³, D. Sosa^{59b},
 C.L. Sotropoulou^{124a,124b}, R. Soualah^{163a,163c}, A.M. Soukharev^{109,c}, D. South⁴⁴, B.C. Sowden⁷⁸,
 S. Spagnolo^{74a,74b}, M. Spalla^{124a,124b}, M. Spangenberg¹⁶⁹, F. Spanò⁷⁸, D. Sperlich¹⁷, F. Spettel¹⁰¹,
 R. Spighi^{22a}, G. Spigo³², L.A. Spiller⁸⁹, M. Spousta¹²⁹, R.D. St. Denis^{55,*}, A. Stabile^{92a}, R. Stamen^{59a},
 S. Stamm¹⁷, E. Stanecka⁴¹, R.W. Stanek⁶, C. Stanescu^{134a}, M. Stanescu-Bellu⁴⁴, M.M. Stanitzki⁴⁴,
 S. Stapnes¹¹⁹, E.A. Starchenko¹³⁰, G.H. Stark³³, J. Stark⁵⁷, P. Staroba¹²⁷, P. Starovoitov^{59a}, S. Stärz³²,
 R. Staszewski⁴¹, P. Steinberg²⁷, B. Stelzer¹⁴², H.J. Stelzer³², O. Stelzer-Chilton^{159a}, H. Stenzel⁵⁴,
 G.A. Stewart⁵⁵, J.A. Stillings²³, M.C. Stockton⁸⁸, M. Stoebe⁸⁸, G. Stoica^{28b}, P. Stolte⁵⁶, S. Stonjek¹⁰¹,
 A.R. Stradling⁸, A. Straessner⁴⁶, M.E. Stramaglia¹⁸, J. Strandberg¹⁴⁷, S. Strandberg^{146a,146b},
 A. Strandlie¹¹⁹, M. Strauss¹¹³, P. Strizenec^{144b}, R. Ströhmer¹⁷³, D.M. Strom¹¹⁶, R. Stroynowski⁴²,
 A. Strubig¹⁰⁶, S.A. Stucci²⁷, B. Stugu¹⁵, N.A. Styles⁴⁴, D. Su¹⁴³, J. Su¹²⁵, S. Suchek^{59a}, Y. Sugaya¹¹⁸,
 M. Suk¹²⁸, V.V. Sulin⁹⁶, S. Sultansoy^{4c}, T. Sumida⁶⁹, S. Sun⁵⁸, X. Sun^{35a}, J.E. Sundermann⁵⁰,
 K. Suruliz¹⁴⁹, G. Susinno^{39a,39b}, M.R. Sutton¹⁴⁹, S. Suzuki⁶⁷, M. Svatos¹²⁷, M. Swiatlowski³³,
 I. Sykora^{144a}, T. Sykora¹²⁹, D. Ta⁵⁰, C. Taccini^{134a,134b}, K. Tackmann⁴⁴, J. Taenzer¹⁵⁸, A. Taffard¹⁶²,
 R. Tafirout^{159a}, N. Taiblum¹⁵³, H. Takai²⁷, R. Takashima⁷⁰, T. Takeshita¹⁴⁰, Y. Takubo⁶⁷, M. Talby⁸⁶,
 A.A. Talyshев^{109,c}, K.G. Tan⁸⁹, J. Tanaka¹⁵⁵, M. Tanaka¹⁵⁷, R. Tanaka¹¹⁷, S. Tanaka⁶⁷,
 B.B. Tannenwald¹¹¹, S. Tapia Araya^{34b}, S. Tapprogge⁸⁴, S. Tarem¹⁵², G.F. Tartarelli^{92a}, P. Tas¹²⁹,
 M. Tasevsky¹²⁷, T. Tashiro⁶⁹, E. Tassi^{39a,39b}, A. Tavares Delgado^{126a,126b}, Y. Tayalati^{135e}, A.C. Taylor¹⁰⁵,
 G.N. Taylor⁸⁹, P.T.E. Taylor⁸⁹, W. Taylor^{159b}, F.A. Teischinger³², P. Teixeira-Dias⁷⁸, K.K. Temming⁵⁰,
 D. Temple¹⁴², H. Ten Kate³², P.K. Teng¹⁵¹, J.J. Teoh¹¹⁸, F. Tepel¹⁷⁴, S. Terada⁶⁷, K. Terashi¹⁵⁵,
 J. Terron⁸³, S. Terzo¹³, M. Testa⁴⁹, R.J. Teuscher^{158,l}, A. Thamm^{ao}, T. Theveneaux-Pelzer⁸⁶,
 J.P. Thomas¹⁹, J. Thomas-Wilsker⁷⁸, E.N. Thompson³⁷, P.D. Thompson¹⁹, A.S. Thompson⁵⁵,
 L.A. Thomesen¹⁷⁵, E. Thomson¹²², M. Thomson³⁰, M.J. Tibbetts¹⁶, R.E. Ticse Torres⁸⁶,
 V.O. Tikhomirov^{96,ap}, Yu.A. Tikhonov^{109,c}, S. Timoshenko⁹⁸, P. Tipton¹⁷⁵, S. Tisserant⁸⁶,
 K. Todome¹⁵⁷, T. Todorov^{5,*}, S. Todorova-Nova¹²⁹, J. Tojo⁷¹, S. Tokár^{144a}, K. Tokushuku⁶⁷, E. Tolley⁵⁸,
 L. Tomlinson⁸⁵, M. Tomoto¹⁰³, L. Tompkins^{143,ag}, K. Toms¹⁰⁵, B. Tong⁵⁸, R. Torre^{ar}, E. Torrence¹¹⁶,
 H. Torres¹⁴², E. Torró Pastor¹³⁸, J. Toth^{86,as}, F. Touchard⁸⁶, D.R. Tovey¹³⁹, T. Trefzger¹⁷³, A. Tricoli²⁷,
 I.M. Trigger^{159a}, S. Trincaz-Duvold⁸¹, M.F. Tripiana¹³, W. Trischuk¹⁵⁸, B. Trocmé⁵⁷, A. Trofymov⁴⁴,
 C. Troncon^{92a}, M. Trottier-McDonald¹⁶, M. Trovatelli¹⁶⁸, L. Truong^{163a,163c}, M. Trzebinski⁴¹,
 A. Trzupek⁴¹, J.C.-L. Tseng¹²⁰, P.V. Tsiareshka⁹³, G. Tsipolitis¹⁰, N. Tsirintanis⁹, S. Tsiskaridze¹³,
 V. Tsiskaridze⁵⁰, E.G. Tskhadadze^{53a}, K.M. Tsui^{61a}, I.I. Tsukerman⁹⁷, V. Tsulaia¹⁶, S. Tsuno⁶⁷,
 D. Tsybychev¹⁴⁸, Y. Tu^{61b}, A. Tudorache^{28b}, V. Tudorache^{28b}, A.N. Tuna⁵⁸, S.A. Tupputi^{22a,22b},
 S. Turchikhin⁶⁶, D. Turecek¹²⁸, D. Turgeaman¹⁷¹, R. Turra^{92a,92b}, A.J. Turvey⁴², P.M. Tuts³⁷,
 M. Tyndel¹³¹, G. Ucchielli^{22a,22b}, I. Ueda¹⁵⁵, M. Ughetto^{146a,146b}, F. Ukegawa¹⁶⁰, G. Unal³²,
 A. Undrus²⁷, G. Unel¹⁶², F.C. Ungaro⁸⁹, Y. Unno⁶⁷, C. Unverdorben¹⁰⁰, J. Urban^{144b}, P. Urquijo⁸⁹,
 P. Urrejola⁸⁴, G. Usai⁸, A. Usanova⁶³, L. Vacavant⁸⁶, V. Vacek¹²⁸, B. Vachon⁸⁸, C. Valderanis¹⁰⁰,

E. Valdes Santurio^{146a,146b}, N. Valencic¹⁰⁷, S. Valentinetto^{22a,22b}, A. Valero¹⁶⁶, L. Valery¹³, S. Valkar¹²⁹,
 J.A. Valls Ferrer¹⁶⁶, W. Van Den Wollenberg¹⁰⁷, P.C. Van Der Deijl¹⁰⁷, H. van der Graaf¹⁰⁷,
 N. van Eldik¹⁵², P. van Gemmeren⁶, J. Van Nieuwkoop¹⁴², I. van Vulpen¹⁰⁷, M.C. van Woerden³²,
 M. Vanadia^{132a,132b}, W. Vandelli³², R. Vanguri¹²², A. Vaniachine¹³⁰, P. Vankov¹⁰⁷, G. Vardanyan¹⁷⁶,
 R. Vari^{132a}, E.W. Varnes⁷, T. Varol⁴², D. Varouchas⁸¹, A. Vartapetian⁸, K.E. Varvell¹⁵⁰, J.G. Vasquez¹⁷⁵,
 F. Vazeille³⁶, T. Vazquez Schroeder⁸⁸, J. Veatch⁵⁶, V. Veeraraghavan⁷, L.M. Veloce¹⁵⁸, F. Veloso^{126a,126c},
 S. Veneziano^{132a}, A. Ventura^{74a,74b}, M. Venturi¹⁶⁸, N. Venturi¹⁵⁸, A. Venturini²⁵, V. Vercesi^{121a},
 M. Verducci^{132a,132b}, W. Verkerke¹⁰⁷, J.C. Vermeulen¹⁰⁷, A. Vest^{46,at}, M.C. Vetterli^{142,d}, O. Viazlo⁸²,
 I. Vichou^{165,*}, T. Vickey¹³⁹, O.E. Vickey Boeriu¹³⁹, G.H.A. Viehhauser¹²⁰, S. Viel¹⁶, L. Vigani¹²⁰,
 M. Villa^{22a,22b}, M. Villaplana Perez^{92a,92b}, E. Vilucchi⁴⁹, M.G. Vincter³¹, V.B. Vinogradov⁶⁶,
 C. Vittori^{22a,22b}, I. Vivarelli¹⁴⁹, S. Vlachos¹⁰, M. Vlasak¹²⁸, M. Vogel¹⁷⁴, P. Vokac¹²⁸, G. Volpi^{124a,124b},
 M. Volpi⁸⁹, H. von der Schmitt¹⁰¹, E. von Toerne²³, V. Vorobel¹²⁹, K. Vorobev⁹⁸, M. Vos¹⁶⁶, R. Voss³²,
 J.H. Vossebeld⁷⁵, N. Vranjes¹⁴, M. Vranjes Milosavljevic¹⁴, V. Vrba¹²⁷, M. Vreeswijk¹⁰⁷,
 R. Vuillermet³², I. Vukotic³³, Z. Vykydal¹²⁸, P. Wagner²³, W. Wagner¹⁷⁴, H. Wahlberg⁷²,
 S. Wahr mund⁴⁶, J. Wakabayashi¹⁰³, J. Walder⁷³, R. Walker¹⁰⁰, W. Walkowiak¹⁴¹, V. Wallangen^{146a,146b},
 C. Wang^{35c}, C. Wang^{35d,86}, F. Wang¹⁷², H. Wang¹⁶, H. Wang⁴², J. Wang⁴⁴, J. Wang¹⁵⁰, K. Wang⁸⁸,
 R. Wang⁶, S.M. Wang¹⁵¹, T. Wang²³, T. Wang³⁷, W. Wang^{35b}, X. Wang¹⁷⁵, C. Wanotayaroj¹¹⁶,
 A. Warburton⁸⁸, C.P. Ward³⁰, D.R. Wardrop⁷⁹, A. Washbrook⁴⁸, P.M. Watkins¹⁹, A.T. Watson¹⁹,
 M.F. Watson¹⁹, G. Watts¹³⁸, S. Watts⁸⁵, B.M. Waugh⁷⁹, S. Webb⁸⁴, M.S. Weber¹⁸, S.W. Weber¹⁷³,
 J.S. Webster⁶, A.R. Weidberg¹²⁰, B. Weinert⁶², J. Weingarten⁵⁶, C. Weiser⁵⁰, H. Weits¹⁰⁷, P.S. Wells³²,
 T. Wenaus²⁷, T. Wengler³², S. Wenig³², N. Wermes²³, M. Werner⁵⁰, M.D. Werner⁶⁵, P. Werner³²,
 M. Wessels^{59a}, J. Wetter¹⁶¹, K. Whalen¹¹⁶, N.L. Whallon¹³⁸, A.M. Wharton⁷³, A. White⁸, M.J. White¹,
 R. White^{34b}, D. Whiteson¹⁶², F.J. Wickens¹³¹, W. Wiedenmann¹⁷², M. Wielers¹³¹, P. Wienemann²³,
 C. Wiglesworth³⁸, L.A.M. Wiik-Fuchs²³, A. Wildauer¹⁰¹, F. Wilk⁸⁵, H.G. Wilkens³², H.H. Williams¹²²,
 S. Williams¹⁰⁷, C. Willis⁹¹, S. Willocq⁸⁷, J.A. Wilson¹⁹, I. Wingerter-Seez⁵, F. Winklmeier¹¹⁶,
 O.J. Winston¹⁴⁹, B.T. Winter²³, M. Wittgen¹⁴³, J. Wittkowski¹⁰⁰, T.M.H. Wolf¹⁰⁷, M.W. Wolter⁴¹,
 H. Wolters^{126a,126c}, S.D. Worm¹³¹, B.K. Wosiek⁴¹, J. Wotschack³², M.J. Woudstra⁸⁵, K.W. Wozniak⁴¹,
 M. Wu⁵⁷, M. Wu³³, S.L. Wu¹⁷², X. Wu⁵¹, Y. Wu⁹⁰, T.R. Wyatt⁸⁵, B.M. Wynne⁴⁸, S. Xella³⁸, Z. Xi⁹⁰,
 D. Xu^{35a}, L. Xu²⁷, B. Yabsley¹⁵⁰, S. Yacoob^{145a}, D. Yamaguchi¹⁵⁷, Y. Yamaguchi¹¹⁸, A. Yamamoto⁶⁷,
 S. Yamamoto¹⁵⁵, T. Yamanaka¹⁵⁵, K. Yamauchi¹⁰³, Y. Yamazaki⁶⁸, Z. Yan²⁴, H. Yang^{35e}, H. Yang¹⁷²,
 Y. Yang¹⁵¹, Z. Yang¹⁵, W-M. Yao¹⁶, Y.C. Yap⁸¹, Y. Yasu⁶⁷, E. Yatsenko⁵, K.H. Yau Wong²³, J. Ye⁴²,
 S. Ye²⁷, I. Yeletskikh⁶⁶, A.L. Yen⁵⁸, E. Yildirim⁸⁴, K. Yorita¹⁷⁰, R. Yoshida⁶, K. Yoshihara¹²²,
 C. Young¹⁴³, C.J.S. Young³², S. Youssef²⁴, D.R. Yu¹⁶, J. Yu⁸, J.M. Yu⁹⁰, J. Yu⁶⁵, L. Yuan⁶⁸,
 S.P.Y. Yuen²³, I. Yusuff^{30,au}, B. Zabinski⁴¹, R. Zaidan^{35d}, A.M. Zaitsev^{130,ae}, N. Zakharchuk⁴⁴,
 J. Zalieckas¹⁵, A. Zaman¹⁴⁸, S. Zambito⁵⁸, L. Zanello^{132a,132b}, D. Zanzi⁸⁹, C. Zeitnitz¹⁷⁴, M. Zeman¹²⁸,
 A. Zemla^{40a}, J.C. Zeng¹⁶⁵, Q. Zeng¹⁴³, K. Zengel²⁵, O. Zenin¹³⁰, T. Ženiš^{144a}, D. Zerwas¹¹⁷,
 D. Zhang⁹⁰, F. Zhang¹⁷², G. Zhang^{35b,an}, H. Zhang^{35c}, J. Zhang⁶, L. Zhang⁵⁰, R. Zhang²³,
 R. Zhang^{35b,av}, X. Zhang^{35d}, Z. Zhang¹¹⁷, X. Zhao⁴², Y. Zhao^{35d}, Z. Zhao^{35b}, A. Zhemchugov⁶⁶,
 J. Zhong¹²⁰, B. Zhou⁹⁰, C. Zhou⁴⁷, L. Zhou³⁷, L. Zhou⁴², M. Zhou¹⁴⁸, N. Zhou^{35f}, C.G. Zhu^{35d},
 H. Zhu^{35a}, J. Zhu⁹⁰, Y. Zhu^{35b}, X. Zhuang^{35a}, K. Zhukov⁹⁶, A. Zibell¹⁷³, D. Ziemińska⁶², N.I. Zimine⁶⁶,
 C. Zimmermann⁸⁴, S. Zimmermann⁵⁰, Z. Zinonos⁵⁶, M. Zinser⁸⁴, M. Ziolkowski¹⁴¹, L. Živković¹⁴,
 G. Zobernig¹⁷², A. Zoccoli^{22a,22b}, M. zur Nedden¹⁷, L. Zwalski³².

¹ Department of Physics, University of Adelaide, Adelaide, Australia

² Physics Department, SUNY Albany, Albany NY, United States of America

³ Department of Physics, University of Alberta, Edmonton AB, Canada

⁴ ^(a) Department of Physics, Ankara University, Ankara; ^(b) Istanbul Aydin University, Istanbul; ^(c)

- Division of Physics, TOBB University of Economics and Technology, Ankara, Turkey
- ⁵ LAPP, CNRS/IN2P3 and Université Savoie Mont Blanc, Annecy-le-Vieux, France
- ⁶ High Energy Physics Division, Argonne National Laboratory, Argonne IL, United States of America
- ⁷ Department of Physics, University of Arizona, Tucson AZ, United States of America
- ⁸ Department of Physics, The University of Texas at Arlington, Arlington TX, United States of America
- ⁹ Physics Department, University of Athens, Athens, Greece
- ¹⁰ Physics Department, National Technical University of Athens, Zografou, Greece
- ¹¹ Department of Physics, The University of Texas at Austin, Austin TX, United States of America
- ¹² Institute of Physics, Azerbaijan Academy of Sciences, Baku, Azerbaijan
- ¹³ Institut de Física d'Altes Energies (IFAE), The Barcelona Institute of Science and Technology, Barcelona, Spain, Spain
- ¹⁴ Institute of Physics, University of Belgrade, Belgrade, Serbia
- ¹⁵ Department for Physics and Technology, University of Bergen, Bergen, Norway
- ¹⁶ Physics Division, Lawrence Berkeley National Laboratory and University of California, Berkeley CA, United States of America
- ¹⁷ Department of Physics, Humboldt University, Berlin, Germany
- ¹⁸ Albert Einstein Center for Fundamental Physics and Laboratory for High Energy Physics, University of Bern, Bern, Switzerland
- ¹⁹ School of Physics and Astronomy, University of Birmingham, Birmingham, United Kingdom
- ²⁰ ^(a) Department of Physics, Bogazici University, Istanbul; ^(b) Department of Physics Engineering, Gaziantep University, Gaziantep; ^(d) Istanbul Bilgi University, Faculty of Engineering and Natural Sciences, Istanbul, Turkey; ^(e) Bahcesehir University, Faculty of Engineering and Natural Sciences, Istanbul, Turkey, Turkey
- ²¹ Centro de Investigaciones, Universidad Antonio Narino, Bogota, Colombia
- ²² ^(a) INFN Sezione di Bologna; ^(b) Dipartimento di Fisica e Astronomia, Università di Bologna, Bologna, Italy
- ²³ Physikalisches Institut, University of Bonn, Bonn, Germany
- ²⁴ Department of Physics, Boston University, Boston MA, United States of America
- ²⁵ Department of Physics, Brandeis University, Waltham MA, United States of America
- ²⁶ ^(a) Universidade Federal do Rio De Janeiro COPPE/EE/IF, Rio de Janeiro; ^(b) Electrical Circuits Department, Federal University of Juiz de Fora (UFJF), Juiz de Fora; ^(c) Federal University of Sao Joao del Rei (UFSJ), Sao Joao del Rei; ^(d) Instituto de Fisica, Universidade de Sao Paulo, Sao Paulo, Brazil
- ²⁷ Physics Department, Brookhaven National Laboratory, Upton NY, United States of America
- ²⁸ ^(a) Transilvania University of Brasov, Brasov, Romania; ^(b) National Institute of Physics and Nuclear Engineering, Bucharest; ^(c) National Institute for Research and Development of Isotopic and Molecular Technologies, Physics Department, Cluj Napoca; ^(d) University Politehnica Bucharest, Bucharest; ^(e) West University in Timisoara, Timisoara, Romania
- ²⁹ Departamento de Física, Universidad de Buenos Aires, Buenos Aires, Argentina
- ³⁰ Cavendish Laboratory, University of Cambridge, Cambridge, United Kingdom
- ³¹ Department of Physics, Carleton University, Ottawa ON, Canada
- ³² CERN, Geneva, Switzerland
- ³³ Enrico Fermi Institute, University of Chicago, Chicago IL, United States of America
- ³⁴ ^(a) Departamento de Física, Pontificia Universidad Católica de Chile, Santiago; ^(b) Departamento de Física, Universidad Técnica Federico Santa María, Valparaíso, Chile
- ³⁵ ^(a) Institute of High Energy Physics, Chinese Academy of Sciences, Beijing; ^(b) Department of Modern Physics, University of Science and Technology of China, Anhui; ^(c) Department of Physics, Nanjing University, Jiangsu; ^(d) School of Physics, Shandong University, Shandong; ^(e) Department of

Physics and Astronomy, Shanghai Key Laboratory for Particle Physics and Cosmology, Shanghai Jiao Tong University, Shanghai; (also affiliated with PKU-CHEP); ^(f) Physics Department, Tsinghua University, Beijing 100084, China

³⁶ Laboratoire de Physique Corpusculaire, Clermont Université and Université Blaise Pascal and CNRS/IN2P3, Clermont-Ferrand, France

³⁷ Nevis Laboratory, Columbia University, Irvington NY, United States of America

³⁸ Niels Bohr Institute, University of Copenhagen, Kobenhavn, Denmark

³⁹ ^(a) INFN Gruppo Collegato di Cosenza, Laboratori Nazionali di Frascati; ^(b) Dipartimento di Fisica, Università della Calabria, Rende, Italy

⁴⁰ ^(a) AGH University of Science and Technology, Faculty of Physics and Applied Computer Science, Krakow; ^(b) Marian Smoluchowski Institute of Physics, Jagiellonian University, Krakow, Poland

⁴¹ Institute of Nuclear Physics Polish Academy of Sciences, Krakow, Poland

⁴² Physics Department, Southern Methodist University, Dallas TX, United States of America

⁴³ Physics Department, University of Texas at Dallas, Richardson TX, United States of America

⁴⁴ DESY, Hamburg and Zeuthen, Germany

⁴⁵ Lehrstuhl für Experimentelle Physik IV, Technische Universität Dortmund, Dortmund, Germany

⁴⁶ Institut für Kern- und Teilchenphysik, Technische Universität Dresden, Dresden, Germany

⁴⁷ Department of Physics, Duke University, Durham NC, United States of America

⁴⁸ SUPA - School of Physics and Astronomy, University of Edinburgh, Edinburgh, United Kingdom

⁴⁹ INFN Laboratori Nazionali di Frascati, Frascati, Italy

⁵⁰ Fakultät für Mathematik und Physik, Albert-Ludwigs-Universität, Freiburg, Germany

⁵¹ Section de Physique, Université de Genève, Geneva, Switzerland

⁵² ^(a) INFN Sezione di Genova; ^(b) Dipartimento di Fisica, Università di Genova, Genova, Italy

⁵³ ^(a) E. Andronikashvili Institute of Physics, Iv. Javakhishvili Tbilisi State University, Tbilisi; ^(b) High Energy Physics Institute, Tbilisi State University, Tbilisi, Georgia

⁵⁴ II Physikalisches Institut, Justus-Liebig-Universität Giessen, Giessen, Germany

⁵⁵ SUPA - School of Physics and Astronomy, University of Glasgow, Glasgow, United Kingdom

⁵⁶ II Physikalisches Institut, Georg-August-Universität, Göttingen, Germany

⁵⁷ Laboratoire de Physique Subatomique et de Cosmologie, Université Grenoble-Alpes, CNRS/IN2P3, Grenoble, France

⁵⁸ Laboratory for Particle Physics and Cosmology, Harvard University, Cambridge MA, United States of America

⁵⁹ ^(a) Kirchhoff-Institut für Physik, Ruprecht-Karls-Universität Heidelberg, Heidelberg; ^(b)

Physikalisches Institut, Ruprecht-Karls-Universität Heidelberg, Heidelberg; ^(c) ZITI Institut für technische Informatik, Ruprecht-Karls-Universität Heidelberg, Mannheim, Germany

⁶⁰ Faculty of Applied Information Science, Hiroshima Institute of Technology, Hiroshima, Japan

⁶¹ ^(a) Department of Physics, The Chinese University of Hong Kong, Shatin, N.T., Hong Kong; ^(b) Department of Physics, The University of Hong Kong, Hong Kong; ^(c) Department of Physics, The Hong Kong University of Science and Technology, Clear Water Bay, Kowloon, Hong Kong, China

⁶² Department of Physics, Indiana University, Bloomington IN, United States of America

⁶³ Institut für Astro- und Teilchenphysik, Leopold-Franzens-Universität, Innsbruck, Austria

⁶⁴ University of Iowa, Iowa City IA, United States of America

⁶⁵ Department of Physics and Astronomy, Iowa State University, Ames IA, United States of America

⁶⁶ Joint Institute for Nuclear Research, JINR Dubna, Dubna, Russia

⁶⁷ KEK, High Energy Accelerator Research Organization, Tsukuba, Japan

⁶⁸ Graduate School of Science, Kobe University, Kobe, Japan

⁶⁹ Faculty of Science, Kyoto University, Kyoto, Japan

- ⁷⁰ Kyoto University of Education, Kyoto, Japan
⁷¹ Department of Physics, Kyushu University, Fukuoka, Japan
⁷² Instituto de Física La Plata, Universidad Nacional de La Plata and CONICET, La Plata, Argentina
⁷³ Physics Department, Lancaster University, Lancaster, United Kingdom
⁷⁴ ^(a) INFN Sezione di Lecce; ^(b) Dipartimento di Matematica e Fisica, Università del Salento, Lecce, Italy
⁷⁵ Oliver Lodge Laboratory, University of Liverpool, Liverpool, United Kingdom
⁷⁶ Department of Physics, Jožef Stefan Institute and University of Ljubljana, Ljubljana, Slovenia
⁷⁷ School of Physics and Astronomy, Queen Mary University of London, London, United Kingdom
⁷⁸ Department of Physics, Royal Holloway University of London, Surrey, United Kingdom
⁷⁹ Department of Physics and Astronomy, University College London, London, United Kingdom
⁸⁰ Louisiana Tech University, Ruston LA, United States of America
⁸¹ Laboratoire de Physique Nucléaire et de Hautes Energies, UPMC and Université Paris-Diderot and CNRS/IN2P3, Paris, France
⁸² Fysiska institutionen, Lunds universitet, Lund, Sweden
⁸³ Departamento de Fisica Teorica C-15, Universidad Autonoma de Madrid, Madrid, Spain
⁸⁴ Institut für Physik, Universität Mainz, Mainz, Germany
⁸⁵ School of Physics and Astronomy, University of Manchester, Manchester, United Kingdom
⁸⁶ CPPM, Aix-Marseille Université and CNRS/IN2P3, Marseille, France
⁸⁷ Department of Physics, University of Massachusetts, Amherst MA, United States of America
⁸⁸ Department of Physics, McGill University, Montreal QC, Canada
⁸⁹ School of Physics, University of Melbourne, Victoria, Australia
⁹⁰ Department of Physics, The University of Michigan, Ann Arbor MI, United States of America
⁹¹ Department of Physics and Astronomy, Michigan State University, East Lansing MI, United States of America
⁹² ^(a) INFN Sezione di Milano; ^(b) Dipartimento di Fisica, Università di Milano, Milano, Italy
⁹³ B.I. Stepanov Institute of Physics, National Academy of Sciences of Belarus, Minsk, Republic of Belarus
⁹⁴ National Scientific and Educational Centre for Particle and High Energy Physics, Minsk, Republic of Belarus
⁹⁵ Group of Particle Physics, University of Montreal, Montreal QC, Canada
⁹⁶ P.N. Lebedev Physical Institute of the Russian Academy of Sciences, Moscow, Russia
⁹⁷ Institute for Theoretical and Experimental Physics (ITEP), Moscow, Russia
⁹⁸ National Research Nuclear University MEPhI, Moscow, Russia
⁹⁹ D.V. Skobeltsyn Institute of Nuclear Physics, M.V. Lomonosov Moscow State University, Moscow, Russia
¹⁰⁰ Fakultät für Physik, Ludwig-Maximilians-Universität München, München, Germany
¹⁰¹ Max-Planck-Institut für Physik (Werner-Heisenberg-Institut), München, Germany
¹⁰² Nagasaki Institute of Applied Science, Nagasaki, Japan
¹⁰³ Graduate School of Science and Kobayashi-Maskawa Institute, Nagoya University, Nagoya, Japan
¹⁰⁴ ^(a) INFN Sezione di Napoli; ^(b) Dipartimento di Fisica, Università di Napoli, Napoli, Italy
¹⁰⁵ Department of Physics and Astronomy, University of New Mexico, Albuquerque NM, United States of America
¹⁰⁶ Institute for Mathematics, Astrophysics and Particle Physics, Radboud University Nijmegen/Nikhef, Nijmegen, Netherlands
¹⁰⁷ Nikhef National Institute for Subatomic Physics and University of Amsterdam, Amsterdam, Netherlands

- ¹⁰⁸ Department of Physics, Northern Illinois University, DeKalb IL, United States of America
¹⁰⁹ Budker Institute of Nuclear Physics, SB RAS, Novosibirsk, Russia
¹¹⁰ Department of Physics, New York University, New York NY, United States of America
¹¹¹ Ohio State University, Columbus OH, United States of America
¹¹² Faculty of Science, Okayama University, Okayama, Japan
¹¹³ Homer L. Dodge Department of Physics and Astronomy, University of Oklahoma, Norman OK, United States of America
¹¹⁴ Department of Physics, Oklahoma State University, Stillwater OK, United States of America
¹¹⁵ Palacký University, RCPTM, Olomouc, Czech Republic
¹¹⁶ Center for High Energy Physics, University of Oregon, Eugene OR, United States of America
¹¹⁷ LAL, Univ. Paris-Sud, CNRS/IN2P3, Université Paris-Saclay, Orsay, France
¹¹⁸ Graduate School of Science, Osaka University, Osaka, Japan
¹¹⁹ Department of Physics, University of Oslo, Oslo, Norway
¹²⁰ Department of Physics, Oxford University, Oxford, United Kingdom
¹²¹ ^(a) INFN Sezione di Pavia; ^(b) Dipartimento di Fisica, Università di Pavia, Pavia, Italy
¹²² Department of Physics, University of Pennsylvania, Philadelphia PA, United States of America
¹²³ National Research Centre "Kurchatov Institute" B.P.Konstantinov Petersburg Nuclear Physics Institute, St. Petersburg, Russia
¹²⁴ ^(a) INFN Sezione di Pisa; ^(b) Dipartimento di Fisica E. Fermi, Università di Pisa, Pisa, Italy
¹²⁵ Department of Physics and Astronomy, University of Pittsburgh, Pittsburgh PA, United States of America
¹²⁶ ^(a) Laboratório de Instrumentação e Física Experimental de Partículas - LIP, Lisboa; ^(b) Faculdade de Ciências, Universidade de Lisboa, Lisboa; ^(c) Department of Physics, University of Coimbra, Coimbra; ^(d) Centro de Física Nuclear da Universidade de Lisboa, Lisboa; ^(e) Departamento de Física, Universidade do Minho, Braga; ^(f) Departamento de Física Teórica y del Cosmos and CAFPE, Universidad de Granada, Granada (Spain); ^(g) Dep Física and CEFITEC of Faculdade de Ciencias e Tecnologia, Universidade Nova de Lisboa, Caparica, Portugal
¹²⁷ Institute of Physics, Academy of Sciences of the Czech Republic, Praha, Czech Republic
¹²⁸ Czech Technical University in Prague, Praha, Czech Republic
¹²⁹ Faculty of Mathematics and Physics, Charles University in Prague, Praha, Czech Republic
¹³⁰ State Research Center Institute for High Energy Physics (Protvino), NRC KI, Russia
¹³¹ Particle Physics Department, Rutherford Appleton Laboratory, Didcot, United Kingdom
¹³² ^(a) INFN Sezione di Roma; ^(b) Dipartimento di Fisica, Sapienza Università di Roma, Roma, Italy
¹³³ ^(a) INFN Sezione di Roma Tor Vergata; ^(b) Dipartimento di Fisica, Università di Roma Tor Vergata, Roma, Italy
¹³⁴ ^(a) INFN Sezione di Roma Tre; ^(b) Dipartimento di Matematica e Fisica, Università Roma Tre, Roma, Italy
¹³⁵ ^(a) Faculté des Sciences Ain Chock, Réseau Universitaire de Physique des Hautes Energies - Université Hassan II, Casablanca; ^(b) Centre National de l'Energie des Sciences Techniques Nucléaires, Rabat; ^(c) Faculté des Sciences Semlalia, Université Cadi Ayyad, LPHEA-Marrakech; ^(d) Faculté des Sciences, Université Mohamed Premier and LPTPM, Oujda; ^(e) Faculté des sciences, Université Mohammed V, Rabat, Morocco
¹³⁶ DSM/IRFU (Institut de Recherches sur les Lois Fondamentales de l'Univers), CEA Saclay (Commissariat à l'Energie Atomique et aux Energies Alternatives), Gif-sur-Yvette, France
¹³⁷ Santa Cruz Institute for Particle Physics, University of California Santa Cruz, Santa Cruz CA, United States of America
¹³⁸ Department of Physics, University of Washington, Seattle WA, United States of America

- ¹³⁹ Department of Physics and Astronomy, University of Sheffield, Sheffield, United Kingdom
¹⁴⁰ Department of Physics, Shinshu University, Nagano, Japan
¹⁴¹ Fachbereich Physik, Universität Siegen, Siegen, Germany
¹⁴² Department of Physics, Simon Fraser University, Burnaby BC, Canada
¹⁴³ SLAC National Accelerator Laboratory, Stanford CA, United States of America
¹⁴⁴ ^(a) Faculty of Mathematics, Physics & Informatics, Comenius University, Bratislava; ^(b) Department of Subnuclear Physics, Institute of Experimental Physics of the Slovak Academy of Sciences, Kosice, Slovak Republic
¹⁴⁵ ^(a) Department of Physics, University of Cape Town, Cape Town; ^(b) Department of Physics, University of Johannesburg, Johannesburg; ^(c) School of Physics, University of the Witwatersrand, Johannesburg, South Africa
¹⁴⁶ ^(a) Department of Physics, Stockholm University; ^(b) The Oskar Klein Centre, Stockholm, Sweden
¹⁴⁷ Physics Department, Royal Institute of Technology, Stockholm, Sweden
¹⁴⁸ Departments of Physics & Astronomy and Chemistry, Stony Brook University, Stony Brook NY, United States of America
¹⁴⁹ Department of Physics and Astronomy, University of Sussex, Brighton, United Kingdom
¹⁵⁰ School of Physics, University of Sydney, Sydney, Australia
¹⁵¹ Institute of Physics, Academia Sinica, Taipei, Taiwan
¹⁵² Department of Physics, Technion: Israel Institute of Technology, Haifa, Israel
¹⁵³ Raymond and Beverly Sackler School of Physics and Astronomy, Tel Aviv University, Tel Aviv, Israel
¹⁵⁴ Department of Physics, Aristotle University of Thessaloniki, Thessaloniki, Greece
¹⁵⁵ International Center for Elementary Particle Physics and Department of Physics, The University of Tokyo, Tokyo, Japan
¹⁵⁶ Graduate School of Science and Technology, Tokyo Metropolitan University, Tokyo, Japan
¹⁵⁷ Department of Physics, Tokyo Institute of Technology, Tokyo, Japan
¹⁵⁸ Department of Physics, University of Toronto, Toronto ON, Canada
¹⁵⁹ ^(a) TRIUMF, Vancouver BC; ^(b) Department of Physics and Astronomy, York University, Toronto ON, Canada
¹⁶⁰ Faculty of Pure and Applied Sciences, and Center for Integrated Research in Fundamental Science and Engineering, University of Tsukuba, Tsukuba, Japan
¹⁶¹ Department of Physics and Astronomy, Tufts University, Medford MA, United States of America
¹⁶² Department of Physics and Astronomy, University of California Irvine, Irvine CA, United States of America
¹⁶³ ^(a) INFN Gruppo Collegato di Udine, Sezione di Trieste, Udine; ^(b) ICTP, Trieste; ^(c) Dipartimento di Chimica, Fisica e Ambiente, Università di Udine, Udine, Italy
¹⁶⁴ Department of Physics and Astronomy, University of Uppsala, Uppsala, Sweden
¹⁶⁵ Department of Physics, University of Illinois, Urbana IL, United States of America
¹⁶⁶ Instituto de Física Corpuscular (IFIC) and Departamento de Física Atomica, Molecular y Nuclear and Departamento de Ingeniería Electrónica and Instituto de Microelectrónica de Barcelona (IMB-CNM), University of Valencia and CSIC, Valencia, Spain
¹⁶⁷ Department of Physics, University of British Columbia, Vancouver BC, Canada
¹⁶⁸ Department of Physics and Astronomy, University of Victoria, Victoria BC, Canada
¹⁶⁹ Department of Physics, University of Warwick, Coventry, United Kingdom
¹⁷⁰ Waseda University, Tokyo, Japan
¹⁷¹ Department of Particle Physics, The Weizmann Institute of Science, Rehovot, Israel
¹⁷² Department of Physics, University of Wisconsin, Madison WI, United States of America

- ¹⁷³ Fakultät für Physik und Astronomie, Julius-Maximilians-Universität, Würzburg, Germany
¹⁷⁴ Fakultät für Mathematik und Naturwissenschaften, Fachgruppe Physik, Bergische Universität Wuppertal, Wuppertal, Germany
¹⁷⁵ Department of Physics, Yale University, New Haven CT, United States of America
¹⁷⁶ Yerevan Physics Institute, Yerevan, Armenia
¹⁷⁷ Centre de Calcul de l’Institut National de Physique Nucléaire et de Physique des Particules (IN2P3), Villeurbanne, France
^a Also at Department of Physics, King’s College London, London, United Kingdom
^b Also at Institute of Physics, Azerbaijan Academy of Sciences, Baku, Azerbaijan
^c Also at Novosibirsk State University, Novosibirsk, Russia
^d Also at TRIUMF, Vancouver BC, Canada
^e Also at Department of Physics & Astronomy, University of Louisville, Louisville, KY, United States of America
^f Also at Department of Physics, California State University, Fresno CA, United States of America
^g Also at Department of Physics, University of Fribourg, Fribourg, Switzerland
^h Also at Departament de Fisica de la Universitat Autonoma de Barcelona, Barcelona, Spain
ⁱ Also at Departamento de Fisica e Astronomia, Faculdade de Ciencias, Universidade do Porto, Portugal
^j Also at Tomsk State University, Tomsk, Russia
^k Also at Universita di Napoli Parthenope, Napoli, Italy
^l Also at Institute of Particle Physics (IPP), Canada
^m Also at National Institute of Physics and Nuclear Engineering, Bucharest, Romania
ⁿ Also at Department of Physics, St. Petersburg State Polytechnical University, St. Petersburg, Russia
^o Also at Department of Physics, The University of Michigan, Ann Arbor MI, United States of America
^p Also at Centre for High Performance Computing, CSIR Campus, Rosebank, Cape Town, South Africa
^q Also at Louisiana Tech University, Ruston LA, United States of America
^r Also at Institutio Catalana de Recerca i Estudis Avancats, ICREA, Barcelona, Spain
^s Also at Graduate School of Science, Osaka University, Osaka, Japan
^t Also at Department of Physics, National Tsing Hua University, Taiwan
^u Also at Institute for Mathematics, Astrophysics and Particle Physics, Radboud University Nijmegen/Nikhef, Nijmegen, Netherlands
^v Also at Department of Physics, The University of Texas at Austin, Austin TX, United States of America
^w Also at CERN, Geneva, Switzerland
^x Also at Georgian Technical University (GTU), Tbilisi, Georgia
^y Also at Ochadai Academic Production, Ochanomizu University, Tokyo, Japan
^z Also at Manhattan College, New York NY, United States of America
^{aa} Also at Hellenic Open University, Patras, Greece
^{ab} Also at Academia Sinica Grid Computing, Institute of Physics, Academia Sinica, Taipei, Taiwan
^{ac} Also at School of Physics, Shandong University, Shandong, China
^{ad} Also at Department of Physics, California State University, Sacramento CA, United States of America
^{ae} Also at Moscow Institute of Physics and Technology State University, Dolgoprudny, Russia
^{af} Also at Section de Physique, Université de Genève, Geneva, Switzerland
^{ag} Also at Eotvos Lorand University, Budapest, Hungary
^{ah} Also at Departments of Physics & Astronomy and Chemistry, Stony Brook University, Stony Brook NY, United States of America
^{ai} Also at International School for Advanced Studies (SISSA), Trieste, Italy
^{aj} Also at Department of Physics and Astronomy, University of South Carolina, Columbia SC, United States of America

ak Also at School of Physics and Engineering, Sun Yat-sen University, Guangzhou, China

al Also at Institute for Nuclear Research and Nuclear Energy (INRNE) of the Bulgarian Academy of Sciences, Sofia, Bulgaria

am Also at Faculty of Physics, M.V.Lomonosov Moscow State University, Moscow, Russia

an Also at Institute of Physics, Academia Sinica, Taipei, Taiwan

ao Associated at PRISMA Cluster of Excellence & Mainz Institute for Theoretical Physics, Johannes Gutenberg University, Mainz, Germany

ap Also at National Research Nuclear University MEPhI, Moscow, Russia

aq Also at Department of Physics, Stanford University, Stanford CA, United States of America

ar Associated at Institut de Theorie des Phenomene Physiques, EPFL, Lausanne, Switzerland

as Also at Institute for Particle and Nuclear Physics, Wigner Research Centre for Physics, Budapest, Hungary

at Also at Flensburg University of Applied Sciences, Flensburg, Germany

au Also at University of Malaya, Department of Physics, Kuala Lumpur, Malaysia

av Also at CPPM, Aix-Marseille Université and CNRS/IN2P3, Marseille, France

* Deceased